Sensitivity Analysis of Partial Differential Equations With Applications to Fluid Flow

John R. Singler

Dissertation submitted to the Faculty of the
Virginia Polytechnic Institute and State University
in partial fulfillment of the requirements for the degree of

Doctor of Philosophy
in
Mathematics

John A. Burns, Chair
Jeff Borggaard
Gene Cliff
Terry Herdman
Traian Iliescu

June 2005
Blacksburg, Virginia

Keywords: Partial Differential Equations, Sensitivity Analysis, Small Disturbances,
Transition to Turbulence

Sensitivity Analysis of Partial Differential Equations With Applications to Fluid Flow

John R. Singler

ABSTRACT

For over 100 years, researchers have attempted to predict transition to turbulence in fluid flows by analyzing the spectrum of the linearized Navier-Stokes equations. However, for many simple flows, this approach has failed to match experimental results. Recently, new scenarios for transition have been proposed that are based on the non-normality of the linearized operator. These new "mostly linear" theories have increased our understanding of the transition process, but the role of nonlinearity has not been explored. The main goal of this work is to begin to study the role of nonlinearity in transition. We use model problems to illustrate that small unmodeled disturbances can cause transition through movement or bifurcation of equilibria. We also demonstrate that small wall roughness can lead to transition by causing the linearized system to become unstable. Sensitivity methods are used to obtain important information about the disturbed problem and to illustrate that it is possible to have a precursor to predict transition. Finally, we apply linear feedback control to the model problems to illustrate the power of feedback to delay transition and even relaminarize fully developed chaotic flows.

This research was supported in part by the Air Force Office of Scientific Research under grant F49620-03-1-0243 and by the DARPA Special Projects Office.

Dedication

To my wife Susan
and our little one on the way!

Acknowledgments

I would like to thank my advisor, John Burns, for guiding my studies and introducing me to many interesting and important problems. I have really enjoyed working with you. Also, thanks to my committee for listening to all of my questions over the years. A special thanks to Jeff Borggaard for our many discussions about finite elements. Finally, thanks to my wife Susan. Without you, this would not have been possible!

Contents

List of Figures

List of Tables

Nomenclature

$\nabla \cdot \vec{a}$	The divergence of the vector $\vec{a}$ in rectangular coordinates: $\nabla \cdot \vec{a} = \frac{\partial a_1}{\partial x_1} + \cdots + \frac{\partial a_n}{\partial x_n}$.
$\dot{z}$	Derivative with respect to time: $\dot{z} = \frac{\partial z}{\partial t}$.
∇	Gradient operator: $\nabla = \left[\frac{\partial}{\partial x}, \frac{\partial}{\partial y}, \frac{\partial}{\partial z}\right]^T$.
∇^2	The Laplacian in rectangular coordinates: $\nabla^2 = \nabla \cdot \nabla = \frac{\partial^2}{\partial x^2} + \frac{\partial^2}{\partial y^2} + \frac{\partial^2}{\partial z^2}$.
$\langle \cdot, \cdot \rangle$	An inner product. It will usually be accompanied by a subscript to denote an inner product over a certain space.
$\Lambda(\mathcal{A})$	The spectrum of a linear operator $\mathcal{A}$; see definition 2.1.3.
$\mathbf{A}$	A capital letter in this font will normally denote a matrix.
$\mathcal{A}$, $\mathfrak{A}$	A capital letter in one of these fonts will normally denote an operator which acts on an infinite dimensional space.
$\mathcal{A}^*$	The adjoint of the linear operator $\mathcal{A}$; see definition 2.4.2
$\mathcal{I}$	The identity operator.
$\mathcal{R}(\lambda; \mathcal{A})$	The resolvent operator; see definition 2.1.2.
$\mathrm{cl}(E)$	The closure of a set E.
$\mathrm{Re}(z)$	The real part of the complex number z. The imaginary part of z is denoted $\mathrm{Im}(z)$.
$\|\cdot\|$	A norm. It will usually be accompanied by a subscript to denote the norm over a certain space. If not accompanied by a subscript, then it is the operator norm unless otherwise specified.
$\tilde{\Delta}$	The Fourier transform of the Laplacian in the x and z directions: $\tilde{\Delta} = \frac{\partial^2}{\partial y^2} - k_x^2 - k_z^2$.
$\vec{v} \cdot \nabla$	The nonlinear operator in the Navier-Stokes equations: $\vec{v} \cdot \nabla = v_1 \frac{\partial}{\partial x} + v_2 \frac{\partial}{\partial y} + v_3 \frac{\partial}{\partial z}$.
$A := B$	A is defined by expression B. Similarly, $A =: B$ means expression A defines B.

f_x	All subscripts indicate partial derivatives, e.g., $f_x = \frac{\partial f}{\partial x}$.
$H^m(\Omega)$	The Hilbert space of all functions in $L^2(\Omega)$ whose generalized partial derivatives up to the m^{th} order back are all in $L^2(\Omega)$. See section 1.2.1.
$H_0^m(\Omega)$	The closure of the infinitely smooth functions with compact support in Ω in the H^m norm. See section 1.2.1.
$L^2(\Omega)$	The Hilbert space of all Lebesgue measurable functions f such that $\int_\Omega \lvert f\rvert^2 < \infty$. It is usually accompanied by the inner product $\langle f, g\rangle = \int_\Omega fg$.
R	The Reynolds number of a flow (or a mock Reynolds number for a model problem).

Chapter 1

Introduction

One of the most longstanding problems in fluid dynamics is to predict when a flow will transition from laminar to turbulent. This problem has been investigated experimentally, numerically and analytically for well over a century. Some of the pioneering research in this area was done by Osborne Reynolds in the 1880's [49]. Reynolds experimentally studied water flow through a pipe and noticed that the flow became turbulent when a parameter exceeded a certain value. This parameter, now called the Reynolds number, depends only on the dimensions of the pipe, the mean velocity of the flow and the kinematic viscosity of the fluid. However, Reynolds also noticed that the transition was very sensitive to small disturbances in the fluid.

Reynolds' original experiments showed the value of the critical Reynolds number at which transition invariably occurred to be approximately 13000. Later experiments by many different researchers all confirm that transition occurred when the Reynolds number increased past a certain critical value. However, these experiments predicted a wide range of critical Reynolds numbers from anywhere between 2000 to up to 100000 in the most carefully controlled experiments. It is not surprising then that researchers agree that transition is extremely sensitive to small disturbances.

Despite this range of values for the critical Reynolds number for pipe flow, many modern experiments yield a critical value of about 2200. This same phenomenon is also seen in many other types of flow. Various experiments give a wide range of possible values for the critical Reynolds number. However most experimentalists accept a critical value within a certain range. In Poiseuille flow for example, the accepted critical Reynolds number is about 1000, although certain experiments have yielded much higher values.

Of course, the critical Reynolds number for various flows has not only been estimated experimentally but also numerically and analytically. This approach to the problem of predicting transition has traditionally entailed linear stability analysis. The governing equations of motion, the incompressible Navier-Stokes equations, are linearized about the laminar flow and an eigenvalue analysis is performed. When the real part of an eigenvalue crosses into the right half plane, the laminar flow is unstable and the linear analysis implies that transition to turbulence is possible. However, as has been known for quite some time, the predictions of

the critical Reynolds number using linear stability analysis fail to match the accepted values in many types of fluid flow. For example, using numerical approximations Orszag produced approximately 5772 as the critical Reynolds number for Poiseuille flow [104], while as mentioned above the accepted experimental value is about 1000. For Couette and pipe flow the situation is even worse. Linear stability analysis predicts that these flows will never become unstable ([119], [68], and [120], [69], respectively), while accepted experimental values are given by approximately 360 and 2200, respectively.

Remark: It is important to note here that much of the linear stability analysis discussed above was not applied directly to the Navier-Stokes equations. For example, for channel flows such as Poiseuille flow, researchers often transform the linearized Navier-Stokes equations and then study the eigenvalues of the transformed problem. This process leads to the Orr-Sommerfeld equations. However, if the transformation is not valid, then it is possible that the spectrum of the Orr-Sommerfeld operator does not coincide with the spectrum of the linearized Navier-Stokes operator. This could be one possible cause for the failure of the linear stability analysis to predict transition. However, the validity of the transformation is seldom questioned in the literature.

The failure of classical eigenvalue analysis to accurately predict transition led to other nonlinear stability theories. These methods have had limited success (see [49]). However, during the past 25 years many researchers have begun to use non-classical linear stability techniques to attack the problem of transition. These methods have produced new insights into the transition process and have generated two new "*mostly linear*" theories on the mechanism of transition. First, it was discovered that certain small perturbations to the laminar flow can cause an extremely large transient energy growth in the linearized system before the flow relaminarizes. This transient energy growth in the linear system can be studied using the resolvent operator or, equivalently, the pseudospectra. It has been suggested that when the transient growth becomes "sufficiently large", then the flow is "mixed" by the nonlinearity, producing turbulence. Another new approach to transition uses ideas from robust control theory to study the effects of small forcing terms on the linear system. Because of the non-normality of the linear term, energy could be greatly amplified due to the small forcing term. The conservative nonlinearity is again thought to "mix" the energy leading to transition. As noted above, energy amplification in the linear system is possible because the linear operator $\mathcal{A}$ is non-normal, i.e., $\mathcal{A}\mathcal{A}^* \neq \mathcal{A}^*\mathcal{A}$ where $\mathcal{A}^*$ is the adjoint operator. This will be discussed in more detail in the following sections.

These new mostly linear theories have not yet provided a complete theory explaining the role that the nonlinearity plays in the transition process. This is due to the fact that the theories are primarily concerned with energy growth and the nonlinearity in the Navier-Stokes equations conserves energy. It is the non-normality of the linear term that causes the great increase in energy and therefore much of the work has focused on the linearized system. **The main goal of this work is to begin to provide an understanding of the role that the nonlinearity plays in the transition process.** We will not abandon the non-classical linear theories on transition. In fact, by examining the nonlinearity we hope to provide a basis for completing these mostly linear theories.

In particular, we focus on model problems that have the same mathematical structure as the Navier-Stokes equations and investigate the effects of small disturbances on the dynamics of such systems. Our work on these model problems can be classified into two categories. First, if the small disturbances enter the equations as (roughly) a small forcing function, the disturbed system can experience bifurcations of equilibria which would otherwise have not occurred without the disturbances. This can cause an equilibrium to move an order of magnitude or disappear entirely and requires an analysis of bifurcation under uncertainty. Second, if the small disturbances enter the equations as "unmodeled terms" in the linear and nonlinear terms, the model uncertainty can cause an equilibrium to become unstable and even cause new equilibria to appear.

We also use the continuous sensitivity equation method to study the dynamics of perturbed model problems. In this case, the solution to the disturbed problem is assumed to depend on a small disturbance parameter ε. Taking the derivative of the solution with respect to ε and setting $\varepsilon = 0$ provides a measure of the sensitivity of the solution with respect to a small disturbance. Solving for this sensitivity is equivalent to solving a linear equation and hence is often feasible even for complex nonlinear systems. For the model problems in this thesis, we show that the sensitivities yield important information about the disturbed problem. Therefore, the sensitivity equation method is quite useful in studying transition in flow systems.

Finally, motivated by flow control applications, we consider the problem of using linear feedback to control a flow system. We use the model problems to illustrate how linear feedback can drastically reduce the sensitivity of solutions with respect to small disturbances in the equations. This effort can be considered as a first step in illustrating how linear feedback might be used to delay transition and even relaminarize fully developed turbulent flow.

1.1 Outline of Thesis

In the remainder of this introduction, we present an abstract formulation of the Navier-Stokes equations and review what is known about existence and uniqueness of solutions to both the time dependent and steady problems. The steady problem will provide motivation for small disturbances possibly causing bifurcation of equilibria in flow problems. Again, we will see that bifurcation under uncertainty has the potential to be the trigger for transition to turbulence.

In chapter 2, we review classical spectral theory and indicate how it may be applied to study the stability of equilibrium states in both finite and infinite dimensional problems. This has been the most popular method of predicting transition in flow problems and hence we review the known results concerning the Navier-Stokes and Orr-Sommerfeld equations. We also discuss two recent nonclassical (mostly linear) approaches to stability analysis that have led to two new transition scenarios. Although these theories are incomplete, they provide motivation for the study of the effects of small disturbances on the dynamics of nonlinear systems.

Chapter 3 will focus on the one dimensional Burgers' equation over a finite interval. This partial differential equation will serve both as a motivating example and a test case for many of the ideas presented in this thesis. As with the Navier-Stokes equations, an abstract formulation of the problem will be presented and small disturbances will be added to the model. We then review the existence and uniqueness theory for solutions. The equilibrium problem and the long time behavior of solutions will be used to illustrate how small disturbances can be an essential part of the transition problem.

Chapter 4 focuses on the continuous sensitivity equation method (CSEM) for computing sensitivities. We use this method to predict the effects of small disturbances on solutions of differential equations. The ideas are first illustrated on low order ODE model problems. A one dimensional Burgers' equation will be used to show how the method can be rigorously extended to infinite dimensional systems. We also use the CSEM to explore the effects of a simplified form of wall roughness on solutions of a two dimensional Burgers' equation.

Chapter 5 contains numerical results for the finite and infinite dimensional model problems considered in the previous sections. We begin with the one dimensional Burgers' equation and demonstrate how a small disturbance can move an equilibrium state by an order of magnitude. This causes solutions to the time dependent problem to transition to an order one steady state. The CSEM is used to show that sensitivities can be used to predict important information about the solution of the disturbed problem. We present a numerically study of the two dimensional Burgers' equation and illustrate how a simplified form of wall roughness perturbs the nonlinear part of the equations. For the ODE model problems, we show how a small disturbance can cause an asymptotically stable "laminar flow" state to cease to be an equilibrium. Any flow beginning near this state will then transition. Finally, we apply linear feedback control to these model ODE systems. An LQR controller is used to demonstrate how a linear control can be used to suppress the sensitivity of solutions with respect to small disturbances and delay transition.

In the conclusion we summarize the contributions of this thesis and comment on open problems and future directions for research.

1.2 The Navier-Stokes Equations

In this section, we review the incompressible Navier-Stokes equations which are widely accepted as the standard model for fluid flow. Specifically, we formulate the equations as an abstract differential equation and discuss the existence and uniqueness theory for solutions.

The incompressible Navier-Stokes (NS) equations are given by

$$\frac{\partial \vec{v}}{\partial t} + (\vec{v} \cdot \nabla)\, \vec{v} = -\nabla p + \frac{1}{R}\nabla^2 \vec{v} + f \tag{1.1}$$

$$\nabla \cdot \vec{v} = 0, \tag{1.2}$$

where $\vec{v} = [u(t,\vec{x}), v(t,\vec{x}), w(t,\vec{x})]^T$ is the velocity vector, $p = p(t,\vec{x})$ is the pressure, $f = f(t,\vec{x})$ is a forcing function and R is the Reynolds number. The equations are defined on an

open domain Ω in $\mathbb{R}^n$, where $n = 2$ or 3. On the boundary of Ω, denoted by $\partial\Omega$, we specify zero Dirichlet boundary conditions (the so called no slip condition)

$$\vec{v} = \vec{0}, \quad \vec{x} \in \partial\Omega. \tag{1.3}$$

In the case of an unbounded domain, other boundary conditions are applied. For example, it is common to specify that the flow approaches a given flow in the far field, i.e.,

$$\lim_{\|\vec{x}\|\to\infty} \vec{v} = \vec{v}_\infty. \tag{1.4}$$

We also prescribe the initial flow velocity

$$\vec{v}(0,\vec{x}) = \vec{v}_0(\vec{x}), \quad \vec{x} \in \Omega. \tag{1.5}$$

The equations (1.1)-(1.5) fully describe the flow problem.

Linearization is concerned with the velocity and pressure fluctuations around a base flow $\vec{U}$ and a base pressure state P that solve the Navier-Stokes equations (1.1)-(1.5). Define the velocity and pressure fluctuations, $\vec{u}$ and q, by $\vec{v} = \vec{U} + \vec{u}$ and $p = P + q$. Substituting these equations into the NS equations yields

$$\begin{aligned}
\frac{\partial\vec{u}}{\partial t} + (\vec{u}\cdot\nabla)\,\vec{u} &= -\nabla q + \frac{1}{R}\nabla^2\vec{u} + \left(\vec{U}\cdot\nabla\right)\vec{u} + (\vec{u}\cdot\nabla)\,\vec{U}, \quad \vec{x}\in\Omega && (1.6)\\
\nabla\cdot\vec{u} &= 0, \quad \vec{x}\in\Omega && (1.7)\\
\vec{u} &= \vec{0}, \quad \vec{x}\in\partial\Omega && (1.8)\\
\lim_{\|\vec{x}\|\to\infty} \vec{u} &= \vec{0} && (1.9)\\
\vec{u}(0,\vec{x}) &= \vec{u}_0(\vec{x}) := \vec{v}_0(\vec{x}) - \vec{U}(0,\vec{x}), \quad \vec{x}\in\Omega. && (1.10)
\end{aligned}$$

Throughout this thesis, equations (1.6)-(1.10) will be referred to as the fluctuation Navier-Stokes equations.

In the remainder of this section, we use the standard abstract state space formulation in order to describe properties of the equations and their solutions.

1.2.1 Abstract Formulation

In order to provide a framework to discuss the basic properties of the Navier-Stokes equations and the existence and uniqueness theory for solutions, it is beneficial to place the equations into an abstract state space formulation. The following derivation may be found in several standard references (see [43], [85], [128], [134], [135], [136]) and hence we omit many details.

First, we introduce the standard L^p and H^m function spaces. To simplify notation, we drop the vector notation ($\vec{}$) unless additional clarity is needed. For $1 < p < \infty$, let $L^p(\Omega)^n$

denote the Banach space of functions $f : \Omega \to \mathbb{R}^n$ such that the norm

$$\|f\|_{L^p} = \left(\int_\Omega \|f\|_{\mathbb{R}^n}^p \, dx \right)^{1/p}$$

is finite. Also, $L^\infty(\Omega)^n$ is the Banach space of all functions with finite norm

$$\|f\|_{L^\infty} = \operatorname*{ess\,sup}_{x \in \Omega} \|f\|_{\mathbb{R}^n}.$$

The space $L^2(\Omega)^n$ is a Hilbert space with inner product

$$\langle f, g \rangle_{L^2} = \int_\Omega f \cdot g \, dx$$

and corresponding norm $\|f\|_{L^2}^2 = \langle f, f \rangle_{L^2}$. Let $H^m(\Omega)^n$ be the set of all functions $f : \Omega \to \mathbb{R}^n$ whose generalized partial derivatives up to order m are all square integrable. For a multi-index $\alpha = (\alpha_1, \ldots, \alpha_n)$, let $[\alpha] = \alpha_1 + \cdots + \alpha_n$ and define the differentiation operator D^α by

$$D^\alpha = \frac{\partial^{[\alpha]}}{\partial x_1^{\alpha_1} \cdots \partial x_n^{\alpha_n}}.$$

Then $H^m(\Omega)^n$ is a Hilbert space with inner product

$$\langle f, g \rangle_{H^m} = \sum_{[\alpha] \leq m} \langle D^\alpha f, D^\alpha g \rangle_{L^2}$$

and corresponding norm. Let $C_0^\infty(\Omega)^n$ be the space of all infinitely smooth functions mapping Ω to $\mathbb{R}^n$ with compact support in Ω. The space $H_0^m(\Omega)^n$ is the closure of $C_0^\infty(\Omega)^n$ in the H^m norm.

With the standard function spaces defined, we introduce divergence free function spaces which play an important role for the abstract formulation of the Navier-Stokes equations. In particular, these spaces allow us to eliminate the pressure from the state space formulation. Let $X = L^2(\Omega)^n$ and define $\mathbf{D}(\Omega)$ to be the closure of all functions $f \in C_0^\infty(\Omega)^n$ that are divergence free, i.e., $\nabla \cdot f = 0$. Then $\mathbf{H}(\Omega)$ and $\mathbf{V}(\Omega)$ are defined as the closure of $\mathbf{D}(\Omega)$ in $L^2(\Omega)^n$ and in $H_0^1(\Omega)^n$, respectively. These spaces can be explicitly characterized by

$$\mathbf{H}(\Omega) = \{ u \in X \, : \, \nabla \cdot u = 0, \; u \cdot n = 0 \text{ on } \partial\Omega, \text{where } n \text{ is the outward normal to } \Omega \}$$

and

$$\mathbf{V}(\Omega) = \left\{ u \in H_0^1(\Omega)^n \, : \, \nabla \cdot u = 0 \right\}.$$

Define a scalar product on $\mathbf{V}(\Omega)$ by

$$\langle u, v \rangle_{\mathbf{V}(\Omega)} = \sum_{j=1}^n \langle \nabla u_j, \nabla v_j \rangle_X$$

If the domain Ω is bounded in at least one direction, then the Poincaré inequality (see, e.g., [101, Theorem 3.5.9]) guarantees that the scalar product is actually an inner product on $\mathbf{V}(\Omega)$. This inner product on $\mathbf{V}(\Omega)$ generates the norm $\|f\|^2_{\mathbf{V}(\Omega)} = \langle f, f\rangle_{\mathbf{V}(\Omega)}$ which is equivalent to the H^1 norm defined above.

The space $\mathbf{V}(\Omega)$ allows one to define weak velocity solutions of the Navier-Stokes equations since functions in $\mathbf{V}(\Omega)$ automatically satisfy the divergence free condition (1.2), the no slip boundary conditions (1.3) and are once differentiable. We now derive the weak form of the Navier-Stokes equations (1.1)-(1.5). In the following, we assume that for an unbounded domain the flow approaches zero in the far field (see (1.4)). Multiplying the equations of motion (1.1) by a test function $v \in \mathbf{V}(\Omega)$, integrating over the domain Ω and integrating by parts (by the divergence theorem) eliminates the pressure and yields

$$\frac{\partial}{\partial t}\langle u, v\rangle_X + b(u, u, v) = -\frac{1}{R}\langle u, v\rangle_{\mathbf{V}(\Omega)} + \langle f, v\rangle_X ,$$

where the trilinear form $b(\cdot,\cdot,\cdot)$ is given by

$$b(u, v, w) = \sum_{i,j=1}^{n} \int_\Omega u_i \frac{\partial v_i}{\partial x_j} w_j \, dx. \tag{1.11}$$

The weak form for the fluctuation NS equations (1.6)-(1.10) is obtained in the same way as

$$\frac{\partial}{\partial t}\langle u, v\rangle_X + b(u, u, v) = -\frac{1}{R}\langle u, v\rangle_{\mathbf{V}(\Omega)} + b(U, u, v) + b(u, U, v).$$

These equations are accompanied by the initial conditions (1.5) and (1.10), respectively.

The weak form above can now be recast as an abstract differential equation on $\mathbf{V}(\Omega)'$. Recall that the dual space of a space Y, denoted Y', is the set of all bounded linear functionals acting on that space (see [82]). The dual space Y' is always a Banach space with the operator norm

$$\|f\|_{Y'} = \sup\{\, |f(y)| \,:\, y \in Y, \|y\|_Y = 1\},$$

where $|f(y)|$ is the absolute value of the real (or, more generally, complex) number $f(y)$. If Y is a Hilbert space, then Y may be identified with its dual (denoted $Y \cong Y'$) via the Riesz Representation Theorem. The dual space of H^1_0 is denoted H^{-1}. For the NS system, the following inclusions

$$\mathbf{V}(\Omega) \subset \mathbf{H}(\Omega) \cong \mathbf{H}(\Omega)' \subset \mathbf{V}(\Omega)',$$

are continuous and each space is dense in the next. Define the linear operator $\mathcal{A} : \mathbf{V}(\Omega) \to \mathbf{V}(\Omega)'$ which takes a velocity field in $\mathbf{V}(\Omega)$ and maps it to a bounded linear functional on $\mathbf{V}(\Omega)$ by

$$[\mathcal{A}u]\, v = -\frac{1}{R}\langle u, v\rangle_{\mathbf{V}(\Omega)} .$$

We also require an abstract formulation of the linear operator involving the base velocity field U and an abstract formulation of the nonlinear operator. Therefore, define the linear

operator $\mathcal{R} : \mathbf{V}(\Omega) \to \mathbf{V}(\Omega)'$ as $[\mathcal{R}u]\, v = b(U, u, v) + b(u, U, v)$ and the nonlinear operator $\mathcal{F} : \mathbf{V}(\Omega) \to \mathbf{V}(\Omega)'$ as $[\mathcal{F}(u)]\, v = -b(u, u, v)$.

The Navier-Stokes system (1.1)-(1.5) can now be written as the abstract differential equation on $\mathbf{V}(\Omega)'$ given by

$$u_t(t) = \mathcal{A}u(t) + \mathcal{F}(u(t)) + f, \tag{1.12}$$
$$u(0) = u_0 \in \mathbf{H}(\Omega), \tag{1.13}$$

where $f \in \mathbf{V}(\Omega)'$. Similarly, the fluctuation NS equations (1.6)-(1.10) can be written as the system

$$u_t(t) = (\mathcal{A} + \mathcal{R})u(t) + \mathcal{F}(u(t)), \tag{1.14}$$
$$u(0) = u_0 \in \mathbf{H}(\Omega). \tag{1.15}$$

These state space formulations provide rigorous mathematical frameworks to study properties of the equations and their solutions. In particular, these formulations are central to the study of stability and transition to turbulence.

During the remainder of this chapter, we let H stand for $\mathbf{H}(\Omega)$ and V for $\mathbf{V}(\Omega)$. Unless otherwise indicated H and V are divergent free vector fields.

1.2.2 Existence and Uniqueness of Solutions

One reason to formulate the Navier-Stokes equations as an abstract differential equation is so that one can apply the rigorous techniques of functional analysis to study existence, uniqueness and regularity of solutions as well as the existence of absorbing sets and attractors. In particular, the above framework falls into the class of systems covered by the general theory of Ghidaglia and Temam (see [135]). We will not go into details of their theory here, but note that in order to apply this theory one only needs to obtain bounds for certain expressions involving the operators $\mathcal{A}$ and $\mathcal{R}$ and the trilinear form $b(\cdot, \cdot, \cdot)$. A crucial assumption in this theory is that the nonlinearity is conservative in the sense that

$$b(v, v, v) = 0, \quad \text{for all } v \text{ in } V.$$

It is well known that the nonlinearity in the Navier-Stokes equations accompanied by either zero Dirichlet boundary conditions (including in the far field for unbounded domains) or periodic boundary conditions is conservative in this sense.

This general framework is sufficient to prove the existence and uniqueness of solutions for all time to the Navier-Stokes equations for two dimensional domains. However in three dimensions the theory is inadequate and one can only prove the uniqueness of solutions under certain restricted conditions. Proving the existence and uniqueness of solutions in three dimensions is an important open problem. In what follows, we briefly outline the main results for existence and uniqueness of solutions in two and three dimensions for both bounded and unbounded domains.

We assume the following conditions on the data for the Navier-Stokes and fluctuation NS problems:

(A1) The domain Ω is open in $\mathbb{R}^n$, where $n = 2$ or 3, and is bounded in at least one direction with Lipschitz boundary.

(A2) $f \in V'$ and is independent of time.

(A3) The initial condition $u(0) = u_0 \in H$.

(A4) $\lim_{\|x\|\to\infty} u = 0$ for unbounded domains.

Many of these statements can be weakened (see [43], [85], [109], [128], [134], [136]). However we focus on the cases covered by (A1)-(A4).

The weak formulations of the Navier-Stokes problem deals with functions of time with values in a dual space. Therefore, if Y is a general Banach space, define the Banach spaces $L^p(0,T;Y)$ to be the space of all measurable functions $f : (0,T) \to Y$ such that the norm defined by

$$\|f\|_{L^p(0,T;Y)} = \left(\int_0^T \|f(t)\|_Y^2 \, dt\right)^{1/p}$$

is finite. The space $L^2(0,T;Y)$ is also a Hilbert space. Similarly, define the Banach space $L^\infty(0,T;Y)$ to be the space of all measurable functions $f : (0,T) \to Y$ with finite norm

$$\|f\|_{L^\infty(0,T;Y)} = \operatorname*{ess\,sup}_{t\in[0,T]} \|f(t)\|_Y .$$

Finally, let $C(0,T;Y)$ be the space of all continuous functions $f : (0,T) \to Y$ with finite norm

$$\|f\|_{C(0,T;Y)} = \sup_{t\in[0,T]} \|f(t)\|_Y .$$

We now state the basic existence result for both bounded and unbounded domains in two or three dimensions [136, Theorem 3.1].

Theorem 1.2.1 *Suppose $n = 2$ or 3 and the assumptions (A1)-(A4) hold. For every $T > 0$, there exists at least one function u which satisfies the weak formulation of the Navier-Stokes equations (1.12) on the time interval $(0,T)$. Specifically, $u \in L^2(0,T;V) \cap L^\infty(0,T;H)$.*

As we indicated above, in two dimensions this solution is actually unique and is continuous in time (see [135, Theorems 2.1 and 8.1], [136, Theorem 3.2]).

Theorem 1.2.2 *If (A1)-(A4) hold and $n = 2$, the solution u of the weak formulation of the Navier-Stokes equations is unique. Furthermore, $u \in C(0,T;H)$.*

A similar existence and uniqueness theorem holds for the fluctuation NS equations (1.14) in two dimensions [128].

If $n = 3$, it is not known if weak solutions are unique. However, there are certain instances where specific results do exist and these results often depend on restrictions that require small problem data. For example, in [136] Temam defines a constant $d = d(f, u_0)$ by

$$d(f, u_0) := \|f\|_{L^2} + \frac{c_0}{R}\|u_0\|_{H^2} + c_1\|u_0\|_{H^2}^2,$$

and proves existence and uniqueness when an expression involving d is "small". Here, R is the Reynolds number and c_0 and c_1 are specific positive constants (see [136, Theorem 3.7] for the complete details). In particular, Temam proves the following uniqueness result [136, Theorem 3.7].

Theorem 1.2.3 *Assume the domain $\Omega \subset \mathbb{R}^3$ is bounded and the initial condition u_0 and the forcing function f satisfy $u_0 \in V \cap H^2(\Omega)^3$ and $f \in H$, respectively. If (A1)-(A4) hold, then the solution u of the weak formulation of the Navier-Stokes equations is unique provided that the data f and u_0 satisfy the bound*

$$R\|f\|_{V'} + \left(1 + d(f, u_0)^2\right)\left(\|u_0\|_X^2 + RT\|f\|_{V'}\right)^{1/2} < c^{-2}R^{-3},$$

where R is the Reynolds number, T is the final time and the constants c and d are defined in [136, Theorem 3.7].

If the Reynolds number or the time interval $(0, T)$ is large, then this theorem only guarantees uniqueness in the three dimensional case if the problem data (f and u_0) is truly small. A similar uniqueness result again holds for the fluctuation Navier-Stokes equations [128].

Another restriction on the three dimensional problem that guarantees uniqueness is not to restrict the data, but instead to restrict the "thickness" of the domain Ω. Let Ω be a bounded domain in $\mathbb{R}^2$ and define $\Omega_\varepsilon = \Omega \times (0, \varepsilon)$. Raugel and Sell [111] first considered the three dimensional Navier-Stokes equations on this thin domain with periodic and other boundary conditions and proved global uniqueness of solutions for small ε even when the problem data, f and u_0, is large. Other researchers have improved and extended their results (see [72] for a short review). Avrin [4] also showed that the thin domain restriction is a special case of another assumption that yields uniqueness for the Dirichlet problem on a general bounded three dimensional domain. Let λ_1 be the smallest eigenvalue of the operator $-\nabla^2$ with domain $[H^2(\Omega) \cap H_0^1(\Omega)]^3 \subset L^2(\Omega)^n$. Avrin showed that if λ_1 is large enough, then the Navier-Stokes equations admit unique solutions.

We emphasize that the results presented here only comprise a brief summary of the main theory concerning solutions of the time dependent Navier-Stokes equations. For additional results concerning the long time behavior and regularity of solutions among other topics, see the references [43], [85], [128], [134], [136]. Even though the theory is incomplete in three dimensions, the Navier-Stokes equations are still the basis for most standard mathematical models for fluid flows.

1.2.3 The Equilibria Problem

Here we consider the steady state problem for the Navier-Stokes equations given by

$$\begin{aligned}(\vec{v}\cdot\nabla)\,\vec{v} &= -\nabla p + \frac{1}{R}\nabla^2\vec{v} + f, \quad \vec{x}\in\Omega,\\ \nabla\cdot\vec{v} &= 0, \quad \vec{x}\in\Omega,\\ \vec{v} &= \vec{0}, \quad \vec{x}\in\partial\Omega,\\ \lim_{\|\vec{x}\|\to\infty}\vec{v} &= \vec{0},\end{aligned}$$

where R is the Reynolds number. The steady problem can be formulated as the abstract nonlinear algebraic problem on the dual space V' given by

$$\mathcal{A}u + \mathcal{F}(u) + f = 0, \tag{1.16}$$

where $f\in V'$ and the operators $\mathcal{A}$ and $\mathcal{F}$ both map V to V' and are defined by

$$[\mathcal{A}u]\,v = -\frac{1}{R}\langle u, v\rangle_V, \quad \text{and} \quad [\mathcal{F}(u)]\,v = -b(u,u,v) = -\sum_{i,j=1}^{n}\int_\Omega u_i\frac{\partial u_i}{\partial x_j}v_j\,dx.$$

The main existence and uniqueness theory for the equilibrium problem is summarized below. A more extensive treatment may be found in [58] and in the references given above for the time dependent problem.

It is known that there exists at least one solution to the steady problem for both two and three dimensional bounded domains [136, Theorem 1.2].

Theorem 1.2.4 *Let $\Omega\in\mathbb{R}^n$ be bounded for $n=2$ or 3. If $f\in H^{-1}(\Omega)^n$, then there exists at least one solution $u\in V$ to the steady weak Navier-Stokes equations (1.16).*

A similar result holds for unbounded domains with some slight modifications in the functional framework [136, Theorem 1.4]. In order to obtain the uniqueness of steady solutions the problem can again be restricted. In particular, for bounded domains one can restrict the size of the problem data to obtain a unique solution [136, Theorem 1.3].

Theorem 1.2.5 *Let $\Omega\in\mathbb{R}^n$ be bounded for $n=2$ or 3. If $f\in H^{-1}(\Omega)^n$ satisfies the bound*

$$\|f\|_{V'} < C^{-1}R^{-2},$$

then there exists a unique solution $u\in V$ to the steady weak Navier-Stokes equations (1.16). Here, C is any constant satisfying $\|b(u,v,w)\|_X \le C\,\|u\|_{H^1}\|v\|_{H^1}\|w\|_{H^1}$ for all $u,v,w\in V$.

Again, if the Reynolds number R is large, the above theorem only guarantees the uniqueness of solutions to the steady problem if the forcing function f is small.

For non-homogeneous Dirichlet boundary conditions (corresponding to, say, moving walls), uniqueness of solutions can again be guaranteed by restricting the size of the forcing function and also the boundary conditions [136, Theorem 1.6]. Again, these bound depends on

the inverse of the Reynolds number. When the data does not satisfy this bound, there are certain cases where the uniqueness of solutions is known to break down (see [136, Section 4.1]). This observation can have implications for transition to turbulence.

1.3 Possible Connections Between Bifurcation Under Uncertainty and Transition

Consider the Navier-Stokes equations (1.1)-(1.5) and let the base flow U and base pressure state P satisfy the NS equations. Suppose for simplicity that U and P do not depend on time, i.e., they are equilibrium states. The velocity flow U is then a solution to the weak steady NS equations. Furthermore, in the absence of forcing (i.e., $f = 0$) the above theorem implies that in a bounded domain U is the only equilibrium solution. We shall see in chapter 2 that if U is a stable equilibrium, then for a smooth initial condition near to U the time dependent flow will remain near the base flow U for all time (see Theorem 2.2.3 and Section 2.3 below). Therefore, in this case, "perfect" laboratory conditions should produce a stable flow.

However, laboratory conditions are never ideal and one must assume that some small disturbance enters the system or that equipment imperfections such as wall roughness are always present. This disturbance is an "uncertainty" in the system that is not modeled by the standard Navier-Stokes equations. In order to account for this uncertainty, one can include additional terms in the model or adjust the equations and boundary conditions. For example, one might add a "small" forcing function f to the equations. We assumed above that U was an equilibrium for the NS equations when $f = 0$. With the addition of a nonzero forcing term f, U is no longer an equilibrium state for the disturbed problem. However, Theorem 1.2.4 guarantees the existence of another equilibrium state, but it is not known whether the small perturbation to the NS equations has caused a small movement in the equilibrium state. Also, if the Reynolds number is large, then the above theorem implies that equilibrium for the disturbed problem (i.e., with f small but nonzero) may no longer be unique. It is therefore possible that a small imperfection in a laboratory experiment can cause movement or *bifurcation* in the Navier-Stokes system. An initial flow near the supposed stable flow U may not relaminarize since U is no longer an equilibrium and this could lead to transition and turbulence. In this case, classical stability analysis might fail.

This "bifurcation under uncertainty" scenario could explain the sometimes drastic differences in experimental predictions of critical Reynolds numbers for various flows. We noted above that in the case of pipe flow, experiments have predicted critical values in the range between 2000 and 100000. It is possible that the theoretical predictions of the critical Reynolds number using linear stability analysis of the Orr-Sommerfeld equation actually give the true critical values for an idealized (i.e., completely undisturbed) flow system. As we illustrate below, small imperfections in actual experiments may cause extreme changes in the value of the critical Reynolds number.

As noted above, the theory concerning solutions of the Navier-Stokes equations in three

dimensions is incomplete. Therefore, we focus on low order finite dimensional models and less complex partial differential equation that share similarities with the Navier-Stokes system. We use these model problems to illustrate the basic ideas and to demonstrate how specific unmodeled disturbances may be an important piece of the transition process. Sensitivity methods will be used to demonstrate that one can quantify these ideas and to illustrate that it is possible to have a precursor to predict transition. Also, we apply linear feedback to the model problems to illustrate the power of feedback to delay transition and even relaminarize fully developed chaotic flows.

Chapter 2

Classical and Nonclassical Stability Analysis of the Navier-Stokes Equations

We begin with a brief review of both classical and nonclassical hydrodynamic stability theory. As noted above, stability analysis has been one of the main analytical tools used over the years to investigate transition to turbulence in fluid flow. Almost all of the transition scenarios involve linearizing about an equilibrium (laminar flow) and analyzing the stability of the linearized system for various values of the Reynolds number. The basic idea is that at a critical Reynolds number, the laminar flow becomes unstable and nearby flows "transition" to another attracting set (equilibrium state, periodic orbit or chaotic attractor). However, this scenario fails when the laminar flow is stable for all values of the Reynolds number (such as for Couette flow). Also, even when the linearized equations become unstable, this method has failed to predict the critical values of the Reynolds number usually observed in experiments. Recently, new approaches to linear stability analysis have been developed in an attempt to close this gap. However, much of this work is still based on an analysis of the linearized system and is often incomplete.

In this chapter, we review the classical spectral approach and two nonclassical approaches to stability analysis with an emphasis on their applications to the Navier-Stokes equations. The review will begin with a survey of spectral approaches to stability analysis for linear systems in finite and infinite dimensions. We also discuss how the stability theory for the finite dimensional case does not generally extend to infinite dimensions. Here, we concentrate on spectral approaches for stability analysis although there is a body of work based on Lyapunov and energy methods. However, many of the papers that apply Lyapunov and energy methods to flow equations use a formal analysis and do not address the technical requirements that are essential to a rigorous application of the theory to infinite dimensional systems.

After presenting the short survey of the classical spectral stability methods, we review how these ideas have been applied to the Navier-Stokes. We present results concerning the

spectrum of the linearized Navier-Stokes operator and other approximations such as the Orr-Sommerfeld equations. We then turn to two new linear methods that have had some success in describing the transition problem.

We begin with precise definitions of stability for finite dimensional dynamical systems. Consider an autonomous initial value problem (IVP) over $\mathbb{R}^n$ of the form

$$\dot{x}(t) = f(x(t)) \quad \text{for } t > 0, \quad x(0) = x_0. \tag{2.1}$$

Here, $x(t)$ is a vector in $\mathbb{R}^n$ for each $t \geq 0$, f is a function mapping $\mathbb{R}^n$ to $\mathbb{R}^n$ and the dot denotes differentiation with respect to t.

Definition 2.0.1 *Consider the initial value problem (2.1) with solution $x(t)$ and initial state x_0 and let $\|\cdot\|$ be any norm on $\mathbb{R}^n$. A state $x_e \in \mathbb{R}^n$ is an **equilibrium** of the IVP if $f(x_e) = 0$. This equilibrium is **stable** if for every $\varepsilon > 0$, there exists a $\delta > 0$ such that if $\|x_0 - x_e\| < \delta$, then the solution $x(t)$ exists for all $t > 0$ and satisfies $\|x(t) - x_e\| < \varepsilon$ for all $t > 0$. A stable equilibrium is **asymptotically stable** if in addition $\|x(t) - x_e\| \to 0$ as $t \to \infty$. Furthermore, the equilibrium is **exponentially asymptotically stable** if there exists positive constants M and ω such that $\|x(t) - x_e\| \leq Me^{-\omega t}$ for all $t > 0$. A stability property is **global** if it holds independent of δ. Also, an equilibrium is said to be **unstable** if it is not stable.*

Roughly, an equilibrium is stable if given any initial condition "near the equilibrium", the solution must exist and stay close to the equilibrium for all positive time. The equilibrium is asymptotically stable if the solution also converges to the equilibrium and it is exponentially asymptotically stable if the convergence is exponential. Any norm may be used in the above definition since all norms on finite dimensional spaces are equivalent (see [82]).

Remark: When dealing with PDE systems, one formulates the problem as an ODE over an infinite dimensional space. Although the above definition remains relatively the same, since all norms in infinite dimensional spaces are not equivalent, one must choose a specific norm with which to study stability properties of an equilibrium. In some cases, this specific norm is only defined on a proper subspace V of X. This is not necessarily unnatural since many abstract initial value problems are only known to have globally defined unique solutions when the initial condition is contained in a certain subspace of the state space.

Even if all solutions converge to an equilibrium, then the equilibrium may not be stable. This can be seen from the following example due to Hahn [65, p. 87]. The system of ordinary differential equations are defined by

$$\dot{x}_1 = \begin{cases} \dfrac{x_1^2(x_2 - x_1) + x_2^5}{\|x\|^2 (1 + \|x\|^4)}, & \|x\| \neq 0 \\ 0, & \|x\| = 0 \end{cases}, \quad \dot{x}_2 = \begin{cases} \dfrac{x_2^2(x_2 - 2x_1)}{\|x\|^2 (1 + \|x\|^4)}, & \|x\| \neq 0 \\ 0, & \|x\| = 0 \end{cases},$$

where $\|x\|^2 = x_1^2 + x_2^2$. In this system, $x = 0$ is an equilibrium and solutions converge to the origin. However, the origin is not stable. In particular, for any $\varepsilon > 0$ there are initial conditions arbitrarily near the origin such that the solution grows larger than ε before

returning to the origin. This is not a stable motion since the solution does not remain near the equilibrium state for all positive time.

2.1 Stability Analysis for Linear Systems

Consider the linear autonomous initial value problems

$$\dot{x}(t) = \mathbf{A}x(t) \quad \text{for } t > 0, \qquad x(0) = x_0 \in \mathbb{R}^n, \tag{2.2}$$

$$\dot{x}(t) = \mathcal{A}x(t) \quad \text{for } t > 0, \qquad x(0) = x_0 \in X, \tag{2.3}$$

where the dot denotes differentiation with respect to t. The first equation is defined on $\mathbb{R}^n$ with $\mathbf{A}$ a constant $n \times n$ matrix. The second equation is defined on an infinite dimensional Banach space X with norm $\|\cdot\|_X$ and $\mathcal{A}$ a linear operator mapping its domain $\mathcal{D}(\mathcal{A}) \subset X$ into X. In both cases the zero state is an equilibrium solution. This section is devoted to the study of the long time behavior of solutions to the above linear equations. In particular, we focus on how spectral information from the matrix or linear operator impacts the stability of the zero equilibrium and contrast the results from the finite dimensional case with the infinite dimensional case.

2.1.1 The Finite Dimensional Case

First consider the above ordinary differential equation (2.2). It is well known that the solution of the initial value problem is given by

$$x(t) = e^{\mathbf{A}t}x_0,$$

where the matrix exponential is given by the power series

$$e^{\mathbf{A}t} = \sum_{k=0}^{\infty} \frac{1}{k!}\mathbf{A}^k t^k.$$

The series converges in the operator norm defined by

$$\|\mathbf{A}\| = \sup\left\{ \|\mathbf{A}x\|_{\mathbb{R}^n} \,:\, \|x\|_{\mathbb{R}^n} = 1 \right\}. \tag{2.4}$$

Since the solution is given by the matrix exponential acting on the initial data, the operator norm of the matrix exponential provides a bound on the norm of the solution. In particular, it follows that

$$\|x(t)\|_{\mathbb{R}^n} \leq \| e^{\mathbf{A}t}\| \, \|x_0\|_{\mathbb{R}^n}.$$

Let $\Lambda(\mathbf{A})$ denote the set of the eigenvalues of $\mathbf{A}$. The following result may be found in [102, Theorem 5.5.5].

Theorem 2.1.1 *Consider the linear initial value problem (2.2) and let $\|\cdot\|$ be the operator norm defined in (2.4). If the matrix $\mathbf{A}$ has all of its eigenvalues strictly in the left half plane, i.e., if*

$$\alpha := \max_{\lambda \in \Lambda(\mathbf{A})} \mathrm{Re}(\lambda) < 0, \tag{2.5}$$

then for any ω satisfying $-\alpha > \omega > 0$, there exists a constant $M = M(\omega) \geq 1$ such that the matrix exponential defined above satisfies the bound

$$\| e^{\mathbf{A}t} \| \leq M e^{-\omega t},$$

for all $t \geq 0$. Therefore, the zero equilibrium is globally exponentially asymptotically stable. Furthermore, if $\mathbf{A}$ has at least one eigenvalue with positive real part, then the zero equilibrium is unstable.

In light of this theorem, a matrix will be said to be **stable** if all of its eigenvalues lie in the left half plane, i.e., (2.5) is satisfied. Of course, if the largest eigenvalue of the matrix $\mathbf{A}$ lies on the imaginary axis, this theorem does not provide any information about the stability of the zero state. In this case, one must resort to Lyapunov methods.

2.1.2 The Infinite Dimensional Case: The Unique Solvability of the Linear Initial Value Problem

In the infinite dimensional case, it is not even clear whether the abstract initial value problem (2.3) has a unique solution that exists for all time. In order to address this question, we begin with a review of linear operators, their spectrum and C_0-semigroups. Suppose the linear operator $\mathcal{A}$ maps its domain $\mathcal{D}(\mathcal{A}) \subset X$ into X. Many important operators arising in applications satisfy two basic properties:

1. The space $\mathcal{D}(\mathcal{A})$ is a dense linear subspace of X. In this case, we say that $\mathcal{A}$ is densely defined.

2. The operator $\mathcal{A}$ is **closed**, i.e., for any sequence $\{x_k\} \subset \mathcal{D}(\mathcal{A})$ such that $x_k \to x \in X$ and $\mathcal{A}x_k \to y \in X$, then $x \in \mathcal{D}(\mathcal{A})$ and $\mathcal{A}x = y$.

We will not comment on these properties now except to note that they are essential if one is to define an operator exponential. An operator is **bounded** if there exists a constant $C > 0$ such that $\|\mathcal{A}x\|_X \leq C \|x\|_X$ for any $x \in \mathcal{D}(\mathcal{A})$. If $\mathcal{A}$ is bounded, then define the norm

$$\|\mathcal{A}\| = \sup \{ \|\mathcal{A}x\|_X \, : \, x \in \mathcal{D}(\mathcal{A}), \, \|x\|_X = 1 \}. \tag{2.6}$$

Note that the operator norm changes if the norm on the space X is changed. A bounded operator is necessarily continuous on its domain. Also, if the domain is dense, the operator may be uniquely extended to X. An operator that is not bounded (or equivalently, not continuous) is said to be **unbounded**.

In most practical applications, such as systems governed by partial differential equations, the operator $\mathcal{A}$ is never bounded. In this case, a power series does not make sense and we must define the matrix exponential in a different manner.

Definition 2.1.1 *A family of bounded operators $\{\mathcal{S}(t) : X \to X\}$ for each $t \geq 0$ is called a* **$\mathbf{C_0}$-*semigroup*** *on X if*

1. $\lim_{t\to 0^+} \mathcal{S}(t)x = x$ *for all* $x \in X$,
2. $\mathcal{S}(0) = \mathcal{I}$, *the identity operator on* X,
3. $\mathcal{S}(t+\tau) = \mathcal{S}(t)\mathcal{S}(\tau)$, *for all* $t, \tau \geq 0$.

If $\mathcal{S}(t)$ is a C_0-semigroup, then the ***generator*** *$\mathcal{A}$ of $\mathcal{S}(t)$ is defined on the domain*

$$\mathcal{D}(\mathcal{A}) = \left\{ x \in X \, : \, \lim_{t\to 0^+} \frac{\mathcal{S}(t)x - x}{t} \text{ exists} \right\}$$

by

$$\mathcal{A}x = \lim_{t\to 0^+} \frac{\mathcal{S}(t)x - x}{t}.$$

The generator is simply the (right) strong derivative of the semigroup at $t = 0$ and it is closed and densely defined [105, Corollary 1.2.5]. To show that a semigroup is indeed an generalization of the matrix exponential, we have the following theorem [105, Theorem 1.8.3]).

Theorem 2.1.2 *Let $\mathcal{S}(t)$ be a C_0-semigroup on X with generator $\mathcal{A}$ as defined above. If $x \in X$, then*

$$\mathcal{S}(t)x = \lim_{n\to\infty} \left(\mathcal{I} - \frac{t}{n}\mathcal{A} \right)^{-n} x.$$

If $\mathcal{A}$ generates a C_0-semigroup, then we define an operator exponential by $e^{\mathcal{A}t} = \mathcal{S}(t)$.

The following theorem may be found in [105, Theorem 1.2.4].

Theorem 2.1.3 *If X is a Banach space and $\mathcal{A} : \mathcal{D}(\mathcal{A}) \subset X \to X$ is the generator of a C_0-semigroup $\mathcal{S}(t)$, then $\mathcal{S}(t)x$ is differentiable for $x \in \mathcal{D}(\mathcal{A})$ and*

$$\frac{d}{dt}\mathcal{S}(t)x = \mathcal{A}\mathcal{S}(t)x.$$

Therefore, if $x_0 \in \mathcal{D}(\mathcal{A})$, the linear initial value problem (2.3) has a solution given by $x(t) = \mathcal{S}(t)x_0$.

The solvability of the initial value problem (2.3) is then reduced to showing that the linear operator $\mathcal{A}$ generates a C_0-semigroup. If $x_0 \notin \mathcal{D}(\mathcal{A})$, then $x(t) = \mathcal{S}(t)x_0$ is well defined and is called a **mild solution** of (2.3).

We now define the resolvent and spectrum of a linear operator.

Definition 2.1.2 *A complex number λ is in the **resolvent set**, denoted $\rho(\mathcal{A})$, if the **resolvent operator** $\mathcal{R}(\lambda;\mathcal{A}) := (\lambda\mathcal{I}-\mathcal{A})^{-1}$ exists, is densely defined and is bounded.*

Definition 2.1.3 *The **spectrum** of $\mathcal{A}$, denoted $\Lambda(\mathcal{A})$, is the complement of the resolvent set in the complex plane, i.e., $\Lambda(\mathcal{A}) = \rho(\mathcal{A})^c$. The spectrum can be further classified as follows.*

1. $\Lambda_p(\mathcal{A}) = \{\, \lambda \in \Lambda(\mathcal{A}) \,:\, \lambda\mathcal{I}-\mathcal{A}$ *is not invertible* $\}$
2. $\Lambda_c(\mathcal{A}) = \{\, \lambda \in \Lambda(\mathcal{A}) \,:\, (\lambda\mathcal{I}-\mathcal{A})^{-1}$ *exists but is unbounded* $\}$
3. $\Lambda_r(\mathcal{A}) = \{\, \lambda \in \Lambda(\mathcal{A}) \,:\, (\lambda\mathcal{I}-\mathcal{A})^{-1}$ *is bounded but not densely defined* $\}$

*The sets $\Lambda_p(\mathcal{A})$, $\Lambda_c(\mathcal{A})$ and $\Lambda_r(\mathcal{A})$ are called the point spectrum, continuous spectrum and residual spectrum of $\mathcal{A}$, respectively. If $\lambda \in \Lambda_p(\mathcal{A})$, then λ is called an eigenvalue of $\mathcal{A}$. The multiplicity of an eigenvalue λ is defined to be the dimension of the nullspace of $\lambda\mathcal{I}-\mathcal{A}$. Furthermore, $\lambda \in \Lambda(\mathcal{A})$ is in the **essential spectrum** if either (see [114])*

1. *λ is a limit point of the set of eigenvalues, i.e., there exists a sequence of eigenvalues λ_k such that $\lambda_k \to \lambda$,*
2. *λ is an eigenvalue with infinite multiplicity,*
3. *λ is in the continuous or residual spectrum.*

*Also, $\lambda \in \Lambda(\mathcal{A})$ is in the **discrete spectrum** if it is not part of the essential spectrum.*

Notice that linear operators with essential spectrum are in a sense far removed from matrices which can only have discrete spectrum.

If a linear operator $\mathcal{A}$ generates a C_0-semigroup, we may classify $\mathcal{A}$ by the type of semigroup it generates. The following result can be found in [105, Theorem 1.2.2].

Theorem 2.1.4 *If $\mathcal{S}(t)$ is a C_0-semigroup on X, then there exists constants $M \geq 1$ and $\omega \geq 0$ such that*

$$\|\mathcal{S}(t)\| \leq Me^{\omega t} \quad \text{for all } t \geq 0. \tag{2.7}$$

If there is an $\omega < 0$ such that (2.7) holds, then the semigroup is **exponentially asymptotically stable**. The above exponential bound has implications for the behavior of solutions to the initial value problem (2.3). If $x_0 \in X$, then the mild solution $x(t) = \mathcal{S}(t)x_0$ satisfies

$$\|x(t)\|_X = \|\mathcal{S}(t)x_0\|_X \leq Me^{\omega t}\|x_0\|_X .$$

Remark: If $\omega < 0$ and the constant M is equal to 1, this solution $x(t)$ cannot experience any growth, i.e., $\|x(t)\|_X \leq \|x_0\|_X$ for all $t \geq 0$. However if the constant M is greater than 1, solutions may exhibit transient growth before they eventually decay to zero. In section 2.4.2, it will be seen that this is a crucial point for the new theories on transition to turbulence. Therefore, it is important to know when $\mathcal{A}$ generates a C_0-semigroup of contractions $\mathcal{S}(t)$, i.e., $\mathcal{S}(t)$ satisfies $\|\mathcal{S}(t)\| \leq 1$. A complete classification of the linear operators that generate such a C_0-semigroup is given by the Hille-Yoshida Theorem [105, Theorem 1.3.1].

Theorem 2.1.5 (The Hille-Yoshida Theorem) *$\mathcal{A}$ is the generator of a C_0-semigroup $\mathcal{S}(t)$ on X satisfying $\|\mathcal{S}(t)\| \leq 1$ if and only if*

1. *$\mathcal{A}$ is closed and densely defined on X and*
2. *the resolvent set of $\mathcal{A}$, $\rho(\mathcal{A})$ contains $[0,\infty)$ and the resolvent operator satisfies the bound*
$$\|\mathcal{R}(\lambda;\mathcal{A})\| \leq 1/\lambda \quad \text{for all } \lambda > 0.$$

The following theorem completely characterizes the linear operators that generate C_0-semigroups [105, Theorem 1.5.3].

Theorem 2.1.6 *Let X be a Banach space and assume $\mathcal{A} : \mathcal{D}(\mathcal{A}) \subset X \to X$. Then $\mathcal{A}$ generates a C_0-semigroupup $\mathcal{S}(t)$ satisfying $\|\mathcal{S}(t)\| \leq Me^{\omega t}$ if and only if*

1. *The linear operator $\mathcal{A}$ is closed and densely defined and*
2. *the resolvent set of $\mathcal{A}$, $\rho(\mathcal{A})$, contains the segment of the real line (ω,∞) and the resolvent operator satisfies*
$$\|\mathcal{R}(\lambda,\mathcal{A})^n\| \leq \frac{M}{(\lambda-\omega)^n} \quad \text{for all } \lambda > \omega \text{ and each } n = 1, 2, \ldots$$

This theorem shows that $\mathcal{A}$ must be closed and densely defined and also reveals the importance of the resolvent. Also, the theorem gives insight into the unique solvability of the linear initial value problem (2.3). While there are weaker conditions the guarantee unique solvability (see [105, Theorem 4.1.2]), the following theorem shows that the semigroup approach is sufficient to guarantee that the solution is "classical" (see [105, Section 4.1]).

Theorem 2.1.7 *Let X be a Banach space and suppose $\mathcal{A} : \mathcal{D}(\mathcal{A}) \subset X \to X$ generates a C_0-semigroup. Then for any initial condition $x_0 \in X$, the linear initial value problem (2.3) has a unique mild solution which exists for all $t \geq 0$. Moreover, if $x_0 \in \mathcal{D}(\mathcal{A})$, then $x(t)$ is continuously differentiable on $[0,\infty)$.*

2.1.3 The Infinite Dimensional Case: Spectral Analysis and the Stability of the Zero State

Recall that in the finite dimensional case, if the eigenvalues of the matrix $\mathbf{A}$ all lie in the left half plane, then all solutions to the linear problem tend to zero exponentially fast (Theorem 2.1.1). The following example dashes all hopes that this theorem extends to the infinite dimensional case (see [105, Example 4.4.2]).

Let X be the space of all functions $f : [0,\infty) \to \mathbb{R}$ such that

$$\|f\|_X = \int_0^\infty e^x |f(x)| \, dx + \left(\int_0^\infty |f(x)|^2 \, dx \right)^{1/2} < \infty.$$

It can be shown that $\|\cdot\|_X$ is a norm on X and with this norm, X is a Banach space. Moreover, define a linear operator $\mathcal{A}$ on the domain $\mathcal{D}(\mathcal{A}) = \{f \in X \ : \ f \text{ is absolutely continuous and } f_x \in X\}$ by $\mathcal{A}f = f_x$. Here, the subscript denotes differentiation with respect to x. It can be shown that the resolvent set is contained in $\{\lambda \in \mathbb{C} : \text{Re}(\lambda) > -1\}$ and therefore the spectrum of $\mathcal{A}$ lies entirely to the left of the line $\{\lambda \in \mathbb{C} : \text{Re}(\lambda) = -1\}$. Also, $\mathcal{A}$ generates a C_0-semigroup $\mathcal{S}(t)$ on X and $\mathcal{S}(t)f(x) = f(t+x)$ for $t \geq 0$. This semigroup satisfies $\|\mathcal{S}(t)\| = 1$ for all $t \geq 0$ and therefore no nontrivial solution to the initial value problem will decay to the zero state.

The linear operator $\mathcal{A}$ in the above example is only one in a class of operators for which the **spectral abscissa**

$$\alpha(\mathcal{A}) = \begin{cases} \sup\limits_{\lambda \in \Lambda(\mathcal{A})} \text{Re}(\lambda), & \Lambda(\mathcal{A}) \neq \emptyset \\ -\infty, & \Lambda(\mathcal{A}) = \emptyset \end{cases}$$

and the **growth abscissa**

$$\omega_0(\mathcal{A}) = \lim_{t \to \infty} t^{-1} \log \|\mathcal{S}(t)\|$$

are not equal. Other examples can be found in the references [44], [115] and [140]. Note that the limit defining the growth abscissa always exists since the norm of a C_0-semigroup is always exponentially bounded. The growth abscissa determines the growth or decay of solutions to the linear initial value problem. There are theorems that guarantee the equality of the growth and spectral abscissas (see [44], [107]), but in general $\alpha(\mathcal{A}) \leq \omega_0(\mathcal{A})$. If the growth abscissa is negative, then the semigroup is exponentially stable and all solutions will decay to zero. We concentrate here on conditions that force the exponential stability of the semigroup.

In light of the above example, it is clear that the linear operator $\mathcal{A}$ must be restricted in order to extend the finite dimensional spectral condition that guarantees all solutions of the linear problem decay exponentially to zero. One condition assuring this extension that often arises in applications is that $\mathcal{A}$ generates an analytic semigroup.

Definition 2.1.4 *Let Δ be the sector in the complex plane given by $\{z \in \mathbb{C} : \varphi_1 < \arg(z) < \varphi_2, \ \varphi_1 < 0 < \varphi_2\}$ and suppose $\mathcal{S}(z)$ is a bounded operator for each $z \in \Delta$. The family of bounded linear operators $\{\mathcal{S}(z) : z \in \Delta\}$ is called an analytic semigroup over Δ if*

1. *$\mathcal{S}(z)$ is analytic throughout Δ,*
2. *$\mathcal{S}(0) = \mathcal{I}$, the identity operator on X and $\lim_{z \to 0} \mathcal{S}(z)x = x$ for any $x \in X$, where the limit is taken over $z \in \Delta$,*
3. *$\mathcal{S}(z+w) = \mathcal{S}(z)\mathcal{S}(w)$ for all $z, w \in \Delta$.*

Roughly, a C_0-semigroup $\mathcal{S}(t)$, $t \geq 0$, is analytic if $\mathcal{S}(t)$ can be extended analytically from the positive real axis to a sector in the complex plane and this extension also has the semigroup properties in that sector. If $\mathcal{A}$ generates an analytic semigroup, Theorem 2.1.1 for the finite dimensional case naturally extends to infinite dimensions [105, Theorem 4.4.3 and Corollary 4.1.5].

Theorem 2.1.8 *Consider the linear initial value problem (2.3). If $\mathcal{A}$ generates an analytic semigroup $\mathcal{S}(t)$ and its spectrum is bounded away from the imaginary axis in the left half plane, i.e., if*

$$\alpha := \sup_{\lambda \in \Lambda(\mathcal{A})} \mathrm{Re}(\lambda) < 0, \tag{2.8}$$

then for any ω satisfying $-\alpha > \omega > 0$, there exists a constant $M = M(\omega) \geq 1$ such that the semigroup satisfies the bound

$$\|\mathcal{S}(t)\| \leq Me^{-\omega t},$$

for all $t \geq 0$. Furthermore, $\mathcal{S}(t)x$ is differentiable for every $x \in X$ and $t > 0$. Therefore for any initial data $x_0 \in X$ the IVP (2.3) has a unique classical solution which tends to zero exponentially in the X-norm.

Definition 2.1.5 *A linear operator $\mathcal{A} : \mathcal{D}(\mathcal{A}) \subset X \to X$ defined on a complex Banach space X is **sectorial** if it is closed, densely defined and there exist $M \geq 1$, $a \in \mathbb{R}$ and $\theta \in (\pi/2, \pi)$ such that the sector of the complex plane $S = \{ \lambda : 0 \leq |\arg(\lambda - a)| \leq \theta \}$ is contained in the resolvent set of $\mathcal{A}$ and*

$$\|\mathcal{R}(\lambda; \mathcal{A})\| \leq M / |\lambda - a| \quad \text{for all } \lambda \in S.$$

Sectorial operators arise frequently in parabolic PDEs and certain delay equations among other applications. In particular, they often arise when the linear operator can be derived from a bilinear form (see section 4.3). The following result (see [67, Theorem 1.3.4], [101, Section 4.5]) will be useful in later sections.

Theorem 2.1.9 *If $\mathcal{A}$ is a sectorial operator, then $\mathcal{A}$ generates an analytic semigroup. Furthermore, for any $a \in \mathbb{R}$ such that $a > \lambda$ for any $\lambda \in \Lambda(\mathcal{A})$, the operator $\mathcal{A} - a\mathcal{I}$ satisfies the spectral bound (2.8) and generates an exponentially stable semigroup.*

Therefore, sectorial operators generate analytic semigroups. To give a concrete example, the linearized Navier-Stokes operator over a bounded domain $\Omega \subset \mathbb{R}^n$, $n = 2$ or 3, is a sectorial operator.

If the state space X is a Hilbert space, the linear operators that generate exponentially stable C_0-semigroups can be completely characterized [107, Corollary 4].

Theorem 2.1.10 (Prüss) *Suppose $\mathcal{A} : \mathcal{D}(\mathcal{A}) \subset X \to X$ generates a C_0-semigroup $\mathcal{S}(t)$ over a Hilbert space X. Then there exist constants $M \geq 1$ and $\omega > 0$ such that $\|\mathcal{S}(t)\| \leq Me^{-\omega t}$ if and only if the closed right half plane $\{ \lambda \in \mathbb{C} : \mathrm{Re}(\lambda) \geq 0 \}$ is contained in the resolvent set $\rho(\mathcal{A})$ and there exists a constant $K > 0$ such that*

$$\|\mathcal{R}(\lambda; \mathcal{A})\| \leq K \quad \text{for all } \lambda = i\gamma,\ \gamma \in \mathbb{R}.$$

Thus, the resolvent operator is required to be bounded in the closed right half plane in order for a linear operator to generate an exponentially stable semigroup over a Hilbert space.

In this section, we have seen how the stability of the zero state to the linear autonomous initial value problem over $\mathbb{R}^n$ can be ascertained from spectral information of the matrix $\mathbf{A}$. In infinite dimensions, however, one must impose extra conditions on the linear operator $\mathcal{A}$ to ensure that the abstract linear IVP has a globally defined unique solution. Also, the spectral condition governing the stability of the zero state from the finite dimensional case does not necessarily extend to infinite dimensions. Therefore, one must be cautious when using spectral methods to determine stability properties of an equilibrium in infinite dimensions.

2.2 Stability Analysis for Nonlinear Systems

In this section, we study the stability of equilibria for both finite and infinite dimensional nonlinear autonomous initial value problems. In particular, consider the following problems with the special form

$$\dot{x}(t) = \mathbf{A}x(t) + F(x(t)) \quad \text{for } t > 0, \qquad x(0) = x_0 \in \mathbb{R}^n, \tag{2.9}$$

$$\dot{x}(t) = \mathcal{A}x(t) + \mathcal{F}(x(t)) \quad \text{for } t > 0, \qquad x(0) = x_0 \in X, \tag{2.10}$$

where the dot again denotes differentiation with respect to t. The first equation is defined on $\mathbb{R}^n$ with $\mathbf{A}$ a constant $n \times n$ matrix and $F(\cdot)$ a nonlinear function mapping $\mathbb{R}^n$ to $\mathbb{R}^n$. The second equation is defined on an infinite dimensional Banach space X with norm $\|\cdot\|_X$ where $\mathcal{A} : \mathcal{D}(\mathcal{A}) \subset X \to X$ and $\mathcal{F} : \mathcal{D}(\mathcal{F}) \subset X \to X$ are linear and nonlinear operators, respectively. Also, we assume $F(0) = 0$ and $\mathcal{F}(0) = 0$ so that the zero state is an equilibrium for both systems. It will be seen below that this is not a restriction.

2.2.1 The Finite Dimensional Case

We begin with a general autonomous nonlinear initial value problem on $\mathbb{R}^n$ of the form

$$\dot{y}(t) = f(y(t)) \quad \text{for } t > 0, \quad y(0) = y_0 \in \mathbb{R}^n, \tag{2.11}$$

where $f : \mathbb{R}^n \to \mathbb{R}^n$. Suppose y_e is an equilibrium for this system. If $f(\cdot)$ is continuously differentiable in a neighborhood of y_e and

$$\mathbf{A} = \left[\frac{\partial f_i}{\partial y_j}\right]_{y = y_e} \tag{2.12}$$

is the Jacobian at $y = y_e$, then the change of variables $x(t) = y(t) - y_e$ produces the initial value problem

$$\dot{x}(t) = \mathbf{A}x(t) + F(x(t)) \quad \text{for } t > 0, \quad x(0) = x_0 := y_0 - y_e,$$

where $F(x) = f(x + y_e) - \mathbf{A}x$. Note that $F(0) = 0$. This motivates the study of the above specific form (2.9) of the initial value problem.

The matrix $\mathbf{A}$ may formally be viewed as the first term in a Taylor expansion of $f(\cdot)$ about y_e and so it seems plausible that $F(x) = o(\|x\|)$ as $\|x\| \to 0$, i.e.,

$$\lim_{\|x\|\to 0} \frac{\|F(x)\|}{\|x\|} = 0.$$

Here, $\|\cdot\|$ is any norm on $\mathbb{R}^n$. Returning to the specific IVP (2.9), we examine the stability properties of the zero state under this hypothesis.

Perron's Theorem relates the stability of the zero equilibrium of the nonlinear system (2.9) to the spectrum of the matrix $\mathbf{A}$ (see [102, Theorems 6.2.1 and 6.2.3])

Theorem 2.2.1 (Perron's Theorem) *Consider the nonlinear initial value problem (2.9) and let $\|\cdot\|$ be any norm on $\mathbb{R}^n$. Suppose $F(\cdot)$ is continuous in some neighborhood about the origin and satisfies $F(x) = o(\|x\|)$ as $\|x\| \to 0$. If $\mathbf{A}$ is a stable matrix in the sense of (2.5), then the origin is asymptotically stable. Furthermore, if at least one of the eigenvalues of $\mathbf{A}$ has positive real part, then the origin is unstable.*

Corollary 2.2.1 *Let y_e be an equilibrium state for the general initial value problem (2.11) and suppose $f(\cdot)$ is continuously differentiable in a neighborhood of y_e. If the matrix $\mathbf{A}$ defined in (2.12) is stable, then y_e is an asymptotically stable equilibrium. Furthermore, if at least one of the eigenvalues of $\mathbf{A}$ has positive real part, then y_e is an unstable equilibrium.*

This result implies that in some cases the stability of an equilibrium state for a nonlinear ordinary differential equation can be determined by analyzing the linear problem. It is important to note that the basin of attraction for the nonlinear problem can be extremely small even if all of the eigenvalues of $\mathbf{A}$ are bounded far away from the imaginary axis in the left half plane.

2.2.2 The Infinite Dimensional Case

Now we consider the nonlinear infinite dimensional initial value problem (2.10). We extend Perron's theorem for finite dimensions to a specific class of infinite dimensional problems. This extension requires that $\mathcal{A}$ generate an exponentially stable C_0-semigroup $\mathcal{S}(t)$. Also, Perron's theorem for finite dimensional systems assumes that the nonlinearity $\mathcal{F}(\cdot)$ is continuous in some neighborhood about zero and that $\mathcal{F}(x) = o(\|x\|)$ as $\|x\| \to 0$. This condition is severely restricting in the infinite dimensional case. Many important types of nonlinearities are unbounded and therefore fail to satisfy this condition. In particular, the nonlinearities arising in the Navier-Stokes equation is unbounded. Therefore, to extend Perron's theorem to infinite dimensional nonlinear systems one must resort to different techniques.

One extension of Perron's theorem involves fractional powers of the linear operator $-\mathcal{A}$ and the underlying state space X (see [67], [101]).

Definition 2.2.1 *Suppose $\mathcal{A}$ generates an exponentially stable C_0-semigroup $\mathcal{S}(t)$ over X. Then for any $x \in X$ and $\alpha > 0$ define*

$$(-\mathcal{A})^{-\alpha} x = \frac{1}{\Gamma(\alpha)} \int_0^\infty t^{\alpha-1} \mathcal{S}(t) x \, dt.$$

This operator is bounded and invertible. Define the fractional power $(-\mathcal{A})^\alpha$ as the inverse of the above operator with domain equal to the range of $(-\mathcal{A})^{-\alpha}$.

Theorem 2.1.9 in the previous section leads to the following definition of the fractional powers of the state space X.

Definition 2.2.2 *Suppose $\mathcal{A} : \mathcal{D}(\mathcal{A}) \subset X \to X$ is sectorial over a Banach space X and let $a \in \mathbb{R}$ satisfy $\operatorname{Re}(\lambda) < a$ for any $\lambda \in \Lambda(\mathcal{A})$. For $\alpha \geq 0$, define the space $X^\alpha := \mathcal{D}((a\mathcal{I} - \mathcal{A})^\alpha)$ with the norm $\|x\|_\alpha := \|(a\mathcal{I} - \mathcal{A})^\alpha x\|_X$.*

Note that Theorem 2.1.9 guarantees that $\mathcal{A} - a\mathcal{I}$ generates an exponentially stable semigroup and therefore the fractional powers of $a\mathcal{I} - \mathcal{A}$ are well defined. The following theorem collects some basic properties of the fractional powers of X (see [67, Theorem 1.4.8]).

Theorem 2.2.2 *Suppose $\mathcal{A} : \mathcal{D}(\mathcal{A}) \subset X \to X$ is sectorial on a Banach space X. It follows that*

1. *For $\alpha \geq 0$ the normed space $(X^\alpha, \|\cdot\|_\alpha)$ is a Banach space. Also, $X^0 = X$.*
2. *Different choices of the constant a in the definition of X^α induce equivalent norms.*
3. *If $\alpha \geq \beta \geq 0$, then $X^\alpha \subset X^\beta$ and the embedding is continuous. Furthermore, if $\mathcal{A}$ has compact resolvent, the embedding is compact.*

In this framework, an operator that is unbounded on X may be bounded on X^α. The framework allows us to extend Perron's theorem and to examine the stability of equilibria in the norm of this alternate space (see [67, Chapter 5], [101, Sections 6.4 and 6.6]).

Theorem 2.2.3 *Suppose $\mathcal{A} : \mathcal{D}(\mathcal{A}) \subset X \to X$ is sectorial and the spectrum of $\mathcal{A}$ satisfies the bound*

$$\sup_{\lambda \in \Lambda(\mathcal{A})} \operatorname{Re}(\lambda) < 0.$$

Assume that $\mathcal{F} : U \subset X^\alpha \to X$ where U is open in X^α for some $\alpha \in (0, 1)$ and $\|\mathcal{F}(x)\|_X = o(\|x\|_\alpha)$ as $\|x\|_\alpha \to 0$. Then there exists a $\delta > 0$ such that if $x_0 \in X^\alpha$ and $\|x_0\|_\alpha < \delta$, then the nonlinear initial value problem (2.10) has a unique solution $x(t)$ that exists for all $t > 0$ and satisfies $\|x(t)\|_\alpha \to 0$ as $t \to \infty$.

Therefore, in this special framework, the stability of the zero state depends on the spectrum of the underlying linear operator and the specific form of the operators. One must be careful when trying to extend classical stability results from finite dimensions to the infinite dimensional case. In particular, one must provide the appropriate abstract framework to extend Perron's theorem. These technical details are not often addressed in the literature on hydrodynamic stability.

2.3 Classical Stability Analysis of the Navier-Stokes Equations

Spectral methods for linear stability analysis have been one of the main tools used to investigate transition to turbulence in fluid flow. In this section, we discuss the spectrum of the linearized Navier-Stokes (NS) operator and review how this knowledge has been applied to study transition. Next, the more popular approach of transforming the linearized NS operator to the Orr-Sommerfeld/Squire operator will be presented. Both approaches have limitations and gaps which remain to be filled.

Recall, in section 1.2.3 the Navier-Stokes equations (1.1)-(1.5) were transformed by a change of variables to arrive at the fluctuation equations (1.6)-(1.10) about a base flow and pressure state. Assuming these base states are a constant equilibrium state for the Navier-Stokes equations, then zero is an equilibrium for the fluctuation Navier-Stokes equations. The linear operator in the fluctuation equations is the linearization of the NS equations about the base states.

For bounded domains, the linearized Navier-Stokes operator has very nice properties (see [128, Theorems 3.6 and 4.2]).

Theorem 2.3.1 *Let Ω be a bounded domain in $\mathbb{R}^n$, with $n = 2$ or 3, with smooth boundary and suppose the base flow is smooth. Then the spectrum of the linearized fluctuation Navier-Stokes operator $\mathcal{A}$ consists entirely of eigenvalues, each with finite multiplicity, that can accumulate only at $-\infty$. Furthermore, $\mathcal{A}$ is sectorial and generates an analytic semigroup on V.*

For unbounded domains, the analysis is much more complex. When the boundary of Ω is compact, such as in an external flow problem (i.e., flows over an obstacle), the spectrum is known to contain essential spectrum (see [128]). However, when the boundary is not compact, such as in channel or pipe flow, the difficulties are even more pronounced. Because of this difficulty, it is standard to transform the linear system and employ Fouier analysis to study linear stability.

In this alternate method, the linear fluctuation NS equations are transformed to yield the Orr-Sommerfeld and Squire equations. This transformation is popular since it leads to two coupled one dimensional partial differential equations over a finite interval. These equations are much easier to analyze analytically than the linearized Navier-Stokes operator over an unbounded three dimensional domain. However, the transformation only works for certain equilibria states and it is unknown whether the transformation is entirely rigorous as we will discuss below.

To begin, assume the domain Ω is an unbounded infinite three dimensional channel given by

$$\Omega = \left\{ (x, y, z) \in \mathbb{R}^3 \, : \, -\infty < x < \infty, \, -1 < y < 1, \, -\infty < z < \infty \right\}.$$

This geometry allows one to study the stability of base flows of the form of plane Couette and Poiseuille flow. Other flows such as pipe flow or Blasius boundary layer flow can be considered

in a similar fashion (see [49] or [123]). Plane Couette flow is given by $\vec{U}(y) = [y, 0, 0]^T$ with the pressure a linear function of y, while plane Poiseuille flow is given by $\vec{U}(y) = [1-y^2, 0, 0]$ with the pressure constant in y. More generally, we assume the velocity base flow has the form $\vec{U} = [U(y), 0, 0]^T$.

If one drops the nonlinear term $(\vec{u} \cdot \nabla)\vec{u}$ from the fluctuation Navier-Stokes equations (1.6)-(1.10), then the resulting linear equations are given by

$$\begin{aligned} u_t + Uu_x + U'v &= -q_x + R^{-1}\nabla^2 u \quad (2.13)\\ v_t + Uv_x &= -q_y + R^{-1}\nabla^2 v \quad (2.14)\\ w_t + Uw_x &= -q_z + R^{-1}\nabla^2 w, \quad (2.15) \end{aligned}$$

where $\vec{u}$ has been decomposed into $[u, v, w]^T$. Here, prime ($'$) denotes differentiation with respect to y and subscripts denote partial derivatives. Also, one has the divergence free condition (also called the continuity equation)

$$u_x + v_y + w_z = 0. \quad (2.16)$$

To derive the Orr-Sommerfeld equations, one (formally) takes the divergence of the equations of motion (2.13)-(2.15) and uses the divergence free condition (2.16) to obtain a Poisson equation for the pressure fluctuation

$$\nabla^2 q = -2U'v_x. \quad (2.17)$$

Substituting this expression into the second equation of motion (2.14) eliminates the pressure and gives an equation for the normal velocity component (i.e., the velocity in the y direction):

$$\left[\left(\frac{\partial}{\partial t} + U\frac{\partial}{\partial x}\right)\nabla^2 - U''\frac{\partial}{\partial x} - \frac{1}{R}\nabla^4\right] v = 0. \quad (2.18)$$

In order to capture the three dimensional flow field, one derives an equation for the normal vorticity $\eta := u_z - w_x$. In particular, η satisfies

$$\left[\frac{\partial}{\partial t} + U\frac{\partial}{\partial x} - \frac{1}{R}\nabla^2\right]\eta = -U'\frac{\partial v}{\partial z}. \quad (2.19)$$

Using the continuity equation (2.16) it follows that the other velocity components can be recovered by solving the Poisson equations

$$u_{xx} + u_{zz} = \eta_z - v_{xy} \quad \text{and} \quad w_{xx} + w_{zz} = -\eta_x - v_{yz}. \quad (2.20)$$

For fixed constants k_x and k_z, define the Fourier transform of the normal velocity (and

similarly for the normal vorticity) by

$$\tilde{v}(t,y,k_x,k_z) = \int_{-\infty}^{\infty}\int_{-\infty}^{\infty} v(t,x,y,z)e^{-i(k_x x+k_z z)}\,dx\,dz,$$

where i is the imaginary unit. Here, k_x and k_z are called the wave numbers in the streamwise (x-direction) and spanwise (z-direction), respectively. Formally taking the Fourier transform of the normal velocity and vorticity equations (2.18) and (2.19) in the streamwise and spanwise directions yields the equations

$$\left[\left(\frac{\partial}{\partial t} + ik_xU\right)\tilde{\Delta} - ik_xU'' - \frac{1}{R}\tilde{\Delta}^2\right]\tilde{v} = 0 \tag{2.21}$$

$$\left[\frac{\partial}{\partial t} + ik_xU - \frac{1}{R}\tilde{\Delta}\right]\tilde{\eta} = -ik_zU'\tilde{v}, \tag{2.22}$$

where $\tilde{\Delta}$ is the transformed operator given by $\tilde{\Delta} = \frac{\partial^2}{\partial y^2} - k_x^2 - k_z^2$. These equations are accompanied by the boundary conditions

$$\tilde{v}(t,\pm 1,k_x,k_z) = \tilde{v}_y(t,\pm 1,k_x,k_z) = \tilde{\eta}(t,\pm 1,k_x,k_z) = 0, \tag{2.23}$$

which can be derived by taking the Fourier transform of the continuity equation (2.16) and using the original no-slip boundary conditions (1.8). Again, the Fourier transforms of the streamwise and spanwise velocity components ($\tilde{u}$ and $\tilde{w}$, respectively) can be recovered given only the Fourier transforms of the normal velocity and vorticity. Taking the Fourier transforms of the Poisson equations (2.20) yields

$$\tilde{u} = \frac{-i}{k_x^2+k_z^2}\left(k_z\tilde{\eta} - k_x\tilde{v}_y\right), \quad \tilde{w} = \frac{i}{k_x^2+k_z^2}\left(k_x\tilde{\eta} + k_z\tilde{v}_y\right). \tag{2.24}$$

The above partial differential equations (2.21), (2.22) along with the boundary conditions (2.23) are called the Orr-Sommerfeld and Squire equations, respectively. In order to place these equations in an abstract form, the domains of the operators $\tilde{\Delta}$ and $\tilde{\Delta}^2$ need to be specified. In view of the boundary conditions (2.23), the natural domains are given by $\mathcal{D}(\tilde{\Delta}) = H^2(-1,1)\cap H_0^1(-1,1)$ and $\mathcal{D}(\tilde{\Delta}^2) = H^4(-1,1)\cap H_0^2(-1,1)$. With these domains, $\tilde{\Delta}$ is invertible, but $\tilde{\Delta}^{-1}\tilde{\Delta}^2 \neq \tilde{\Delta}$. Letting $\varphi = [\,\tilde{v},\tilde{\eta}\,]^T$, the Orr-Sommerfeld and Squire equations can be written as the formal abstract linear differential equation

$$\dot{\varphi}(t) = \mathcal{A}\varphi(t) := \begin{bmatrix} \mathcal{A}_{OS} & 0 \\ \mathcal{C} & \mathcal{A}_S \end{bmatrix}\varphi(t) \tag{2.25}$$

where

$$\mathcal{A}_{OS} \;=\; \tilde{\Delta}^{-1}\left(-ik_xU\tilde{\Delta} + ik_xU'' + \frac{1}{R}\tilde{\Delta}^2\right),$$

$$\begin{aligned} \mathcal{C} &= -ik_z U' \quad \text{and} \\ \mathcal{A}_S &= -ik_x U + \frac{1}{R}\tilde{\Delta} \end{aligned}$$

are called the Orr-Sommerfeld, coupling and Squire operators, respectively.

In order to properly define the operator $\mathcal{A}$ one must specify a state space and the operator's domain. Let $H = [H^2 \cap H_0^1] \times L^2$, $\varphi = [\,\tilde{v}, \tilde{\eta}\,]^T$ and define the inner product on H by

$$\langle \varphi, \psi \rangle_H = \langle \mathcal{Q}\varphi, \psi \rangle_{L^2 \times L^2} = \frac{1}{8(k_x^2 + k_z^2)} \Big(\langle -\Delta\tilde{v}, \psi_1 \rangle_{L^2} + \langle \tilde{\eta}, \psi_2 \rangle_{L^2} \Big),$$

where $\mathcal{Q}$ is the positive definite operator given by

$$\mathcal{Q}\varphi = \frac{1}{8(k_x^2 + k_z^2)} \begin{bmatrix} -\tilde{\Delta} & 0 \\ 0 & I \end{bmatrix} \begin{bmatrix} \tilde{v} \\ \tilde{\eta} \end{bmatrix}$$

on the space H. This inner product can be interpreted as an average kinetic energy of the flow velocity over a bounded region by using the relations (2.24), inverting the Fourier transforms and integrating by parts (see [9], [52]). The domain of the $\mathcal{A}$ operator is defined by $\mathcal{D}(\mathcal{A}) = [H^4 \cap H_0^2] \times [H^2 \cap H_0^1] \subset H$. We will refer to this operator as the Orr-Sommerfeld/Squire operator.

We emphasize here that many of these manipulations are purely formal. To begin, we assumed the velocity field is in H^4 to arrive at the normal velocity and vorticity equations (2.18), (2.19). Also, as noted by Bamieh and Dahleh in [9], little attention is paid in the literature as to whether the above Fourier transforms are valid. This would require the solutions of the normal velocity and vorticity equations to be L^2 which is also not known to hold. Nevertheless, once the transformation has been made, the linear operator can be placed in an entirely rigorous setting and analyzed completely (see [91] and the references therein). In particular, the spectrum of the Orr-Sommerfeld operator $\mathcal{A}_{OS}$ defined over various domains is known to be consist entirely of eigenvalues.

Remark: This last result seems curious to the author. The linearized Navier-Stokes operator over an unbounded channel is likely to have essential spectrum (see definition 2.1.3). This is a familiar property of the spectrum of differential operators over unbounded domains (see [67, Appendix to Chapter 5]). On the other hand, the Orr-Sommerfeld/Squire operator is known only to have a discrete spectrum for each pair of wave numbers k_x and k_z. The actual spectrum of the linearized Navier-Stokes operator is thought to be the union of the spectra of the Orr-Sommerfeld/Squire operator over all values of the wave numbers. If this is the case, then it is possible that the union of the spectra will create an essential spectrum. However, this is not known and therefore it is possible that some spectral information has been lost in the transformation. It is known that no spectral information is lost in a similar transformation to study the stability properties of an asymptotic suction velocity profile [100]. However, the author is not aware of other rigorous justifications for the Fourier transformation leading to the Orr-Sommerfeld and Squire equations.

Now we briefly discuss the deficiencies of both of these linear operators to actually predict

transition to turbulence. In the first case, to actually predict the critical Reynolds number at which the spectrum of the linearized Navier-Stokes operator crosses into the right half plane can be extremely difficult. The main problem here is that one must deal with divergence free function spaces. This creates problems in computing or estimating eigenvalues both theoretically and numerically. In addition, unbounded domains only serve to complicate the issues. Therefore, for many classes of unbounded domains the Orr-Sommerfeld and Squire equations (and variations thereof) have been the primary focus of linear stability analysis for fluid flow for about 100 years. The theoretical and numerical analysis of the spectrum of the Orr-Sommerfeld/Squire operator proves much easier. However, the transformation used to arrive at these equations is not completely justified. Also, as mentioned in the introduction, the critical Reynolds numbers found by a spectral analysis of the Orr-Sommerfeld/Squire operator for various flows is known to differ substantially from experimental values for many flow types. One possible explanation of this could lie in the fact that the spectral abscissa and the growth abscissa are different.

The failure of the classical linear stability analysis has led many researchers to consider alternative linear methods to investigate stability. Two of these approaches will be outlined in the next section.

2.4 Two New Approaches to Stability Analysis of the Navier-Stokes Equations

As noted above, the transformation that takes the linearized Navier-Stokes equations to the Orr-Sommerfeld and Squire equations is not always justified. However, during the past 25 years considerable attention has been devoted to understanding the failure of classical linear stability analysis to predict transition. In the past decade, several new theories have appeared. As noted in the introduction, these new approaches are primarily concerned with energy growth (or amplification) of small disturbances in the flow. In this section, we describe the details of two of these theories, discuss the advances each has made in understanding transition, and highlight what some gaps in these methods. For more details on these approaches see the review articles [121] and [143] and Schmid and Henningson's recent book [123].

2.4.1 A Resolvent/Pseudospectra Approach

A non-classical approach to linear stability that can be based on the analysis of the resolvent operator or, equivalently, the pseudospectra. In this approach, the pseudospectra of the Orr-Sommerfeld/Squire operator $\mathcal{A}$ defined in (2.25) is used to study the transient growth of energy in flows that begin near the laminar state. Certain small perturbations to the laminar flow state are found to cause a substantial energy growth. When the base flow is known to be asymptotically stable, researchers have argued that when this energy growth becomes "sufficiently large" the nonlinearity becomes important and mixes the flow leading

to transition. Even if the laminar flow is asymptotically stable, the premise is that a domain of attraction rapidly shrinks with increasing Reynolds number. Therefore, the laminar flow state would be practically unstable in laboratory experiments despite being theoretically stable.

To formulate these ideas into precise mathematical statements requires infinite dimensional stability theory. Assume the linear system

$$\dot{z}(t) = \mathcal{A}z(t), \quad z(0) = z_0 \in X, \tag{2.26}$$

is exponentially stable. In particular, suppose $\mathcal{A}$ generates a C_0-semigroup $\mathcal{S}(t)$ and there are constants $M \geq 1$ and $\omega > 0$ such that $\|\mathcal{S}(t)\| \leq Me^{-\omega t}$ for all $t \geq 0$. As above, the solutions of the above linear differential equation satisfy

$$\|z(t)\|_X = \|\mathcal{S}(t)z_0\|_X \leq Me^{-\omega t} \|z_0\|_X .$$

If $M = 1$, then solutions cannot experience any transient growth. However, if the constant M is strictly greater than 1, solutions may exhibit transient growth before they eventually decay to zero. The Hille-Yoshida theorem (see Theorem 2.1.5) completely characterizes the generators of the former type of semigroup using a bound on the resolvent operator. Therefore, the resolvent is involved in the behavior of solutions to a linear differential equation. To examine this further, we need the concept of the ε-pseudospectra.

Definition 2.4.1 *The ε-pseudospectra of a linear operator $\mathcal{A}$ is defined to be the set*

$$\Lambda_\varepsilon(\mathcal{A}) := \{\lambda \in \rho(\mathcal{A}) \ : \ \| \mathcal{R}(\lambda; \mathcal{A})\| > 1/\varepsilon\} \cup \Lambda(\mathcal{A}),$$

where $\Lambda(\mathcal{A})$ is the spectrum of $\mathcal{A}$.

Roughly, the pseudospectra of an operator is the portions of the complex plane where the resolvent operator is "large". If $\lambda \in \Lambda_p(\mathcal{A})$ or $\Lambda_c(\mathcal{A})$, then it is reasonable to define the norm of the resolvent as $+\infty$ since the resolvent either does not exist or is unbounded. It is not clear how to deal with the residual spectrum. The following equivalent form of the pseudospectra can be found in [118, Proposition 4.15].

Theorem 2.4.1 *Let X be a Banach space. The ε-pseudospectra of a linear operator $\mathcal{A} : \mathcal{D}(\mathcal{A}) \subset X \to X$ is also given by*

$$\Lambda_\varepsilon(\mathcal{A}) = \bigcup \{ \Lambda(\mathcal{A} + \mathcal{A}_\varepsilon) \ : \ \mathcal{A}_\varepsilon \text{ is bounded and } \|\mathcal{A}_\varepsilon\| < \varepsilon \} .$$

Therefore, the pseudospectra is the union of all the spectra of operators that are small bounded perturbations to the operator $\mathcal{A}$.

We will explore the role of the pseudospectra in the transient growth of solutions to differential equations. Therefore, we focus on the properties of the pseudospectra that are essential to this study. Trefethen's review articles [139] and [140] or Trefethen and Embree's

forthcoming book [142] contain more information on the gerenal theory. Also, Embree and Trefethen maintain an extensive online resource for pseudospectra [51]. We also note that the above equivalent definitions of the pseudospectra has been extended to the case of perturbations having a certain structure. In some cases these structured perturbations can be unbounded [59].

To explore the transient growth of solutions through the resolvent and pseudospectra, we need to make use of properties of the adjoint operator. For simplicity we now assume that X is a Hilbert space with inner product $\langle \cdot, \cdot \rangle_X$ and corresponding norm $\|\cdot\|_X$.

Definition 2.4.2 *Let $\mathcal{A} : \mathcal{D}(\mathcal{A}) \subset X \to X$ be a closed, densely defined linear operator on a Hilbert space X. The **adjoint operator** $\mathcal{A}^* : \mathcal{D}(\mathcal{A}^*) \subset X \to X$ is defined on the domain*

$$\mathcal{D}(\mathcal{A}^*) = \{\, y \in X \,:\, \text{there exists a } y^* \in X \text{ such that } \langle \mathcal{A}x, y \rangle = \langle x, y^* \rangle \text{ for all } x \in \mathcal{D}(\mathcal{A}) \,\}$$

by $\mathcal{A}^* y = y^*$ for all $y \in \mathcal{D}(\mathcal{A}^*)$.

It is well known that if the operator $\mathcal{A}$ is densely defined, then the adjoint operator is uniquely defined, closed and densely defined [77]. We also define two very important classes of operators.

Definition 2.4.3 *A linear operator $\mathcal{A}$ is self-adjoint if $\mathcal{D}(\mathcal{A}) = \mathcal{D}(\mathcal{A}^*)$ and $\mathcal{A}x = \mathcal{A}^* x$ for all $x \in \mathcal{D}(\mathcal{A})$. A linear operator $\mathcal{A}$ is normal if $\mathcal{A}\mathcal{A}^* = \mathcal{A}^*\mathcal{A}$, i.e., these operators have the same domain and action on that domain.*

It was noted above that the transient growth of solutions to the abstract linear differential equation (2.26) is linked to the resolvent operator (by the Hille-Yoshida theorem) which, in turn, is linked to the pseudospectra. For normal operators the following theorem relates the norm of the resolvent (and therefore the pseudospectra) to the spectrum [77].

Theorem 2.4.2 *If $\mathcal{A}$ is a normal operator with spectrum $\Lambda(\mathcal{A})$, then for any $\lambda \in \rho(\mathcal{A})$,*

$$\|\mathcal{R}(\lambda; \mathcal{A})\| = 1/\text{dist}(\lambda, \Lambda(\mathcal{A})) = \sup_{\tilde{\lambda} \in \Lambda(\mathcal{A})} 1/|\, \lambda - \tilde{\lambda}\,|.$$

Therefore, for any $\varepsilon > 0$, the ε-pseudospectra is simply the ε neighborhood surrounding the spectrum, i.e., $\Lambda_\varepsilon(\mathcal{A}) = \{\, \lambda \in \mathbb{C} \,:\, \text{dist}(\lambda, \Lambda(\mathcal{A})) < \varepsilon \}$.

This theorem implies that the pseudospectra for normal operators is "close" to the spectrum when ε is small. This is not true, in general, for non-normal operators. This can be seen from a simple matrix example due to Godunov [62]. Define

$$\mathbf{G} = \begin{bmatrix} 289 & 2064 & 336 & 128 & 80 & 32 & 16 \\ 1152 & 30 & 1312 & 512 & 288 & 128 & 32 \\ -29 & -2000 & 756 & 384 & 1008 & 224 & 48 \\ 512 & 128 & 640 & 0 & 640 & 512 & 128 \\ 1053 & 2256 & -504 & -384 & -756 & 800 & 208 \\ -287 & -16 & 1712 & -128 & 1968 & -30 & 2032 \\ -2176 & -287 & -1565 & -512 & -541 & -1152 & -289 \end{bmatrix}.$$

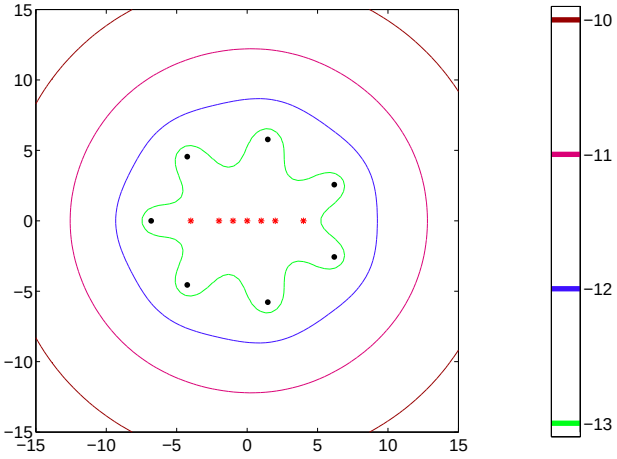

Figure 2.1: Numerical computations of spectra and pseudospectra for Godunov's matrix $\mathbf{G}$ defined above. The true eigenvalues are denoted by the stars and the computed eigenvalues by the dots. The computed ε-pseudospectra are the sets contained in the various contours. The scale is a log 10 scale, i.e., the inner to outer counters correspond to $\varepsilon = 10^{-13}, \ldots 10^{-10}$.

Godunov used this matrix to show how eigenvalue computation can be very ill-conditioned. Define $\mathbf{T}$ to be a 7×7 matrix with ones along the diagonal and in the following entries:

$$\mathbf{T}_{31},\ \mathbf{T}_{61},\ \mathbf{T}_{53},\ \mathbf{T}_{72},\ \mathbf{T}_{73},\ \mathbf{T}_{75}.$$

It can be shown that $\mathbf{T}$ is invertible and that $\mathbf{T}\mathbf{G}\mathbf{T}^{-1}$ is upper triangular with diagonal elements $\{0, \pm 1, \pm 2, \pm 4\}$. These values are therefore the eigenvalues of $\mathbf{G}$. Standard numerical computations fail to approximate the spectrum with any reasonable degree of accuracy. Figure 2.1 shows the actual eigenvalues of $\mathbf{G}$ compared with the eigenvalues computed using Eigtool [148] in Matlab. It is clear that the computed values are nowhere near the actual spectrum. The figure also shows the pseudospectra for various values of ε again computed using Eigtool. The ε-pseudospectra are the sets lying inside the various contours. Notice that the pseudospectra contains points far away from the spectrum even for extremely small values of ε. This phenomenon is not isolated and one can find similar examples in the Eigtool software package as well as in the references given above.

For a general non-normal linear operator, there is no simple relationship between the distance to the spectrum and the norm of the resolvent. The best bounds available are in terms of the spectrum and the numerical range.

Definition 2.4.4 *Let $\mathcal{A} : \mathcal{D}(\mathcal{A}) \subset X \to X$ be a linear operator acting on a Hilbert space X with inner product $\langle \cdot, \cdot \rangle$ and corresponding norm $\|\cdot\|$. The numerical range is the set in the*

complex plane given by

$$\mathrm{Num}(\mathcal{A}) := \{ \langle \mathcal{A}x, x\rangle_X \, : \, x \in \mathcal{D}(\mathcal{A}), \, \|x\|_X = 1\}.$$

The following theorem can be found in [77].

Theorem 2.4.3 *Let $\mathcal{A} : \mathcal{D}(\mathcal{A}) \subset X \to X$ be a closed linear operator acting on a Hilbert space X. For all $\lambda \in \rho(\mathcal{A})$,*

$$1/\mathrm{dist}(\lambda, \Lambda(\mathcal{A})) \leq \|\mathcal{R}(\lambda; \mathcal{A})\|.$$

If, in addition, $\mathbb{C}\backslash\mathrm{cl}(\mathrm{Num}(\mathcal{A}))$ is a connected set which does not intersect the resolvent set $\rho(\mathcal{A})$, then for all $\lambda \notin \mathrm{cl}(\mathrm{Num}(\mathcal{A}))$

$$1/\mathrm{dist}(\lambda, \Lambda(\mathcal{A})) \leq \|\mathcal{R}(\lambda; \mathcal{A})\| \leq 1/\mathrm{dist}(\lambda, \mathrm{Num}(\mathcal{A})).$$

Here, $\mathrm{cl}(E)$ stands for the closure of the set E. In general, the numerical range can be quite large. For example, Eigtool computes the numerical range of Godunov's matrix $\mathbf{G}$ to be roughly a circular region with radius of about 2500. Therefore, the upper bound for the norm of the resolvent (and the pseudospectra) contained in this theorem is too large. This only serves to emphasize the fact that the pseudospectra can be a much larger region than the spectrum.

Let us return to the issue of the transient growth of solutions to the general linear initial value problem (2.26). Recall that the solution is given in terms of the semigroup as $z(t) = \mathcal{S}(t)z_0$, where z_0 is the initial condition. Therefore, a lower bound on the norm of the semigroup will give an estimate of the transient growth of solutions. One such estimate is given by the pseudospectra [140].

Theorem 2.4.4 *If $\mathcal{A} : \mathcal{D}(\mathcal{A}) \subset X \to X$ generates a C_0-semigroupup $\mathcal{S}(t)$ over a Hilbert space X, then*

$$\sup_{t>0} \|\mathcal{S}(t)\| \geq \sup_{\varepsilon>0} \varepsilon^{-1}\beta_\varepsilon(\mathcal{A}), \quad \textit{where} \quad \beta_\varepsilon(\mathcal{A}) := \sup_{\lambda \in \Lambda_\varepsilon(\mathcal{A})} \mathrm{Re}(\lambda). \tag{2.27}$$

$\beta_\varepsilon(\mathcal{A})$ is called the ε-pseudospectral abscissa of $\mathcal{A}$ and measures how far the ε-pseudospectra extends into the right half plane. Therefore, the transient growth of solutions depends on the pseudospectra, or equivalently, the resolvent.

In the late 1980's and early 1990's, researchers began to examine the transient growth of solutions to the Orr-Sommerfeld/Squire equations. These researchers searched for the three-dimensional initial conditions that yield "optimal energy growth". Boberg and Brosa [22] examined energy growth in pipe Poiseuille flow and Gustavsson [63] did the same for plane Poiseuille flow. Butler and Farrell [35] used a variational method to investigate energy growth in plane Couette, plane Poiseuille and Blasius boundary layer flow. Reddy and Henningson [112] then used the above resolvent approach to again study optimal energy growth. These researchers found that certain initial conditions produced transient energy growth on the

order of R^3, where R is the Reynolds number. In certain cases this translates into an energy growth by factors of thousands even if the laminar flow is known to be asymptotically stable.

These efforts were accompanied by further studies which used resolvent techniques to examine transient growth of solutions [122] and the degree of non-normality of the Orr-Sommerfeld/Squire operator [113]. The discoveries of the extreme non-normality of the Orr-Sommerfeld/Squire operator and the large energy growth due to certain initial conditions led to a new transition scenario. Namely, a small perturbation to a laminar flow yields an initial condition that produces large transient growth. The flow is then "mixed" by the nonlinearity to produce turbulence. This scenario (or a slight modification thereof) has been proposed by several groups (see [5], [22], [61] and [143]).

As stated, this theory does not account for the failure of classical linear stability analysis to predict transition. If, for example, one had a Perron type theorem, then initial conditions near the laminar flow should relaminarize. On the other hand, inspired by a simple model ODE system, Trefethen et al. in [143] proposed that the domain of attraction for a laminar flow rapidly shrinks as the Reynolds number increases. Specifically, the authors hypothesized that the largest attracting ball about the laminar flow has radius $O(R^\gamma)$, with $\gamma < -1$. **One problem is that there may not be an attracting ball in the divergence free function space $\mathbf{H}(\Omega)$.** However, if this is the case, the largest attracting ball for the laminar flow would be extremely small for a large Reynolds number. Therefore, the laminar state could be asymptotically stable but practically unstable as far as experiments in a laboratory setting. This hypothesis has been further examined for various ODE model problems in the subsequent studies [5] and [6].

The original energy growth studies provide some heuristic evidence for the "energy growth plus nonlinear mixing" transition theory. However, it is not clear whether naturally arising perturbations to a laminar flow will take an optimal (or nearly optimal) form that will cause an extreme energy growth. Furthermore, even in the case of large energy growth, exactly how the nonlinearity "mixes the energy" and causes transition is not understood. The role of the nonlinearity in this theory has been largely unexplored.

As noted above, the conjecture that the basin of attraction for the laminar state rapidly shrinks mainly arose in light of similar behavior in ODE model problems. It is important to note that the basin of attraction depends on the norm. Thus, in infinite dimensional systems, this can include assuming that the initial data is smooth. For example, the infinite dimensional version of Perron's theorem (2.2.3) is only valid for $x_0 \in X^\alpha$ and $\|x_0\|_\alpha < \delta$. However, early experimental and numerical studies do provide evidence for this conjecture for plane Couette and Poiseuille flow (see [141] for a review). Theoretical evidence for this conjecture has also recently appeared using asymptotic analysis [39] and resolvent bounds (see [27], [93], [94]). However, the asymptotical analysis only gives an indication as to the size of the largest attracting ball for the laminar flow as $R \to \infty$. This is not necessarily an indication that the attracting ball is small for moderate values of the Reynolds number. As for the work based on resolvent methods, the upper bounds on the resolvent only provide *lower* bounds on the size of the largest ball of attraction about the laminar state. As discussed by Kreiss and Lorenz in [81], these estimates can turn out to be very pessimistic.

Therefore, the evidence for this conjecture is again incomplete.

Another possible mechanism for transition to turbulence has been proposed in light of the pseudospectral analysis of the Orr-Sommerfeld/Squire operator. Studies have shown that due to the non-normality of the Orr-Sommerfeld/Squire operator, the pseudospectra extends far into the right half plane even for very small values of ε (see, e.g., [113], [138], [143]). This leads to transient growth of solutions as discussed above (see Theorem 2.4.4). However, the alternate definition of the ε-pseudospectra given in Theorem 2.4.1 allows us to look at the extension of the pseudospectra into the right half plane from a different vantage point. Recall that the pseudospectra may be expressed as the union of the spectra of "nearby" operators (see Theorem 2.4.1) given by

$$\Lambda_\varepsilon(\mathcal{A}) = \{\lambda \in \mathbb{C} \,:\, \lambda \in \Lambda(\mathcal{A} + \mathcal{A}_\varepsilon), \text{ where } \mathcal{A}_\varepsilon \text{ is bounded and } \|\mathcal{A}_\varepsilon\| < \varepsilon\}.$$

Therefore, the fact that the pseudospectra of the Orr-Sommerfeld/Squire operator extends into the right half plane implies that there is a small perturbation to the linear operator that causes it to become unstable.

Trefethen et al. in [143] proposed this mechanism as an alternative to the shrinking domain of attraction theory conjectured in the same work. The authors noted that perhaps some imperfection in an experiment, such as small wall roughness, could possibly be a destabilizing perturbation to the Orr-Sommerfeld/Squire operator. The linearized problem with a small perturbation in the operator would yield an unstable laminar flow that could transition to turbulence at Reynolds numbers well below the critical value predicted by classical linear stability analysis and much nearer to experimental values. They pointed out that most randomly chosen perturbations to the (discretized) Orr-Sommerfeld/Squire operator did cause a destabilizing perturbation for certain Reynolds numbers. The authors also noted that there is no specific reason to expect that a naturally arising imperfection in an experiment can cause the linear operator to become unstable.

We shall show how a small unmodeled perturbation to the boundary can lead to a perturbation of the basic linear operator which is unstable. In particular, in chapter 5, we introduce a simplified form of wall roughness into a model two dimensional partial differential equation. There we show that a small wall roughness leads to a perturbation of both the linear and nonlinear terms in the original problem. Also, in certain cases, the perturbation will cause the linear operator to become unstable and solutions will transition. Therefore, it may not be unreasonable to expect that a small unmodeled disturbance in an experiment can cause the laminar flow state to become unstable. This model uncertainty may in fact be a key to predicting transition.

2.4.2 A Robust Control Theory Approach

In the previous section, we presented a transition scenario which is dependent on noise or imperfections in experiments. This scenario should not be too surprising since it is well known that transition is very sensitive to small disturbances in experiments such as wall roughness. Another "mostly linear" approach to transition, based on robust control theory,

also views small background noise as an important consideration in transition. In fact, this transition scenario is based on the assumption that transition is a noise sustained process. The approach to this theory is different from the resolvent techniques described above. We summarize this second approach below.

Often in applications, techniques from control theory are used to design a feedback control that stabilizes some component of a physical system. The feedback control takes in state information from sensors and acts in response to the state. Researchers have realized that a controller designed for a mathematically idealized system might not work well in applications when noise is present in a system. This sensitivity to noise seems to depend on whether the control is based on full or partial state information. For example, the linear quadratic regulator (LQR) controller, which is based on full state information, is very robust to noise entering the system. However, the linear quadratic Gaussian (LQG) controller, which is based on partial state information, is known to have zero robustness margin (see the simple example by Doyle [48]). In particular, for certain problems an arbitrarily small disturbance could destabilize the closed loop system. This led to the introduction of the more robust $\mathcal{H}^\infty$ (or Min-Max) feedback controller.

One approach to address the sensitivity of a system to noise is to examine the so called input-output properties of the system. Consider a differential equation over a (possibly infinite dimensional) state space X with output of the form

$$\begin{aligned} \dot{x}(t) &= \mathcal{A}x(t) + \mathcal{B}u(t) \\ y(t) &= \mathcal{C}x(t). \end{aligned}$$

Here, $x(\cdot)$ is the state, $u(\cdot)$ is the input (which we regard as a disturbance or noise) and $y(\cdot)$ is the output. The operator $\mathcal{A}$ is assumed to generate a C_0-semigroup, the input operator $\mathcal{B}$ represents how inputs enter the system and the observer $\mathcal{C}$ represents observations of the state. If the input comes from the boundary of a system, this will usually lead to an unbounded input operator $\mathcal{B}$. This will be demonstrated with an example in section 3.1.

Although robust control theory has been extended to infinite dimensional systems (see [44]), one must take care and not apply the finite dimensional theory to infinite dimensional problems. Again, many of the required technical details are ignored by those who use this theory to study energy amplification of noise in fluid flow. Here, we assume that $\mathcal{A}$ generates an exponentially asymptotically stable semigroup $\mathcal{S}(t)$, i.e., $\|\mathcal{S}(t)\| \leq Me^{-\omega t}$ for some $M \geq 1$ and $\omega > 0$. Taking the Laplace transform of the system yields

$$\hat{y}(s) = \mathcal{C}(sI - \mathcal{A})^{-1}\mathcal{B}\,\hat{u}(t) =: \mathcal{G}(s)\hat{u}(t),$$

where $\hat{f}(\cdot)$ represents the Laplace transform of $f(\cdot)$. The operator $\mathcal{G}(\cdot)$ is called the transfer function. Since the Laplace transform preserves norms, a reasonable way to measure the amplification of noise in a system is to use a norm estimate of the form

$$\| \hat{y}(\cdot) \|_Y = \| \mathcal{G}(\cdot)u(\cdot) \|_Y \leq \| \mathcal{G}(\cdot) \| \| u(\cdot) \|_Y.$$

The choice of norm determines the type of result.

Two commonly used norm on $\mathcal{G}(\cdot)$ are the $\mathcal{H}^2$ and $\mathcal{H}^\infty$ norms defined by

$$\|\mathcal{G}\|_{\mathcal{H}^2}^2 := \frac{1}{2\pi}\int_{-\infty}^{\infty} \|\mathcal{G}(i\omega)\|_{HS}^2 \, d\omega$$

and

$$\|\mathcal{G}\|_{\mathcal{H}^\infty}^2 := \sup_{\omega\in\mathbb{R}} \sigma_{\max}[\mathcal{G}(i\omega)],$$

respectively. Here, i is the imaginary unit, $\|\cdot\|_{HS}$ is the Hilbert-Schmidt norm and $\sigma_{\max}[\mathcal{K}]$ denotes the maximum singular value of $\mathcal{K}$. The Hilbert-Schmidt norm is given by $\|\mathcal{K}\|_{HS}^2 := \text{trace}(\mathcal{K}^*\mathcal{K}) = \sum \langle \phi_i, \mathcal{K}^*\mathcal{K}\phi_i\rangle_X = \sum \|\mathcal{K}\phi_i\|_X^2$, where $\{\phi_i\}$ is any orthonormal basis for the underlying Hilbert space X with inner product $\langle\cdot,\cdot\rangle_X$ and associated norm $\|\cdot\|_X$ (see [114]). For a matrix K, computing the Hilbert-Schmidt norm is equivalent to computing the standard matrix trace, $\text{trace}(K^*K)$.

Remark: Observe that these norms only make sense if $\mathcal{G}(\cdot)$ is Hilbert-Schmidt or nuclear. Thus, the infinite dimensional theory is limited by this assumption. If there are only a finite number of inputs or outputs, then the theory is more complete (see [44]). However, for boundary inputs the theory is incomplete.

To examine the sensitivity of fluid flow with respect to small disturbances, one may investigate the input/output properties of a system governed by the Orr-Sommerfeld/Squire operator. To do this, one needs realistic ways to represent disturbances entering the system and outputs leaving the system. An output often used in this approach is the velocity field (or the Fourier transform thereof). The Fourier transformed velocity components can be recovered using the relations (2.24). This allows us to *formally* define the unbounded and infinite rank output operator $\mathcal{C}$ by

$$\begin{bmatrix} \tilde{u} \\ \tilde{v} \\ \tilde{w} \end{bmatrix} = \mathcal{C}\begin{bmatrix} \tilde{v} \\ \tilde{\eta} \end{bmatrix} := \frac{1}{k_x^2+k_z^2}\begin{bmatrix} ik_x\frac{\partial}{\partial y} & -ik_z \\ k_x^2+k_z^2 & 0 \\ ik_z\frac{\partial}{\partial y} & ik_x \end{bmatrix}\begin{bmatrix} \tilde{v} \\ \tilde{\eta} \end{bmatrix}.$$

The input operator $\mathcal{B}$ may take many forms depending on the type of disturbance one wishes to model.

Farrell and Ioannou originally studied the input/output properties of the Orr-Sommerfeld/Squire system with the above output operator $\mathcal{C}$ in [52] and [53]. They chose to model the disturbances with a unitary disturbance operator $\mathcal{B}$ (i.e., $\mathcal{B}$ is bounded and $\mathcal{B}\mathcal{B}^* = I$) acting on stochastic white noise disturbance $u(\cdot)$ with zero mean. Notice that a unitary input operator excludes the possibility that the disturbances enter through the boundary. They computed the $\mathcal{H}^2$ norm and discovered in this case that the energy of small constant forcing disturbances could be amplified by an order of R^3. Bamieh and Dahleh followed in [9] and [10] by investigating the Orr-Sommerfeld/Squire system with the same $\mathcal{B}$ and $\mathcal{C}$ operators and "analytically computed" the $\mathcal{H}^2$ norm. Although this approach was formal, they also found that energy amplification of a constant forcing disturbances of order of R^3 is possible.

Both studies noted that the non-normality of the linear Orr-Sommerfeld/Squire operator was necessary for the large amplification of small disturbances.

These observations suggested another linear approach to transition. The essential idea is that a "small background noise" can be greatly amplified due to the non-normality of the linear operator causing a disturbance in the flow. Small noise then continues to produce disturbances in the flow which are mixed producing turbulence. Farrell and Ioannou in [52] suggest that the nonlinearity may be the cause of the continual mixing of disturbances that produces turbulence. However, the exact mechanism by which the mixing produces turbulence is not discussed.

As with the above pseudospectra/resolvent approach to linear stability analysis, this input/output approach to transition is also not complete. First, the linear analysis is again based on the Orr-Sommerfeld/Squire operator. As noted in the previous section, the transformation from the linearized Navier-Stokes equations to this operator has not been rigorously justified. Furthermore, it is not known whether these robust control theory techniques described here extend without restriction to the infinite dimensional problem defined by the Navier-Stokes equations. Also, this type of input/output analysis requires considerable effort to represent the disturbances causing transition. It has long been known that transition can be quite sensitive with respect to small wall roughness, however it is unknown how to effectively model wall roughness. Jovanović and Bamieh have recently considered the input/output properties of the Orr-Sommerfeld/Squire system with other forms of disturbance operators $\mathcal{B}$ and noise inputs $u(\cdot)$ in [73], [74], [75] and [76]. However, much work remains to be done in this area.

2.5 Summary of Spectral Stability Analysis

In this chapter, we presented a partial survey of methods to determine the stability properties of equilibria for both finite and infinite dimensional dynamical systems. We concentrated on spectral methods since this is currently the most popular method for determining stability characteristics of certain laminar flows. We noted that classical stability theory in finite dimensions may not necessarily extend to the infinite dimensional case. For the latter case, an appropriate abstract framework must be employed to study the stability of equilibria.

Also, we noted that stability analysis for fluid flows is largely incomplete. In the past, the majority of the stability analysis consisted of transforming the linearized Navier-Stokes equations to the Orr-Sommerfeld and Squire equations which are more amenable to analysis. Spectral analysis then provided critical Reynolds numbers at which certain flows should become unstable and thus transition to turbulence. In the fluid dynamics literature, this approach is rarely ever rigorously justified. Lyapunov methods have also be used in the infinite dimensional case. However, as with the spectral methods, to extend the standard theory to infinite dimensions requires care (see [145]). There are again instances where researchers have formally applied the finite dimensional results to flow problems without rigorous verification. In any case, it is well known that the critical Reynolds numbers obtained by the above methods have not always matched experimental values.

The new linear stability methods presented above have shed insight into the transition process. It now seems clear that the linearized Navier-Stokes operator is extremely sensitive with respect to small disturbances. If this is a key in the transition process, it may be possible to control transition by reducing the sensitivity to these disturbances. Also, since this research highlights the sensitivity of the flow to small disturbances in the boundary, it may be possible to take advantage of the sensitivity and develop controls that act on the boundary. Some progress has been made along these lines (see the review articles [18], [78]). We present two simple examples in chapter 5 that further support this point of view and suggest that feedback control may be a practical method to delay or control turbulence.

In spite of this progress, much remains to be done in order to complete the transition picture. In particular, the role of the nonlinearity in these new theories has not been explored. Do the nonlinear terms truly mix the increasing energy and cause the flow to become turbulent? If so, how does this mixing take place? These answers to these questions are very important and may provide further insight into the control of turbulence. One goal of this thesis is to investigate how the nonlinearity factors into the sensitivity of solutions of partial differential equations with respect to small disturbances. In particular, in Chapters 4 and 5, we examine the *sensitivities* of solutions with respect to small disturbances. In particular, we use sensitivity methods to measure how solutions change with respect to the disturbances. This is done by differentiating the solution with respect to the disturbances. We show how this method provides insight into the effects of small disturbances on the dynamics of a system. Also, the ideas from the new theories on transition presented above can be used in this method to show the potential of small disturbances to have a large impact on the behavior of solutions.

Chapter 3

Burgers' Equation

In this chapter, we focus on Burgers' equation to illustrate the basic ideas and to suggest a new transition mechanism. In the previous chapter the question was raised as to whether small wall roughness in a flow system could cause a laminar flow state to become unstable and transition to turbulence. Burgers' equation is an infinite dimensional system that is simple enough to analyze rigorously yet complex enough to capture the essential features of Navier-Stokes type problems. We are motivated by the two dimensional Burgers' equation

$$w_t(t,x,y) + w(t,x,y)w_x(t,x,y) + w(t,x,y)w_y(t,x,y) = \mu\nabla^2 w(t,x,y),$$

on a rectangular domain with periodic boundary conditions in the x direction and nonzero Dirichlet boundary conditions on the top and bottom walls,

$$w(t,x,0) = 1, \quad w(t,x,1) = -1.$$

Later, we examine how a simplified form of small wall roughness affects the formulation of the problem and also the solution.

In order to keep the discussion simple, we begin with the one dimensional Burgers' equation

$$w_t(t,x) + w(t,x)w_x(t,x) = \mu w_{xx}(t,x),$$

over a finite interval with various boundary conditions. We formulate this one dimensional partial differential equation as an abstract infinite dimensional equation so we can address existence and uniqueness of solutions, the equilibrium problem and the long time behavior of solutions. This problem is known to be sensitive with respect to small disturbances in the equation and boundary conditions. We review these results and provide possible connections with transition. This will again motivate the study of small disturbances in the transition problem.

Burgers' equation is among the simplest examples of a nonlinear partial differential equation (PDE) that captures many of the patterns found in the Navier-Stokes equations and thus has been extensively studied by many authors. Among those to originally study Burgers' equation were Burgers [28], Cole [42] and Hopf [71] in the late 1940's and early 1950's.

A more recent general study was done by Fletcher in the early 1980's [55]. Fletcher's work is especially interesting in that it shows how Burgers' equation can be used to model a wide variety of physical phenomena. However, the main reason for the great interest in Burgers' equation is that it can be viewed as a simplified model of fluid flow. In particular, Burgers' equation shares with the Navier-Stokes equations a second order diffusion term balanced against a quadratic nonlinear first order convection term.

Since the Navier-Stokes equations are complex, many researchers use Burgers' equation as a testing ground for tools they hope to eventually use on the Navier-Stokes equations. For instance, due to the immense difficulty in simulating the Navier-Stokes equations, many numerical methods are first tested on Burgers' equation. (See the recent works [7], [46], [57], [84], [92], [110] and the references therein.) Also, due to the great interest in flow control, Burgers' equation has been a model problem for many studies on theoretical and numerical methods for control. (See [3], [31], [32], [50], [79], [83], [96], [144] and the references therein.)

3.1 Weak Formulation

Here we construct a weak formulation of the one dimensional Burgers' equation over a finite interval with Dirichlet or Neumann boundary conditions. In both cases we allow nonhomogeneous boundary conditions which could arise from boundary disturbances or boundary control inputs. The Neumann problem can be formulated weakly in the usual way while the weak Dirichlet problem necessitates a nonstandard framework. This section is similar to the presentation given in [30].

Consider the one dimensional Burgers' equation on a finite interval $\Omega = (a, b)$

$$w_t + ww_x = \mu w_{xx} + f,$$

with constant nonhomogeneous Dirichlet boundary conditions

$$w(t, a) = w_a, \quad w(t, b) = w_b,$$

and initial condition

$$w(0, x) = w_0(x).$$

Here, $\mu > 0$ is a positive constant and the boundary values w_a and w_b are independent of time. Suppose $h(\cdot)$ is an equilibrium for the above system (whose existence we will discuss in section 3.3.2) and define the fluctuations $z(\cdot, \cdot)$ by $w(t, x) = h(x) + z(t, x)$. The fluctuations satisfy the nonlinear convection-diffusion (NLCD) equation

$$z_t + zz_x = \mu z_{xx} - (hz)_x \tag{3.1}$$

with homogeneous Dirichlet boundary conditions

$$z(t, a) = 0, \quad z(t, b) = 0 \tag{3.2}$$

and initial condition

$$z(0,x) = z_0(x) := w_0(x) - h(x). \tag{3.3}$$

We focus on this system to illustrate the main ideas. If there is a "small input" (or unmodeled disturbance) applied at the boundary, then the disturbed NLCD system has the form

$$z_t + zz_x = \mu z_{xx} - (hz)_x, \tag{3.4}$$
$$z(t,a) = u_a(t), \quad z(t,b) = u_b(t), \tag{3.5}$$
$$z(0,x) = z_0(x) := w_0(x) - h(x). \tag{3.6}$$

Here, $u_a(t)$ and $u_b(t)$ are inputs and may be thought of as unmodeled forces acting at the boundary or as control inputs. We also consider this problem with Neumann boundary conditions with input given by

$$z_x(t,a) = u_a(t), \quad z_x(t,b) = u_b(t). \tag{3.7}$$

We place these equations in weak form to demonstrate how the small boundary inputs affect the equations. Let $X = L^2(\Omega)$ with the standard inner product and norm and let $V = H^1(\Omega)$. Multiply the NLCD equation (3.4) by a test function $\varphi \in V$, integrate over the domain and integrate the second order term by parts to get

$$\frac{\partial}{\partial t}\langle z, \varphi\rangle_X = \mu\Big(z_x(b)\varphi(b) - z_x(a)\varphi(a)\Big) - \mu\langle z_x, \varphi_x\rangle_X - \langle (hz)_x, \varphi\rangle_X - \langle zz_x, \varphi\rangle_X . \tag{3.8}$$

For the Neumann problem, the boundary conditions (3.7) can be applied to give

$$\frac{\partial}{\partial t}\langle z, \varphi\rangle_X = \mu\Big(u_b\varphi(b) - u_a\varphi(a)\Big) - \mu\langle z_x, \varphi_x\rangle_X - \langle (hz)_x, \varphi\rangle_X - \langle zz_x, \varphi\rangle_X .$$

This weak problem can be formulated as an abstract differential equation on V' by (see [17], [95])

$$\dot{z}(t) = \mathcal{A}z(t) + \mathcal{F}(z(t)) + \mathcal{B}u(t).$$

We can rewrite the boundary terms resulting from the integration by parts as

$$u_b\varphi(b) - u_a\varphi(a) = (\delta_b\varphi)u_b - (\delta_a\varphi)u_a,$$

where δ_p is the delta functional given by $\delta_p\varphi(\cdot) = \varphi(p)$. Therefore, it appears that the $\mathcal{B}$ operator involves the delta functional and therefore will be unbounded. The precise formulation of the input operator $\mathcal{B}$ provided in the above references confirms that $\mathcal{B}$ is unbounded.

For the Dirichlet problem, the boundary inputs do not enter the above weak form (3.8). If we instead take $V = H_0^1$, then the boundary terms resulting from the integration by parts vanish. In order to explicitly introduce the boundary inputs into the weak form, we must integrate by parts a second time. Therefore, let $W = H^2 \cap H_0^1$ and rewrite the nonlinear

term zz_x as $(z^2/2)_x$. Then for $\varphi \in W$, integrate all terms in (3.8) by parts to get

$$\frac{\partial}{\partial t}\left\langle z,\varphi\right\rangle_X = -\mu\Big(u_b\varphi_x(b) - u_a\varphi_x(a)\Big) + \mu\left\langle z,\varphi_{xx}\right\rangle_X + \left\langle hz,\varphi_x\right\rangle_X + \left\langle z^2/2,\varphi_x\right\rangle_X.$$

This very weak problem can be formulated as a differential equation on W' by (again, see [17], [95])

$$\dot{z}(t) = \mathfrak{A}z(t) + \mathfrak{F}(z(t)) + \mathfrak{B}u(t).$$

For this problem, rewriting the boundary terms gives

$$u_b\varphi_x(b) - u_a\varphi_x(a) = (\delta_b'\varphi)u_b - (\delta_a'\varphi)u_a,$$

where δ_p' is the distributional derivative of the delta functional. Again, this can be made precise and the input operator $\mathfrak{B}$ is unbounded.

3.2 Existence and Uniqueness of Solutions

We now review the basic existence and uniqueness theory for solutions of the one dimensional nonlinear convection-diffusion (NLCD) equation under Dirichlet and Neumann boundary conditions. The solution theory for these systems is more complete than the theory for the Navier-Stokes equations. In contrast to the three dimensional case for the NS equations, the one dimensional NLCD equation under various boundary conditions (and boundary inputs) is known to admit unique solutions that exist for all time. However, we also discuss how the solution theory for the "natural" abstract formulations given above in the case of boundary inputs is incomplete.

We concentrate on solution theory for the one dimensional forced NLCD equation on the finite interval $\Omega = (a,b)$ given by

$$z_t(t,x) + z(t,x)z_x(t,x) = \mu z_{xx}(t,x) - (h(x)z(t,x))_x + f(t,x), \tag{3.9}$$

with initial condition (3.6) and one of three types of boundary conditions. We consider the Dirichlet (3.5) and Neumann (3.7) boundary conditions with small inputs and also mixed boundary conditions given by

$$z_x(t,a) = k_a z(t,a), \quad z_x(t,b) = -k_b z(t,b), \tag{3.10}$$

with k_a and k_b given non-negative constants. The mixed boundary conditions may be viewed as a special case of the Neumann boundary conditions with $u_a(t) = k_a z(t,a)$ and $u_b(t) = -k_b z(t,b)$. The precise nature of the forcing function will be specified later.

For many years, the standard way to examine solution properties of Burgers' equation (the NLCD equation with $h = 0$) has been through the use of the Cole-Hopf transformation

(see [42], [71], or more recently [19]). The change of variables

$$z(t,x) = -2\mu \frac{\partial}{\partial x} \log(\psi(t,x)) = -2\mu \frac{\psi_x(t,x)}{\psi(t,x)}$$

transforms the nonlinear Burgers' equation (3.9) to the *linear* heat equation. This can be seen by computing

$$z_t + zz_x - \mu z_{xx} = \frac{\partial}{\partial x}\left(\frac{\psi_t - \mu\psi_{xx}}{\psi}\right) = \frac{f}{-2\mu},$$

which leads to

$$\psi_t = \mu\psi_{xx} + g\psi, \quad \text{where} \quad g(t,x) = \int_a^x \frac{f(t,s)}{-2\mu}\, ds$$

which makes sense if $f(t,\cdot) \in L^1(\Omega)$ for all t. The initial data for the heat equation is obtained by inverting the transformation to give

$$\psi_0(x) = \exp \int_a^x \frac{z_0(s)}{-2\mu}\, ds,$$

which again makes sense whenever $z_0(\cdot) \in L^1(\Omega)$. One can then use the known properties of the heat equations to draw conclusions about solutions of Burgers' equation.

However, there are limitations to this approach. The Dirichlet boundary conditions are transformed into mixed boundary conditions for the heat equation while other types of boundary conditions can lead to ill-posed problems. There is a more complicated transformation [37] that may be used for the Neumann problem [45] and perhaps for other types of boundary conditions. However, the most significant limitation to this transformation is that it and other similar transformations only work for certain classes of problems. Our motivation for focusing on the NLCD equation is to develop ideas that might extend to more complex problems such as the Navier-Stokes system. Thus, we shall avoid these specialized transformations as they are not valid for most 2D and 3D systems.

We summarize the main existence and uniqueness results for weak solutions. These results have been obtained by employing an abstract framework of the type presented above. Many of the results cited below do not consider the cases of including the convection term $(hz)_x$, the non-homogeneous boundary conditions or non-zero forcing functions. However, in many instances the results can easily be extended to these cases (see [43], [86], [134], [135], [136]). In section 4.3, we present a local uniqueness result for strong solutions to the Dirichlet problem with the convection term. It is likely that this result can be extended to show global uniqueness, but we did not consider this problem here.

For the case of homogeneous Dirichlet boundary conditions, one may place the one dimensional Burgers' equation into an abstract $L^2(\Omega)$ state space formulation quite similar to that given above for the Navier-Stokes equations [97]. In this case one does not need a divergence free subspace of $L^2(\Omega)$ and this allows for more general problem data. Ly, Mease and Titi applied the general theory of Ghidaglia and Temam to this formulation to prove

the existence and uniqueness of weak solutions for all time given very general initial data [97, Theorem 1].

Theorem 3.2.1 *If the initial data $z_0 \in L^2(\Omega)$, then for every $T > 0$ Burgers' equation (the NLCD equation (3.4)-(3.6) with $h = 0$) without forcing and with homogeneous Dirichlet boundary conditions (i.e., $u_a \equiv u_b \equiv 0$) has a unique weak solution z on $[0, T]$ that satisfies*

$$z \in C(0, T; L^2(\Omega)) \cap L^2(0, T; H_0^1(\Omega)).$$

Similar results can be obtained using semigroup methods for parabolic equations (see [64] or [109]).

The case of mixed or Neumann boundary conditions is more difficult due to the fact that the nonlinearity is not conservative as was discussed in section 3.1. However, this obstacle has recently been overcome by employing an abstract formulation which again is similar to that for the Navier-Stokes equations. The following is a result of Byrnes, Gilliam and Shubov [36, Theorem 2.1].

Theorem 3.2.2 *If the initial data $z_0 \in L^2(\Omega)$, then for every $T > 0$ Burgers' equation (the NLCD equation (3.4), (3.6) with $h = 0$) without forcing and with mixed (3.10) or homogeneous Neumann (3.7) boundary conditions (i.e., $u_a \equiv u_b \equiv 0$) has a unique weak solution z on $[0, T]$ that satisfies*

$$z \in C(0, T; L^2(\Omega)) \cap L^2(0, T; H^1(\Omega)).$$

This theorem also holds for a certain class of smooth forcing functions. Similar results have also been obtained for the mixed and Neumann problems by Ly, Mease and Titi [97] and Cao and Titi [38].

3.3 The Equilibrium Problem and Long Time Behavior of Solutions

Now that we have reviewed the main theory concerning solutions of the one dimensional time dependent Burgers' equation, we now turn to the equilibrium problem. Specifically, consider the steady boundary value problem on $\Omega = (a, b)$ given by

$$w(x)w_x(x) - \mu w_{xx}(x) = f(x), \tag{3.11}$$

with μ a positive constant accompanied by either Dirichlet boundary conditions

$$w(a) = u_a, \quad w(b) = u_b, \tag{3.12}$$

or Neumann boundary conditions

$$w_x(a) = u_a, \quad w_x(b) = u_b, \tag{3.13}$$

where u_a and u_b are given constants. For simplicity, we focus on the homogeneous Dirichlet problem, the non-homogeneous Dirichlet problem with $u_a > u_b$ and the homogeneous Neumann problem. We also briefly mention results for the case of mixed boundary conditions as considered in the previous section.

In contrast to the Navier-Stokes equations, the theory for the steady one dimensional Burgers' equation is complete. The Dirichlet problem has a unique equilibrium, the Neumann problem has an infinity of equilibria and the mixed problem bridges the gap with one or more equilibria. We will not discuss the equilibrium problem for the mixed boundary conditions any further here, see [8] for more details. In most cases solutions to the time dependent problem are known to tend to these equilibria asymptotically. Also, it is known that small disturbances to the boundary conditions can have dramatic effects on the nature of the equilibria. This in turn can change the long time behavior of solutions. As discussed in the introduction, this extreme sensitivity of solutions with respect to small disturbances may have implications for transition to turbulence in real flows. We return to this idea at the end of the chapter.

3.3.1 Dirichlet Boundary Conditions

First, consider the steady Dirichlet problem (3.11), (3.12). For the homogeneous case without forcing, i.e., $u_a = u_b = 0$ and $f = 0$, it is clear that the zero function is an equilibrium. Also, due to the conservative nature of the nonlinear term, one can easily show that solutions of the time dependent Burgers' equation without forcing (3.9) approach zero in L^2.

Lemma 3.3.1 *Let $z(t,x)$ be the solution to the time dependent Burgers' equation (the NLCD equation (3.4)-(3.6) with $h = 0$) on $\Omega = (a,b)$ without forcing, with zero Dirichlet boundary conditions (i.e., $u_a \equiv u_b \equiv 0$) and with initial condition $z_0 \in L^2$. Then z approaches zero exponentially fast in the L^2 norm.*

Proof: By Theorem 3.2.1, the solution to the time dependent problem $z(t,\cdot)$ is in H_0^1 for any $t > 0$. Take the L^2 inner product of the Burgers' equation (3.9) with the solution $z(t,x)$, integrate over the domain and integrate by parts to get

$$\frac{d}{dt}\frac{1}{2}\left\|z(t,\cdot)\right\|_{L^2}^2 = -\mu\left\|z_x(t,\cdot)\right\|_{L^2}^2.$$

for any $t > 0$. Note that the nonlinear term has dropped out due to the zero boundary conditions and the integration by parts. Notice that since $z \in H_0^1$,

$$\|z\|_{L^2}^2 = \int_a^b z^2\,dx = \int_a^b 1\cdot z^2\,dx = -\int_a^b 2xzz_x\,dx \le c\left\|z\right\|_{L^2}\left\|z_x\right\|_{L^2},$$

where we have used Hölder's inequality and set $c = \max_{a\le x\le b}|2x| = 2\max\{|a|,|b|\}$. This implies $\left\|z\right\|_{L^2} \le c\left\|z_x\right\|_{L^2}$, or $-\left\|z_x\right\|_{L^2}^2 \le -c^{-2}\left\|z\right\|_{L^2}^2$. Combining this with the above inequality gives

$$\frac{d}{dt}\left\|z(t,\cdot)\right\|_{L^2}^2 = -\mu\left\|z_x(t,\cdot)\right\|_{L^2}^2 \le -\mu c^{-2}\left\|z(t,\cdot)\right\|_{L^2}^2$$

for any $t > 0$. Applying Gronwall's inequality gives

$$\|z(t,\cdot)\|_{L^2}^2 \leq e^{-\mu t/c^2} \|z_0\|_{L^2}^2$$

for any $t > 0$. Therefore, for any initial data in L^2, the solution tends to zero exponentially fast in the L^2 norm. □

The following result is due to Ly, Mease and Titi [97, Theorem 2].

Theorem 3.3.1 *Let $z(t,x)$ be the solution to the time dependent Burgers' equation (the NLCD equation (3.4)-(3.6) with $h = 0$) on $\Omega = (a,b)$ without forcing, with zero Dirichlet boundary conditions (i.e., $u_a \equiv u_b \equiv 0$) and with initial condition $z_0 \in H_0^1$. Then z approaches zero exponentially in the H^1 norm, i.e.,*

$$\|z(t,\cdot)\|_{H^1}^2 \leq Me^{-\mu t/(b-a)^2} \|z_0\|_{H^1}^2,$$

where M is a positive constant depending on a, b, μ and $\|z_0\|_{H^1}$.

Therefore, the zero state is the only equilibrium in this case and all solutions of the time dependent problem converge to zero either in the L^2 or H^1 norm depending on the initial data.

For nonhomogeneous Dirichlet boundary data, the situation is similar. G. Kreiss and H.-O. Kreiss showed that there is a unique equilibrium in [80].

Theorem 3.3.2 *The steady Burgers' Dirichlet problem (3.11), (3.12) with $f \equiv 0$ has a unique smooth solution for any u_a and u_b.*

Due to the simplicity of the problem, the solution can be given in a closed form.

Lemma 3.3.2 *If $f \equiv 0$ and the Dirichlet boundary data satisfies $w(a) = u_a > u_b = w(b)$, then the unique smooth solution to the steady one dimensional Burgers' equation (3.11) with Dirichlet boundary conditions (3.12) is a hyperbolic tangent profile of the form*

$$h(x) = c\tanh\left(\frac{c}{2\mu}(d-x)\right), \tag{3.14}$$

where c and d are constants.

Proof: In the absence of forcing the steady Burgers' equation can be written as

$$\frac{\partial}{\partial x}\left(\frac{1}{2}w^2(x) - \mu w_x(x)\right) = 0, \quad \text{or} \quad \mu w_x(x) = \frac{1}{2}\left(w^2(x) - c_0\right), \tag{3.15}$$

where c_0 is a constant. Since $w(a) = u_a > u_b = w(b)$, the solution $w(\cdot)$ must decrease somewhere in the interval (a,b) and so $w_x(\cdot)$ must be also be negative somewhere in the interval. Then (3.15) implies that c_0 must be positive, say $c_0 = c^2$, and the above equation

can be solved exactly to give

$$w(x) = c \tanh\left(\frac{c}{2\mu}(d-x)\right),$$

where c and d are constants. □

This hyperbolic tangent profile is nearly constant throughout the interval (a, b) with a "shock" located somewhere in the interior of the interval (see figure 3.1). The shock becomes more pronounced as μ becomes small. In certain cases, the shock location can be determined exactly.

Corollary 3.3.1 *Suppose $f \equiv 0$ and $u_a = -u_b$ with $u_b < 0$ and let $h(\cdot)$ be the unique solution of the steady Burgers' Dirichlet problem (3.11), (3.12) given by (3.14). Then , $h(\cdot)$ is odd about $x = (b+a)/2$, i.e., $h(x) = -h(b+a-x)$. Therefore, $d = (b+a)/2$ and $h((b+a)/2) = 0$.*

Proof: Make the change of variable $y = b+a-x$. Then the function $\tilde{w}(y) := -w(b+a-y)$ also satisfies the steady Burgers' equation. Since solutions are unique, it must be that $w(x) = -w(b+a-x)$. The hyperbolic tangent profile (3.14) satisfies this condition only if $d = (b+a)/2$. □

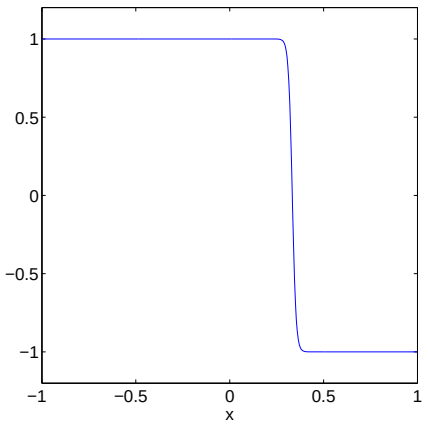

Figure 3.1: A sample hyperbolic tangent profile of the form (3.14) with $c = 1$, $d = 1/3$ and $\mu = .01$.

Using the Cole-Hopf transformation, one can show that the solution to the time dependent problem will converge to this unique equilibrium for any initial data in L^1. Without the transformation, it seems likely that one can use abstract monotonicity arguments (see [106], [126] and the references therein) to prove the convergence of "most" solutions to the unique equilibrium state. In particular, the convergence would only be guaranteed for a certain class of smooth initial data. We will not explore these methods here. Also, in the presence

of a forcing function, Hill and Süli showed that under certain conditions on the problem data that there is a unique equilibrium and that all solutions of the time dependent problem converge to that equilibrium in the L^1 norm [70, Theorem 3.2].

Following the work of Kreiss and Kreiss, researchers began to notice that solutions to the steady Burgers' problem (3.11), (3.12) could move an order of magnitude by slightly perturbing the Dirichlet boundary values. One of the first to notice this phenomenon was Bohé who studied in [25] the more general steady problem

$$\mu w_{xx} = f(w)g(w_x), \quad w(a) = u_a, \quad w(b) = u_b,$$

with certain conditions on $f(\cdot)$ and $g(\cdot)$. Bohé found both theoretically and numerically that solutions could move by an order of magnitude when u_a or u_b was perturbed by a slight amount. Studies of the time dependent Burgers' equation (and other similar problems) followed by Laforgue and O'Malley ([87], [88], [89], [90]), Renya and Ward ([116], [117], [146], [147]) and others [60]. Their studies found that given an arbitrary initial condition for the time dependent problem, the solution could develop a shock after an order one unit of time and *slowly* converge to a steady hyperbolic tangent profile. They found that the location of the shock could move by an order of magnitude by perturbing the equation and/or the boundary conditions by an exponentially small amount.

We briefly present two examples to show how small disturbances to the problem can greatly affect the long time behavior of solutions. Laforgue and O'Malley in [88] studied the following perturbation to the time dependent Burgers' equation with Dirichlet boundary conditions given by

$$\begin{aligned} z_t &= \mu z_{xx} + \left(z + b_1 e^{-a/\mu}\right) z_x + b_2 e^{-a/\mu} \\ z(t,-1) &= -1 + 2b_3 e^{-a/\mu}, \quad z(t,1) = 1 + 2b_4 e^{-a/\mu}, \end{aligned}$$

where $0 < a < 1$ is a constant and the constants b_i are not all zero. (The sign change on the nonlinear term only changes the sign of the unique steady state.) Corollary 3.3.1 implies that if $b_i = 0$ for each i, then the correct steady state solution is given by the hyperbolic tangent profile (3.14) with $d = 0$. This solution has a shock precisely at $x = 0$. If the b_i are not all zero, then set $b(\mu) = \sum_{i=1}^{4} b_i - b_2\mu$. Using asymptotic analysis, Laforgue and O'Malley showed in [88] that as $\mu \to 0$ the shock location x_{shock} of the disturbed steady state problem is given asymptotically by (up to exponentially small terms) [88, Equation 34]

$$x_{\text{shock}} \sim \begin{cases} 1 - a + \mu \log|b(\mu)|, & \text{if} \quad b(\mu) < 0 \\ 0, & \text{if} \quad b(\mu) = 0 \\ -1 + a - \mu \log|b(\mu)|, & \text{if} \quad b(\mu) > 0. \end{cases}$$

Therefore the shock (and thus the solution) can move an incredible amount even though the equation and boundary conditions are only slightly perturbed.

Another example given by Reyna and Ward in [117] involved a time dependent Burgers' equation with perturbed boundary conditions given by

$$z_t + zz_x = \mu z_{xx}$$
$$\mu z_x(t,0) - \kappa_1[z(t,0) - \alpha] = 0, \quad \mu z_x(t,1) + \kappa_2[z(t,1) + \alpha] = 0,$$

where α, κ_1 and κ_2 are all positive constants. With undisturbed Dirichlet boundary conditions $z(t,0) = \alpha$ and $z(t,1) = -\alpha$, Corollary 3.3.1 forces $d = 1/2$ in the steady hyperbolic tangent solution (3.14) and therefore the shock is located at $x = 1/2$. For the disturbed problem, Reyna and Ward used asymptotic analysis to show that as $\mu \to 0$ the shock location x_{shock} of the steady solution is given asymptotically by [117, Proposition 2]

$$x_{\text{shock}} \sim \frac{1}{2} - \frac{\mu}{2\alpha} \log \frac{\kappa_1(\alpha - \kappa_2)}{\kappa_2(\alpha - \kappa_1)},$$

whenever $(\alpha - \kappa_2)(\alpha - \kappa_1) > 0$. Again, the shock location can be moved by an order of magnitude by a small perturbation to the boundary conditions. If this last inequality is not satisfied, the solution undergoes an even more drastic change. The steady solution no longer possesses a "shock" and can also be unstable. In this last case, solutions will "crash" into one of the boundaries of the domain. This is in direct contrast to the undisturbed Dirichlet boundary conditions where solutions must converge to the unique steady equilibrium.

3.3.2 Neumann Boundary Conditions

Solutions to Burgers' equation with nonhomogeneous Dirichlet boundary conditions can be "supersensitive" with respect to exponentially small perturbation to the boundary data. As can be seen from the above two examples, the perturbations cannot necessarily be arbitrarily small and still move the solution by an order of magnitude. However, solutions to the homogeneous Neumann problem can be "infinitely sensitivity" to disturbances.

For this problem, the steady state solutions are again easily determined.

Lemma 3.3.3 *If $f \equiv 0$ and $u_a = u_b = 0$, then constant functions are the only solutions of the steady Burgers' equation (3.11) with homogeneous Neumann boundary conditions (3.13).*

Proof: By inspection, it is easily seen that any constant function is a solution. In a similar manner to the Dirichlet problem, any nonconstant solution must be a hyperbolic tangent profile of the form (3.14). Differentiating, we obtain

$$h_x(x) = -\frac{c^2}{2\mu}\text{sech}^2\left(\frac{c}{2\mu}(d - x)\right)$$

which cannot equal zero at the endpoints $x = a$ or $x = b$ unless $c = 0$. Therefore, constant functions are the only steady solutions. □

Like the Dirichlet case, the precise behavior of the long time behavior of solutions to the time dependent problem is also known. Provided the initial condition is continuous, Cao and Titi recently proved that all trajectories must approach a constant function [38, Theorem 9].

Theorem 3.3.3 *If the initial data $z_0(\cdot) \in C[a,b]$, the forcing $f \equiv 0$, the boundary values $u_a \equiv u_b \equiv 0$ and $z(t,x)$ is the solution to the time dependent Burgers' equation with homogeneous Neumann boundary conditions (the NLCD equation (3.4), (3.6), (3.7) with $h \equiv 0$), then there exists a constant c such that*

$$\sup_{x \in [a,b]} |z(t,x) - c| \longrightarrow 0 \quad as \quad t \to \infty.$$

Unfortunately, this theorem does not reveal the value of the constant c. However, for a certain class of initial data, one can exactly determine the long time behavior of solutions to the time dependent problem. Allen et al. noticed that solutions to the time dependent problem can possess a certain symmetry and proved the following corollary [2, Lemma 2.1].

Corollary 3.3.2 *Define $C_{os}[a,b]$ to be the class of all functions that are continuous and odd symmetric on $[a,b]$, i.e., $z_0(x) = -z_0(b+a-x)$ for all $x \in [a,b]$. If $z_0(\cdot) \in C_{os}[a,b]$, then the solution $z(t,x)$ to the time dependent problem satisfies*

$$\lim_{t \to \infty} z(t,x) = 0, \quad for\ every\ x \in [a,b].$$

In addition, $z(t,\cdot) \in C_{\text{os}}[a,b]$ for all $t > 0$.

Proof: The solution $z(t,x)$ to the time dependent problem in unique by Theorem 3.2.2. Make the change of variable $y = b + a - x$. Then $\tilde{z}(t,y) = -z(t, b+a-y)$ also satisfies the time dependent problem since the odd symmetric initial condition $z_0(\cdot)$ is unchanged by the transformation. Since the solution is unique, it must be that $z(t,x) = -z(t, b+a-x)$ for all $x \in [a,b]$ and all $t > 0$. By theorem 3.3.3, the solution must approach a constant function as $t \to \infty$. That constant function must be odd symmetric and is therefore identically zero. □

In spite of this result, numerical experiments with certain asymmetric initial data have produced numerical solutions which converge to a nonzero steady state as $t \to \infty$ (see [29], [98], [108]). Figure 3.2 shows a solution computed using the group finite element method (see section 5.1) converging to the correct steady state (the zero function), while figure 3.3 shows another numerical solution quickly converging to a nonzero steady state. Notice the nonzero steady state has a "shock" and is an order of magnitude larger than the zero function. This phenomenon was studied extensively by Allen et al. in [2] and was shown to be a result of finite precision arithmetic. The false nonzero steady state solution appearing in the simulations was also shown in [2] to be a solution of the steady Burgers' equation (and therefore a hyperbolic tangent shock profile of the form (3.14)) with *nonzero* Neumann boundary conditions

$$w_x(0) = -\varepsilon = w_x(1),$$

where $\varepsilon > 0$ can be *arbitrarily* small.

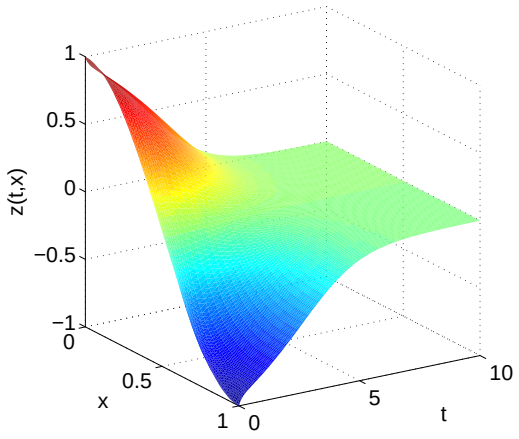

Figure 3.2: Numerical solution of the time dependent Burgers' equation with homogeneous Neumann boundary conditions (3.4), (3.6), (3.7) over $(0,1)$ with $h, f \equiv 0$, $\mu = .1$ and $z_0(x) = \cos(\pi x)$ computed using the group finite element method with 32 equally spaced nodes.

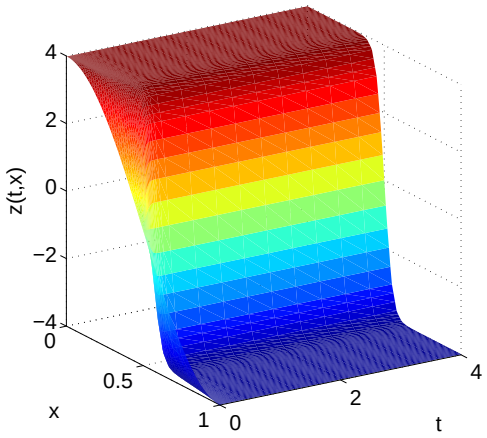

Figure 3.3: Numerical solution of the time dependent Burgers' equation with homogeneous Neumann boundary conditions (3.4), (3.6), (3.7) over $(0,1)$ with $h, f \equiv 0$, $\mu = .1$ and $z_0(x) = 4\cos(\pi x)$ computed using the group finite element method with 32 equally spaced nodes.

Therefore, solutions to Burgers' equation with homogeneous Neumann boundary conditions can be infinitely sensitive to disturbances in the boundary data. An arbitrarily small perturbation causes the solution to undergo an transition to an order one steady state. This phenomenon might be expected from a contrived example, but it is surprising that it can be seen in a relatively simple problem such as Burgers' equation.

3.4 Discussion

In this chapter, we formulated a one dimensional nonlinear convection-diffusion equation with both Dirichlet and Neumann boundary conditions as abstract differential equations. We also considered inputs entering the problem through the boundary conditions. The general framework of Ghidaglia and Temam does not provide existence and uniqueness results for the Neumann problem. Therefore, special techniques were required to construct appropriate theoretical tools to handle this situation.

The motivation for examining the one dimensional Burgers' equation came from a particular two dimensional Burgers' equation presented in the introduction to this chapter. Much of the framework developed above naturally extends to higher dimensions. In particular, once a change of variables is performed to transform the nonhomogeneous Dirichlet problem to a homogeneous problem, the resulting nonlinearity will also be conservative. This is similar to the equations for the fluctuations about an equilibrium for both the Navier-Stokes and Burgers' equations with Dirichlet boundary conditions. A weak formulation for the 2D Burgers' problem with boundary inputs can also be developed in a similar fashion. The Dirichlet map introduced above to define the boundary input operator extends naturally to very general domains in higher dimensions although the exact form of the operator may not be known as it is here (see [17], [95]).

Almost everything is known about solution of the 1D Burgers' equation with various boundary conditions due to its relative simplicity. This is not true of the Navier-Stokes equations. Also, small disturbances can affect the location of equilibria and the long time behavior of solutions to Burgers' equation. For Dirichlet boundary conditions, a small disturbance in the boundary causes the equilibrium state to be moved by an order of magnitude. Even though in the undisturbed system one can prove that all solutions must approach this unique equilibrium, a small perturbation causes solutions to "transition" to another steady state. Solutions to the Neumann problem possesses an even greater sensitivity with respect to small disturbances. In this case, an arbitrarily small perturbation in the boundary condition causes the equilibrium to move an order of magnitude and solutions again transition. This phenomenon occurs in practice when one simulates the undisturbed problem.

Due to the many similarities between Burgers' equation and the Navier-Stokes equations, it is possible that small disturbances can also drastically alter solution to the Navier-Stokes equations. Specifically, this extreme sensitivity with respect to small disturbances might also be present in flow experiments. In many cases, flows should theoretically return to a laminar state for certain values of the Reynolds number, yet in practice the flow will transition to turbulence at these same values. These examples with Burgers' equation raise the possi-

bility that small disturbances in flow systems cannot be neglected in studying transition to turbulence. Extremely small disturbances could cause a flow to transition even though the flow would remain laminar in an idealized system.

More work is required to fully understand the role of small disturbances in flow problems. Therefore, in the upcoming chapters, we examine several model problems that share similarities with the Navier-Stokes equations. In particular, we study the *sensitivities* of solutions with respect to small perturbations in the system. In the next chapter, we formulate the continuous sensitivity equation method for ODE model problems and a one and two dimensional nonlinear convection-diffusion equation.

Chapter 4

The Continuous Sensitivity Equation Method

We now turn to the question of sensitivities for the problems discussed above. In particular, we employ sensitivity analysis to investigate how solutions change as a disturbance parameter is varied. To motivate the ideas, consider the two dimensional Burgers' equation

$$w_t(t,x,y) + w(t,x,y)w_x(t,x,y) + w(t,x,y)w_y(t,x,y) = \mu\nabla^2 w(t,x,y).$$

defined on the rectangular domain $\Omega = (0,1) \times (0,1)$ with periodic boundary conditions in the x direction and nonzero Dirichlet boundary conditions on the top and bottom walls. Thus, $w(t,x,y)$ satisfies the boundary conditions

$$w(t,x,0) = 1, \quad w(t,x,1) = -1.$$

If $h(x,y)$ is an an equilibrium state (whose existence we will discuss in section 4.4), one can examine the fluctuations z about the equilibrium h by setting $z(t,x,y) = w(t,x,y) - h(x,y)$. The fluctuations z satisfy the nonlinear convection diffusion (NLCD) equation

$$z_t + zz_x + zz_y = \mu\nabla^2 z - (hz)_x - (hz)_y,$$

with periodic boundary conditions in the x direction and zero Dirichlet boundary conditions on the top and bottom walls.

Now suppose the bottom and top walls are not perfectly flat but are given by the equations

$$b(x) = \alpha \sin(\beta x), \quad t(x) = 1 + b(x),$$

respectively. If α is small, then the walls are almost "flat". Therefore, the above equations for the walls may be viewed as a simplified form of wall roughness. Figure shows a comparison of the smooth domain with this "rough walled" domain for $\alpha = .01$ and $\beta = 75$. We study how the solution of the 2D nonlinear convection-diffusion equation changes when the height of the roughness, α, changes from zero (perfectly flat walls) to nearly zero (rough walls). The

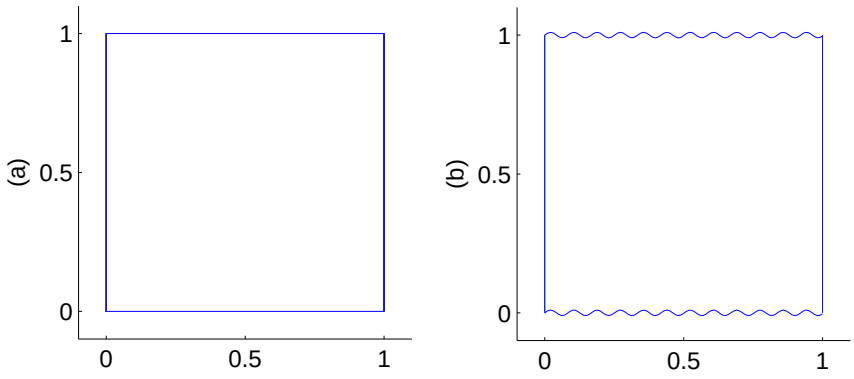

Figure 4.1: A comparison of (a) the smooth domain $\Omega = (0,1) \times (0,1)$ with (b) the "rough walled" domain described in the text for $\alpha = .01$ and $\beta = 75$.

change in the solution can be measured by the derivative of the fluctuations with respect to α. Therefore, define the sensitivity of the fluctuations with respect to α by

$$s(t,x,y) = \frac{\partial z}{\partial \alpha}(t,x,y;\alpha,\beta)\Big|_{\alpha=0,\,\beta=\beta_0},$$

if the derivative exists. Note that we have denoted the dependence of the solution on the parameters α and β and have evaluated the derivative at $\alpha = 0$ and $\beta = \beta_0$. If β_0 is not near zero, this raises the possibility that the walls change from perfectly flat ($\alpha = 0$ and $\beta \neq 0$) to having small but potentially very rough walls ($0 < \alpha \ll 1$ and $0 \ll \beta$).

Finding sensitivities is very important in many practical applications. For example, if a vector of parameters determines the shape of a design, then the sensitivity may be input into an optimization algorithm to determine the optimal shape of the design with respect to some performance requirements. This is an important tool in many aerodynamic design problems and other applications where building and testing various designs may be too costly.

We focus on the continuous sensitivity equation method (CSEM) for computing the sensitivities. Since the sensitivity is a derivative, one could use finite differences to approximate the sensitivity. However, this approach can lead to difficulties in practice. First, one has the problem of finding a good step size for the finite difference calculation. Also, if the evaluation of the function is expensive as is the case in many applications (such as in flow problems), this method can be very inefficient. Another method is to first discretize the problem and then differentiate the resulting discrete system with respect to the parameters of interest. However, when the parameter appears in the boundary as in the problem above, this method requires computing sensitivities of domain transformation with respect to the parameters. This can be quite complicated and can even lead to solving another system of partial differential equations [26].

One method that has both theoretical and numerical advantages is the *continuous sensi-*

tivity equation method (CSEM). Here, the infinite dimensional state equation is differentiated with respect to the parameters of interest leading to *linear* equations for the sensitivities. This linear equation is only weakly coupled to the original equation and can be solved independently. Therefore, one can use different numerical schemes or levels of refinement for each equation. In particular, one can take advantage of the linear nature of the sensitivity equation and solve it at a relatively small computational cost. This is especially advantageous if the original equation is nonlinear and requires a large amount of computational effort to solve. An additional advantage of this method is that in some cases it can be theoretically justified by using an appropriate abstract framework. This framework can then guide the choice of a numerical algorithm to compute the sensitivities. In other computational methods, there is no guarantee that one is computing the "true" sensitivities.

With the basic idea behind us, we turn to model ODE problems to make the concepts more precise. Then we review how the CSEM can be rigorously extended to infinite dimensional semilinear parabolic problems. The one dimensional nonlinear convection-diffusion (NLCD) equation will be used to illustrate the details of this method. We then return to the 2D Burgers' equation and formulate the equation governing the sensitivity of the solution with respect to small changes in the domain as described above. In all of these examples, it will be seen that if the underlying linear operator is non-normal, then the sensitivities can be quite large. Numerical results will be presented in the following chapter. For further details on the CSEM, see the references [26], [33], [34], [66], [129], [130], [131], [132], [133].

4.1 Sensitivities for ODE Model Problems

As mentioned in section 2.4.2, ODE model problem have been used by many researchers to give insight into the transition process for flow problems. In particular, certain ODEs have been used to support the claim that the domain of attraction of a laminar flow may shrink rapidly with increasing Reynold's number. In this section, we describe these ODE model problems and formulate the sensitivity of the solution with respect to a small "unmodeled" disturbance to the equation. In the next chapter, it will be shown that solutions to these problems are very sensitive to these small disturbances.

The basic form of the initial value problem is given by

$$\dot{x}(t) = \mathbf{A}x(t) + \|x(t)\| \, \mathbf{S}x(t) + \varepsilon d, \quad x(0) = x_0 \in \mathbb{R}^n, \tag{4.1}$$

where $\mathbf{A}$ and $\mathbf{S}$ are $n \times n$ constant matrices, $\|\cdot\|$ is the standard Euclidean norm and d is a constant vector. The matrix $\mathbf{S}$ will be taken to be skew-adjoint, i.e., $\mathbf{S}^T = -\mathbf{S}$. In this case, the nonlinear term $F(x) = \|x\| \, \mathbf{S}\, x$ is conservative for the standard Euclidean inner product since

$$\langle F(x), x \rangle = \|x\| \, \langle \mathbf{S}x, x \rangle = 0$$

for all vectors x. The matrix $\mathbf{A}$ will be non-normal, i.e., $\mathbf{A}\mathbf{A}^T \neq \mathbf{A}^T\mathbf{A}$. Therefore, when $\varepsilon = 0$, this class of initial value problems shares a mathematical framework with the Navier-

Stokes equations for a fluctuation about a base flow.

The following lemma summarizes some basic properties of this system when $\varepsilon = 0$.

Lemma 4.1.1 *If* $\mathbf{S}$ *is skew-adjoint and* $\varepsilon = 0$*, then given any initial data* $x_0 \in \mathbb{R}^n$ *there exists a unique solution to the ODE system (4.1) that exists for all time. Also, if all of the eigenvalues of* $\mathbf{A}$ *have negative real part, then the zero state is an asymptotically stable equilibrium.*

Proof: The right hand side of the ODE is locally Lipschitz and therefore, for any initial data a solution exists and is unique on some small time interval. Due to the conservative nature of the nonlinearity, we have

$$\frac{d}{dt}\frac{1}{2}\|x\|^2 = \langle \mathbf{A}x + \|x\|\,\mathbf{S}\,x, x\rangle = \langle \mathbf{A}x, x\rangle \leq \|\mathbf{A}\|\,\|x\|^2.$$

An application of Gronwall's inequality shows that the unique solution is bounded on finite time intervals and thus exists for all time. The nonlinearity $F(x) = \|x\|\,\mathbf{S}x$ is continuous and satisfies $F(x) = o(\|x\|)$ as $\|x\| \to 0$. Also, $F(\cdot)$ is C^1 since the Jacobian exists and is given by

$$D_x F(x) = \begin{cases} \|x\|\,\mathbf{S} + \mathbf{S}\,xx^T/\|x\|, & \text{if } x \neq 0 \\ 0, & \text{if } x = 0, \end{cases} \tag{4.2}$$

which is continuous in x. Therefore, since the spectrum of $\mathbf{A}$ is contained in the left half plane, Perron's theorem (see Theorem 2.2.1) implies that the zero state is asymptotically stable. □

In the next chapter, we consider a specific 2D and 3D system of the above form. Both of these systems have appeared in the literature in connection with the transition problem (see [5], [6] and [143]) and they are also share common features with many other ODE model problems used for this same purpose [6]. The 2D system takes the specific form

$$\mathbf{A} = \begin{bmatrix} -\alpha_1/R & 1 \\ 0 & -\alpha_2/R \end{bmatrix}, \quad \mathbf{S} = \begin{bmatrix} 0 & -1 \\ 1 & 0 \end{bmatrix}, \quad d = \begin{bmatrix} 1 \\ 1 \end{bmatrix},$$

while the 3D system is given by

$$\mathbf{A} = \begin{bmatrix} -\alpha_1/R & 1 & 0 \\ 0 & -\alpha_2/R & 1 \\ 0 & 0 & -\alpha_3/R \end{bmatrix}, \quad \mathbf{S} = \begin{bmatrix} 0 & -s_1 & -s_2 \\ s_1 & 0 & s_3 \\ s_2 & -s_3 & 0 \end{bmatrix}, \quad d = \begin{bmatrix} 1 \\ 1 \\ 1 \end{bmatrix},$$

where all of the parameters are positive. In particular, we fix the values of all the parameters with the exception of R which plays the role of the Reynolds number.

Since the origin is asymptotically stable, there is a ball containing zero such that for any initial data in the ball, the solution will converge to the zero state. However, for these and other similar ODE systems the size of the largest ball of attraction has radius R^γ, with $\gamma \leq -2$ (see [6]). Outside of this ball there are initial conditions where the solution will tend

to an equilibrium or a periodic, quasi-periodic or chaotic orbit depending on the values of the parameters. As mentioned in section 2.4.2, this phenomenon is similar to Couette and pipe flows. We shall see that a small imperfection in the initial condition may cause the flow to transition even though the equilibrium is asymptotically stable.

We also examine another sensitivity. In particular, we consider the problem of determining if solutions to the above ODE systems are sensitive to the small disturbance εd. Notice that as soon as ε is nonzero, the zero state is no longer an equilibrium. That does not of itself imply that solutions are sensitive to the small disturbance. The solution of the disturbed system can still be "nearby" the solution of the undisturbed system. However, note that if the forcing function εd is included in the nonlinear term, the perturbed nonlinear term is no longer conservative or definite since

$$\langle F(x) + \varepsilon d, x\rangle = \varepsilon \langle d, x\rangle = \varepsilon(x_1 + \cdots + x_n).$$

The 1D Burgers' equation with Neumann boundary conditions shows how a nonconservative nonlinearity can cause solutions to be extremely sensitive with respect to small disturbances (see section 3.3.2). Therefore, to investigate the sensitivity of solutions to the above ODEs with respect to ε, compute the derivative

$$s(t) = \frac{\partial}{\partial \varepsilon} x(t;\varepsilon)\Big|_{\varepsilon=0}. \tag{4.3}$$

The derivative is evaluated at zero to measure how the solution changes with the introduction of the disturbance εd to the ODE system. Formally differentiating the initial value problem (4.1), using the chain rule and substituting in $\varepsilon = 0$, yields the sensitivity equation

$$\dot{s}(t) = \mathbf{A}s(t) + D_x F(x(t;0))s(t) + d, \quad s(0) = 0 \in \mathbb{R}^n, \tag{4.4}$$

where the Jacobian $D_x F(\cdot)$ is defined in (4.2).

Note that the sensitivity equation is *linear*. Also, due to the simplicity of the problem, one can couple the sensitivity equation to the original system and simply solve them simultaneously. Even though the sensitivity equation is linear, it is driven by a "large" forcing d. Furthermore, if the matrix $\mathbf{A}$ is non-normal, the discussion in section 2.4.2 implies that solutions can experience significant transient growth. Thus, the constant forcing d or the time dependent linear operator $D_x F(x(t;0))$ has the potential to keep the sensitivity large. These observations raise the possibility that even though the disturbance to the original system is small, the sensitivity with respect to such a perturbation has the potential to be quite large when $\mathbf{A}$ is non-normal.

In formally deriving the above sensitivity equation, we assumed two things. First, we assumed that the derivative defining the sensitivity exists. We also assumed that we could switch the order of differentiation with respect to ε and t. This requires the mixed derivatives of $x(t;\varepsilon)$ to be continuous which again we do not know. However, the following result found in [41, Theorem 1.7.2] and [102, Theorem 2.7.2] guarantees that the above procedure is

justified.

Theorem 4.1.1 *Let $D \subset \mathbb{R}^n$ and $Q \subset \mathbb{R}$ be open domains and assume $f : D \times Q \to \mathbb{R}^n$ is C^1 on $D \times Q$. Suppose for each $(x_0, q_0) \in D \times Q$ there exists a unique solution $x(t; x_0, q_0)$ to the initial value problem*

$$\dot{x}(t; q) = f(x(t; q); q), \quad x(0) = x_0 \in \mathbb{R}^n.$$

defined on an interval $0 < t < T(x_0, q_0)$. Then for each $(x_0, q_0) \in D \times Q$, the sensitivity

$$s(t) = \frac{\partial x}{\partial q}(t; q)\Big|_{q=q_0}$$

exists on $0 < t < T(x_0, q_0)$ and satisfies the initial value problem

$$\dot{s}(t) = [D_x f(x(t; q_0); q_0)]s(t) + [D_q f(x(t; q_0); q_0)], \quad s(0) = 0.$$

Corollary 4.1.1 *Let $x(t; \varepsilon)$ be the solution to the initial value problem (4.1). Then the sensitivity $s(t)$ defined in (4.3) exists for all $t > 0$ and satisfies the sensitivity equation (4.4).*

Proof: For the initial value problem (4.1), $f(x; \varepsilon) = \mathbf{A}x + \|x\| \mathbf{S}\, x + \varepsilon d$ is C^1 over all of $\mathbb{R}$ in both x and ε. The derivatives at $\varepsilon = 0$ are given by

$$D_x f(x(t; 0); 0) = \mathbf{A} + D_x F(x(t; 0); 0), \quad D_\varepsilon f(x(t; 0); 0) = d.$$

Since the solution $x(t; 0)$ exists for all time by Lemma 4.1.1, the above theorem implies that the sensitivity $s(t)$ exists for all $t > 0$ and satisfies the sensitivity equation (4.4). □

The ODE model problems presented here demonstrate the essence of the continuous sensitivity equation method. The next section outlines a framework that rigorously extends the CSEM to a certain class of infinite dimensional dynamical systems.

4.2 Sensitivities for Semilinear Parabolic Equations

We now review how the continuous sensitivity equation method can be rigorously extended to certain abstract parabolic equations. In particular, we focus on the parameter dependent initial value problem over an infinite dimensional state space X given by

$$\dot{x}(t; q) = \mathcal{A}x(t; q) + \mathcal{F}(x(t; q); q), \quad x(0; q) = x_0(q). \tag{4.5}$$

We assume $\mathcal{A}$ is sectorial so that the fractional powers X^α are well defined for some $\alpha \in (0, 1)$. The parameter q is in a Banach space Q. The results presented in this section will be used to study the sensitivities of a one and two dimensional nonlinear convection-diffusion equation in sections 4.3 and 4.4. The sensitivity theory presented here is applicable to a wide range of problems, including the Navier-Stokes equations on bounded domains (see [67, Example 3.8]).

To rigorously extend the continuous sensitivity method to the abstract parabolic initial value problem (4.5), we require the Fréchet derivative and a chain rule.

Definition 4.2.1 *An operator $\mathcal{F}$ mapping a Banach space X into another Banach space Y is Fréchet differentiable at $x_0 \in X$ if there exists a continuous linear operator $D_x\mathcal{F}(x_0)$ such that*

$$\|\mathcal{F}(x) - \mathcal{F}(x_0) - [D_x\mathcal{F}(x_0)](x - x_0)\|_Y = o(\|x - x_0\|_X) \quad as \ \|x - x_0\|_X \to 0$$

for every x in a neighborhood of x_0. The linear operator $D_x\mathcal{F}(x_0)$ is the Fréchet derivative of $\mathcal{F}(\cdot)$ at x_0.

The following version of the chain rule for Fréchet derivatives can be found in [145, Proposition II.4.1].

Lemma 4.2.1 *Let X and Y be Banach spaces and let Q be open in $\mathbb{R}$. If $x : Q \subset \mathbb{R} \to X$ is Fréchet differentiable at $q_0 \in Q$ and if $\mathcal{F} : X \to Y$ is Fréchet differentiable at $x(q_0)$, then $\mathcal{F}(x(\cdot)) : Q \subset \mathbb{R} \to Y$ is Fréchet differentiable at q_0 and*

$$D_q\mathcal{F}(x(q))\Big|_{q=q_0} = D_x\mathcal{F}(x(q))\Big|_{q=q_0} D_q x(q)\Big|_{q=q_0}.$$

The following result extends the CSEM to abstract semilinear parabolic equations and can be found in Henry's text [67, Theorem 3.4.4].

Theorem 4.2.1 *Suppose X and Y are Banach spaces, $\mathcal{A}$ is sectorial on X, $\alpha \in (0, 1)$, U is open in X^α and Q is open in Y. Suppose also that $\mathcal{F} : U \times Q \to X$ and the Fréchet derivatives $D_x\mathcal{F}$ and $D_q\mathcal{F}$ are all continuous on $U \times Q$. For $x_0 \in U$, $\mu > 0$ and $q \in Q$, let $x = x(t; x_0, \mu, q)$ be the solution of*

$$\dot{x}(t) = \mu\mathcal{A}x(t) + \mathcal{F}(x(t); q), \quad x(0) = x_0,$$

on the interval $0 < t < T(x_0, \mu, q)$. Then x is continuously Fréchet differentiable with respect to x_0, μ and q from $X^\alpha \times \mathbb{R}^+ \times Q$ into X^α. The sensitivities $s_1(t) = D_{x_0}x(t; x_0, \mu, q)$, $s_2(t) = D_\mu x(t; x_0, \mu, q)$ and $s_3(t) = D_q x(t; x_0, \mu, q)$ exist on the interval $0 < t < T(x_0, \mu, q)$ and are given by the solutions of the linear initial value problems

$$\dot{s_1}(t) = \mu\mathcal{A}s_1(t) + [D_x\mathcal{F}(x(t; q); q)]s_1(t), \quad s_1(0) = \mathcal{I}. \tag{4.6}$$

$$\dot{s_2}(t) = \mu\mathcal{A}s_2(t) + [D_x\mathcal{F}(x(t; q); q)]s_2(t) + \mathcal{A}x(t), \quad s_2(0) = 0. \tag{4.7}$$

$$\dot{s_3}(t) = \mu\mathcal{A}s_3(t) + [D_x\mathcal{F}(x(t; q); q)]s_3(t) + [D_q\mathcal{F}(x(t); q); q)], \quad s_3(0) = 0. \tag{4.8}$$

Therefore, in the framework of sectorial operators and fractional powers of the state space X, the sensitivity equation method can be made rigorous. Note that in this result the linear operator $\mathcal{A}$ does not explicitly depend on the parameter q. In certain cases this can be overcome (see [67, Section 3.4]), however we will not deal with this case here.

We are primarily concerned with the differentiability of the solution with respect to the parameter q. This theorem does not cover the case where the initial data depends on q such as in the initial value problem (4.5) above. We will encounter this case for a one dimensional NLCD equation in the next section. However, this theorem can be easily extended using the chain rule for Fréchet derivatives presented above to cover this case when the parameter q is real.

Corollary 4.2.1 *Let the assumptions of Theorem 4.2.1 be satisfied with the space $Y = \mathbb{R}$. Suppose also that the initial data $x_0(q)$ is differentiable with respect to $q \in Q \subset \mathbb{R}$. Then if $x(t;q)$ is the solution of the initial value problem (4.5), then $x(t;q)$ is continuously differentiable in q from Q into X^α. The sensitivity $s(t) = D_q x(t;q)$ exists as long as $x(t;q)$ exists and is the solution of the linear initial value problem*

$$\dot{s}(t) = \mathcal{A}s(t) + [D_x \mathcal{F}(x(t;q);q)]s(t) + [D_q \mathcal{F}(x(t;q);q)], \quad s(0) = D_q x_0(q). \tag{4.9}$$

Proof: First, consider the solution of the initial value problem to depend on x_0 and q, i.e., $x = x(t;x_0,q)$. We momentarily suppress the dependence of x_0 on q. By the above theorem, the sensitivities $s_1(t) = D_{x_0} x(t;x_0,q)$ and $s_3(t) = D_q x(t;x_0,q)$ exist as long as the solution $x(t;x_0,q)$ exists. Since $x_0 = x_0(q)$ maps $\mathbb{R}$ to X^α and is Fréchet differentiable with respect to q, the chain rule for Fréchet derivatives in Lemma 4.2.1 implies that $x = x(t;x_0(q),q)$ is Fréchet differentiable with respect to q and

$$\begin{aligned} D_q x(t;x_0(q),q) &= D_{x_0} x(t;x_0(q),q)\, D_q x_0(q) + D_q x(t;v_0(q),q) \\ &= s_1(t)\, D_q x_0(q) + s_3(t). \end{aligned}$$

Therefore, the sensitivity $s(t) = D_q x(t;x_0(q),q)$ exists as long as $x(t;q) = x(t;x_0(q),q)$ exists. Since $s_1(t)$ and $s_3(t)$ satisfy the initial value problems (4.6) and (4.7), a direct computation shows that $s(t)$ satisfies the linear initial value problem (4.9). □

4.3 Sensitivities for a 1D Burgers' Equation

In this section, we apply the results of the previous section to rigorously formulate the CSEM for the one dimensional nonlinear convection-diffusion (NLCD) equation given by

$$w_t + ww_x = \mu w_{xx} - (hw)_x \tag{4.10}$$

with Dirichlet boundary conditions

$$w(t,-1) = 0, \quad w(t,1) = \varepsilon \tag{4.11}$$

and initial condition

$$w(0,x) = w_0(x). \tag{4.12}$$

Here, $\varepsilon > 0$ is a small constant, $\mu > 0$ is constant and $h(\cdot)$ is the unique solution of the steady problem

$$hh_x = \mu h_{xx}, \quad h(-1) = 1, \;\; h(1) = -1$$

given by the hyperbolic tangent profile (see Corollary 3.3.1)

$$h(x) = c \tanh\left(-cx/2\mu\right). \tag{4.13}$$

The constant c is chosen to satisfy the nonhomogeneous Dirichlet boundary conditions (4.11).

Here, we examine the sensitivity of solutions with respect to the disturbance ε. Let $w = w(t, x; \varepsilon)$ be the solution to (4.10)-(4.12) and define the sensitivity

$$s(t, x) = \frac{\partial w}{\partial \varepsilon}(t, x; \varepsilon)\Big|_{\varepsilon=0}. \tag{4.14}$$

Proceed as with the ODE model problems in section 4.1 and formally differentiate the NLCD equation (4.10)-(4.12) with respect to ε using the chain rule and set $\varepsilon = 0$. This yields a partial differential equation for the sensitivity given by

$$s_t(t, x) = \mu s_{xx}(t, x) - (h(x)s(t, x))_x - (w(t, x; 0)\, s(t, x))_x \tag{4.15}$$

with Dirichlet boundary conditions

$$s(t, -1) = 0, \quad s(t, 1) = 1 \tag{4.16}$$

and zero initial condition

$$s(0, x) = 0. \tag{4.17}$$

Notice again that the sensitivity equation is *linear*. Therefore, the undisturbed NLCD equation may first be solved for $w(t, x; 0)$ and then the linear sensitivity equation solved separately. Also, note that the small disturbance in the boundary condition produces a large boundary condition for the sensitivity equation. Furthermore, as observed in the ODE case, if the underlying time independent linear operator is non-normal, then the solution has the potential for large transient growth. Thus, either the input from the nonzero boundary condition or the time dependent linear term $(w(t, x; 0)\, s(t, x))_x$ has the potential to produce large sensitivities. This can happen even if the undisturbed solution $w(t, x; 0)$ and the time dependent linear term are "small". A similar phenomenon was seen in the sensitivity equation for the ODE model problems considered in the previous section. Therefore, the small disturbance has the potential to cause a large change in the solution $w(t, x; 0)$.

Below, we place the NLCD equation into a strong state space formulation. With the equation in this framework, we can use the results of the previous section to show that the sensitivity formally defined in (4.14) exists and satisfies the sensitivity equation (4.15)-(4.17). The approach outlined here is general and can easily be extended to many other similar problems. Theoretical results such as this are important since they can guide the construction of suitable numerical methods for the problem under consideration.

4.3.1 Abstract Formulation

To place the above nonlinear convection-diffusion equation (4.10)-(4.12) into an abstract strong form, we introduce a change of variables to homogenize the boundary conditions. Let $\psi(x;\varepsilon) = \varepsilon(x+1)/2$ and define $v(t,x;\varepsilon) = w(t,x;\varepsilon) - \psi(x;\varepsilon)$. Then v satisfies the transformed NLCD given by

$$v_t + vv_x = \mu v_{xx} - ((h+\psi)v)_x + f \tag{4.18}$$

with zero Dirichlet boundary conditions

$$v(t,-1;\varepsilon) = 0, \quad v(t,1;\varepsilon) = 0 \tag{4.19}$$

and initial condition

$$v(0,x;\varepsilon) = v_0(x;\varepsilon) := w_0(x) - \psi(x;\varepsilon). \tag{4.20}$$

The forcing function f is defined by

$$f = f(x;\varepsilon) = -h(x)\psi_x(x;\varepsilon) - h_x(x)\psi(x;\varepsilon) - \psi(x;\varepsilon)\psi_x(x;\varepsilon). \tag{4.21}$$

When $\varepsilon = 0$, these equation reduce to the above NLCD equation (4.10)-(4.12). When $\varepsilon \neq 0$, these equations can be viewed as a perturbation to the original fluctuation equations. Note that the perturbation has entered in the linear term as well as adding a forcing function. As in the case of the ODE examples considered in section 4.1, if we view this forcing function as an addition to the nonlinearity, then the perturbed nonlinearity is no longer conservative. Again, this implies that solutions of this transformed equation may behave very differently from solutions to the original equation.

Let $X = L^2(-1,1)$ with the standard inner product and norm. Also let $V = H_0^1(-1,1)$ with inner product $\langle u,v\rangle_V = \langle u_x, v_x\rangle_X$. Multiplying the equation by a test function $\varphi \in V$, integrating over the domain $(-1,1)$ and integrating all of the linear terms by parts yields the weak form of the problem: find $v \in V$ such that

$$\frac{\partial}{\partial t}\langle v,\varphi\rangle_X = -\mu\langle v,\varphi\rangle_V + \langle (h+\psi)v,\varphi_x\rangle_X - \langle vv_x,\varphi\rangle_X + \langle f,\varphi\rangle_X \tag{4.22}$$

for all $\varphi \in V$. The inner products resulting from the linear terms are associated to the bilinear form $a : V \times V \to \mathbb{R}$ defined by

$$a(u,v) = -\mu\langle v,\varphi\rangle_V + \langle (h+\psi)v,\varphi_x\rangle_X .$$

Also, the bilinear form naturally defines the linear operator $\mathcal{A} : \mathcal{D}(\mathcal{A}) \subset X \to X$ given by

$$\langle \mathcal{A}u, v\rangle_X = a(u,v)$$

for all $v \in V$ and all u in the domain $\mathcal{D}(\mathcal{A}) = \{\, u \in V : \mathcal{A}u \in X\}$. For this problem, it is well known that $\mathcal{D}(\mathcal{A}) = H^2 \cap V = H^2 \cap H_0^1$ (see [101]). An application of the Fundamental

Lemma of the Calculus of Variations (see [101, Lemma 2.4.5]) implies that

$$\mathcal{A}u = \mu u_{xx} - ((h+\psi)u)_x$$

for all $u \in \mathcal{D}(\mathcal{A})$.

The following result can be used to ascertain specific information about operators derived from a sesquilinear form (see [101, Sections 2.8, 4.5 and 6.1]).

Theorem 4.3.1 *Suppose the following conditions are satisfied.*

(B1) There exist complex Hilbert spaces X and V with inner products $\langle \cdot, \cdot \rangle_X$ and $\langle \cdot, \cdot \rangle_V$ such that V is dense in X. Also, there exists $M_1 > 0$ such that $\|v\|_X \leq M_1 \|v\|_V$ for all $v \in V$.

(B2) There exists a sesquilinear form $a(\cdot, \cdot) : V \times V \to \mathbb{C}$, i.e., the form is linear in its first argument and conjugate linear in its second argument.

(B3) There exist $M_2, M_3 > 0$ and $a \in \mathbb{R}$ such that for all $u, v \in V$

$$|a(u,v)| \leq M_2 \|u\|_V \|v\|_V, \quad \operatorname{Re} a(v,v) \leq -M_3 \|v\|_V^2 + a\|v\|_X^2.$$

(B4) The linear operator $\mathcal{A} : \mathcal{D}(\mathcal{A}) \subset X \to X$ is defined by $\langle \mathcal{A}u, v \rangle_X = a(u,v)$ for all $v \in V$ and all $u \in \mathcal{D}(\mathcal{A}) = \{ u \in V : \mathcal{A}u \in X \}$.

Then, $\mathcal{A}$ satisfies the following properties.

1. *The numerical range and the spectrum of $\mathcal{A}$ are contained in a sector W in the complex plane given by*

$$W := \left\{ z \in \mathbb{C} : \operatorname{Re}(z) \leq a - M_1^{-2} M_3, \ |\operatorname{Im}(z)| \leq M_2 M_3^{-1} (a - \operatorname{Re}(z)) \right\}.$$

2. *If the embedding $V \subset X$ is compact, then the resolvent operator $\mathcal{R}(\lambda; \mathcal{A})$ is compact and therefore the spectrum of $\mathcal{A}$ is discrete.*

3. *The operator $\mathcal{A}$ is sectorial and generates an analytic C_0-semigroup.*

4. *The fractional power of the state space, $X^{1/2}$, can be taken to be V.*

This theorem can easily be used to show that the convection-diffusion operator defined above generates an analytic semigroup.

Lemma 4.3.1 *Let $X = L^2(-1,1)$, $h \in C^1[-1,1]$ and define $\mathcal{A} : H^2 \cap H_0^1 \subset X \to X$ by $\mathcal{A}u = \mu u_{xx} - (hu)_x$. Then $X^{1/2} = H_0^1$, the spectrum of $\mathcal{A}$ is discrete and $\mathcal{A}$ is sectorial and generates an analytic semigroup.*

Proof: Complexify the Hilbert spaces X and V defined above so that the bilinear form $a(\cdot,\cdot)$ is sesquilinear on $V \times V$. For property (B1), it is well known that $V = H_0^1$ is dense in $X = L^2$. The remainder of the first condition follows directly from the Poincaré inequality. However, to obtain a numerical value for M_1 note that for all $v \in V$

$$\|v\|_X^2 \;=\; \int_{-1}^{1} 1 \cdot v^2 \, dx \;=\; -\int_{-1}^{1} 2x \, v v_x \, dx \;\leq\; 2 \|v\|_X \|v_x\|_X \;=\; 2 \|v\|_X \|v\|_V \,.$$

Here, we have integrated by parts and used Hölder's inequality. Therefore, $\|v\|_X \leq 2 \|v\|_V$ for all $v \in V$ and M_1 can be taken to be 2. For property (B3), note that

$$|a(u,v)| \;\leq\; \mu \|u\|_V \|v\|_V + \int_{-1}^{1} |huv_x| \; dx \;\leq\; (\mu + M_1 \|h\|_{L^\infty}) \|u\|_V \|v\|_V \,.$$

After observing $vv_x = (v^2/2)_x$ and integrating by parts, we obtain

$$\text{Re}\, a(v,v) \;=\; -\mu \|v\|_V^2 - \frac{1}{2}\int_{-1}^{1} h_x v^2 \, dx \;\leq\; -\mu \|v\|_V^2 - \frac{1}{2}\left[\inf_{x\in(-1,1)} h_x(x)\right] \|v\|_X^2 \,.$$

Both of these inequalities depend on the fact that since $h \in C^1$ and therefore h and h_x are bounded above and below. Therefore, we may take

$$M_1 = 2, \quad M_2 = \mu + M_1 \|h\|_{L^\infty}, \quad M_3 = \mu \quad \text{and} \quad a = -\frac{1}{2}\left[\inf_{x\in(-1,1)} h_x(x)\right].$$

Also, it is well known that $V \subset X$ is a compact embedding (see [101, Corollary 3.6.17]). All of the requirements of Theorem 4.3.1 are satisfied and the results follow. □

Note that this lemma holds for any C^1 function $h(\cdot)$. For the specific case of the hyperbolic tangent profile (4.13), h is decreasing everywhere and has a "shock" at $x = 0$ (see section 3.3.2). At the shock, the derivative h_x will be very large and negative and therefore the constant a will also be large and positive. Part 1 of Theorem 4.3.1 gives the following bound on the real part of the spectrum:

$$\text{Re}(\lambda) \leq a - M_3 M_1^{-2} \quad \text{for any} \quad \lambda \in \Lambda(\mathcal{A}).$$

Therefore, when h is given by the hyperbolic tangent profile, it is possible that the spectrum of $\mathcal{A}$ extends into the right half plane since a is large and positive. However, Kreiss and Kreiss showed this is not the case [80].

Theorem 4.3.2 *Let $X = L^2(-1,1)$, μ be a positive constant, $h \in C^1[-1,1]$ and define $\mathcal{A} : H^2 \cap H_0^1 \subset X \to X$ by $\mathcal{A}u = \mu u_{xx} - (hu)_x$. Then the eigenvalues of $\mathcal{A}$ are all real and negative and cannot accumulate at zero.*

Due to this spectral bound and the above lemma, we have the following result.

Corollary 4.3.1 *If $h \in C^1[-1,1]$, then the operator $\mathcal{A}$ defined above generates an exponentially stable C_0-semigroup.*

Proof: By Lemma 4.3.1, $\mathcal{A}$ generates an analytic semigroup. Since the spectrum of $\mathcal{A}$ consists entirely of eigenvalues which are bounded away from the imaginary axis, Theorem 2.1.8 implies that $\mathcal{A}$ generates an exponentially stable semigroup. □

Therefore, the linear operator for the nonlinear convection diffusion equation given by $\mathcal{A}v = \mu v_{xx} - ((h+\psi)v)_x$ on the domain $H^2 \cap H_0^1$ is sectorial and generates an exponentially stable semigroup. However, to apply the theory in the previous section for the derivation of the sensitivity equation, the operator $\mathcal{A}$ cannot depend on the parameter ε. Therefore, we include the term $(\psi(\varepsilon)v)_x$ in the nonlinear operator and redefine the linear operator as

$$\mathcal{A}v = \mu v_{xx} - (hv)_x \tag{4.23}$$

on the same domain. The above corollary still applies and therefore the operator is sectorial and generates an exponentially stable semigroup. To complete the abstract form of the equation, define the ε dependent nonlinear operator $\mathcal{F} : V \times \mathbb{R} \subset X \times \mathbb{R} \to X$ by

$$\mathcal{F}(v;\varepsilon) = -vv_x - (\psi(\varepsilon)\, v)_x + f(\varepsilon), \tag{4.24}$$

where $\psi(\varepsilon) = \psi(x;\varepsilon) = \varepsilon(x+1)/2$ and $f(\varepsilon) = f(x;\varepsilon)$ is defined in (4.21). Therefore, the nonlinear convection diffusion equation takes the form

$$\dot{v}(t;\varepsilon) = \mathcal{A}v(t;\varepsilon) + \mathcal{F}(v(t;\varepsilon);\varepsilon), \quad v(0;\varepsilon) = v_0(\varepsilon) \in V = X^{1/2}. \tag{4.25}$$

This formulation allows us to apply the theory from the previous section (specifically, Corollary 4.2.1) to rigorously study the sensitivity of the solution with respect to ε.

4.3.2 Local Uniqueness and Stability

We now verify that the abstract nonlinear convection diffusion equation (4.23)-(4.25) has a unique solution on some (possibly small) time interval. The following local existence result can be found in [67, Theorem 3.3.3].

Theorem 4.3.3 *Consider an initial value problem over a Banach space X of the form*

$$\dot{x}(t) = \mathcal{A}x(t) + \mathcal{F}(x(t)), \quad x(0) = x_0 \in X,$$

where $\mathcal{A} : \mathcal{D}(\mathcal{A}) \subset X \to X$ is sectorial and X^α is well defined for some $\alpha \in (0,1)$. Let U be open in X^α and suppose $\mathcal{F} : U \subset X^\alpha \to X$ is locally Lipschitz on U, i.e., for every $x \in U$, there exists a ball $B \subset U$ about x and a constant $L > 0$ such that for all $y \in B$,

$$\|\mathcal{F}(x) - \mathcal{F}(y)\|_X \leq L \|x - y\|_\alpha .$$

Then for any $x_0 \in U$, there exists $T = T(x_0)$ such that the initial value problem has a unique solution $x(t)$ on defined on $(0, T)$.

We will not give a precise definition of a solution here (see the above reference for details). However, we note that the solution satisfies the "variation of parameters" integral equation (see [67, Lemma 3.3.2]) given by

$$x(t) = \mathcal{S}(t)x_0 + \int_0^t \mathcal{S}(t-s)\mathcal{F}(x(s))\,ds,$$

where $\mathcal{S}(t)$ is the C_0-semigroup generated by $\mathcal{A}$.

The following proof of local existence and uniqueness for the NLCD problem follows an example in [67, Section 3.3].

Theorem 4.3.4 *Let $\varepsilon > 0$ and $h \in C^1[-1, 1]$. For any $v_0 \in H_0^1$, there exists a $T = T(v_0)$ such that the abstract nonlinear convection diffusion equation (4.23)-(4.25) has a unique solution on $(0, T)$.*

Proof: For $X = L^2(-1, 1)$, Lemma 4.3.1 implies that $\mathcal{A}$ is sectorial and $X^{1/2} = V = H_0^1$. We only need to show that $\mathcal{F}(\cdot)$ is locally Lipschitz. For any $v \in V$, v is absolutely continuous which implies $v(x) = \int_{-1}^x v_\tau\,d\tau$. Therefore,

$$\|v\|_{L^\infty} \leq \int_{-1}^1 |v_x|\,dx \leq \|1\|_X \|v_x\|_X = \sqrt{2}\,\|v\|_V$$

by Hölder's inequality. This inequality is used repeatedly below. For any $u, v \in V$,

$$\|\mathcal{F}(u) - \mathcal{F}(v)\|_X \leq \|uu_x - vv_x\|_X + \|(\psi u)_x - (\psi v)_x\|_X$$

For the first term,

$$\begin{aligned}
\|uu_x - vv_x\|_X &= \|u(u-v)_x + (u-v)v_x\|_X \\
&\leq \|u\|_{L^\infty} \|(u-v)_x\|_X + \|u-v\|_{L^\infty} \|v_x\|_X \\
&\leq \sqrt{2}\,\|u\|_V \|u-v\|_V + \sqrt{2}\,\|u-v\|_V \|v\|_V \\
&\leq \sqrt{2}\,(\|u\|_V + \|v\|_V)\,\|u-v\|_V\,.
\end{aligned}$$

For the second term,

$$\begin{aligned}
\|(\psi u)_x - (\psi v)_x\|_X &= \|\psi_x(u-v) + \psi(u-v)_x\|_X \\
&\leq \|\psi_x\|_X \|u-v\|_{L^\infty} + \|\psi\|_{L^\infty} \|(u-v)_x\|_X \\
&\leq (\sqrt{2}\,\|\psi\|_V + \|\psi\|_{L^\infty})\,\|u-v\|_V\,.
\end{aligned}$$

Therefore, $\mathcal{F}(\cdot)$ is locally Lipschitz over all of V and the result follows. □

In the proof, we derived

$$\|v\|_{L^\infty} \leq \sqrt{2}\,\|v\|_V \quad \text{for all } v \in V = H_0^1. \tag{4.26}$$

This inequality will be useful below. Also, this result only provides local existence and uniqueness for smooth initial data. As mentioned in section 3.2, it is likely that this result can be extended to global uniqueness for arbitrary L^2 initial data.

The infinite dimensional version of Perron's theorem for abstract semilinear parabolic problems (see theorem 2.2.3) can be used to study the stability of the zero state of the undisturbed (i.e., $\varepsilon = 0$) NLCD equation.

Proposition 4.3.1 *If $\varepsilon = 0$ and the initial data $v_0 \in V = H_0^1$ is small enough in the V norm, then the solution $v(t)$ to the nonlinear convection diffusion equation (4.23)-(4.25) exists and is unique for all time and tends to zero asymptotically in the V norm.*

Proof: Since $X^{1/2} = V$ and the linear operator $\mathcal{A}$ is sectorial and generates an exponentially stable semigroup, to apply Theorem 2.2.3 all that remains is to show is $\|\mathcal{F}(v;0)\|_X = o(\|v\|_V)$ as $\|x\|_V \to 0$. Note for $\varepsilon = 0$, the nonlinearity is given by $\mathcal{F}(v;0) = -vv_x$. Using the inequality (4.26) gives

$$\|\mathcal{F}(v;0)\|_X \;=\; \|vv_x\|_X \;\leq\; \|v\|_{L^\infty}\,\|v_x\|_X \;\leq\; \sqrt{2}\,\|v\|_V^2\,.$$

Therefore $\|F(v;0)\|_X = o(\|v\|_V)$ as $\|v\|_V \to 0$. Thus, all of the hypotheses of Theorem 2.2.3 are satisfied and the result follows. □

Note that this result only treats the case where the initial condition is small **and smooth**, i.e., $v_0 \in H_0^1$. Therefore, results such as this do not provide any information about the long time behavior of solutions with small **non-smooth** initial data. In flow systems, it is possible to have non-smooth initial data. Different techniques are required to handle this scenario.

4.3.3 Derivation of the Sensitivity Equation

With the abstract framework presented above, one can use the results from the previous section to rigorously extend the continuous sensitivity equation method to the nonlinear convection-diffusion equation. First, we apply Corollary 4.2.1 to the abstract strong form of the transformation of the NLCD equation (4.23)-(4.25). Once the sensitivity equation is rigorously obtained for the transformed state $v(t;\varepsilon)$, the transformation will be inverted to arrive at the sensitivity equation for the original state $w(t;\varepsilon)$.

Theorem 4.3.5 *Let $v(t,x;\varepsilon)$ be the solution of the transformed NLCD equation (4.18)-(4.20) on $(0,T)$ for some $T > 0$. Then, $v(t,x;\varepsilon)$ is continuously differentiable with respect to ε so that the sensitivity*

$$r(t,x) = \frac{\partial v}{\partial \varepsilon}(t,x;\varepsilon)\,\Big|_{\varepsilon=0} \tag{4.27}$$

exists on $(0,T)$ *and satisfies the linear initial value problem*

$$r_t = \mu r_{xx} - ((h+v)r)_x - ((h+v)\tilde{\psi})_x \tag{4.28}$$

$$r(t,-1) = 0, \quad r(t,1) = 0 \tag{4.29}$$

$$r(0,x) = -\tilde{\psi}(x), \tag{4.30}$$

where $\tilde{\psi}(x) = (x+1)/2$ *and* $v = v(t,x;0)$ *is the solution to the NLCD equation (4.10)-(4.12) with* $\varepsilon = 0$.

Proof: Consider the abstract formulation of the transformed NLCD equation given by (4.23)-(4.25). Recall that $V = X^{1/2}$ and the linear operator $\mathcal{A}$ defined in (4.23) is sectorial and does not depend on ε. To apply Corollary 4.2.1, it remains to show that the nonlinearity $\mathcal{F} : V \times \mathbb{R} \subset X \times \mathbb{R} \to X$ is continuous and the Fréchet derivatives $D_v\mathcal{F}(v;\varepsilon)$, $D_\varepsilon\mathcal{F}(v;\varepsilon)$ and $D_\varepsilon v_0(\varepsilon)$ all exist and are continuous over $V \times \mathbb{R}$. Since the solution $v(t;0)$ to the undisturbed problem exists for all time, it will follow that the sensitivity of the transformed state will exist for all time.

First, we show the continuity of $\mathcal{F}$ in $V \times \mathbb{R}$. For ease of notation, define $\tilde{\psi}(x) = (x+1)/2$ so that $\psi(x;\varepsilon) = \varepsilon(x+1)/2 = \varepsilon\tilde{\psi}(x)$. For any (u,ε) and $(v,\hat{\varepsilon})$ in the product space $V \times \mathbb{R}$,

$$\|\mathcal{F}(u;\varepsilon) - \mathcal{F}(v;\hat{\varepsilon})\|_X \leq \|uu_x - vv_x\|_X + \|(\psi(\varepsilon)\,u)_x - (\psi(\hat{\varepsilon})\,v)_x\|_X + \|f(\varepsilon) - f(\hat{\varepsilon})\|_X .$$

We bound each term separately. In the proof of Theorem 4.3.4, we bounded the first term by

$$\|uu_x - vv_x\|_X \leq \sqrt{2}\,(\|u\|_V + \|v\|_V)\,\|u - v\|_V .$$

For the second term, using the inequality (4.26) and $\psi = \varepsilon\tilde{\psi}$ yields

$$\begin{aligned}
\|(\psi(\varepsilon)\,u)_x - (\psi(\hat{\varepsilon})\,v)_x\|_X &= \|\,\varepsilon(\tilde{\psi}u)_x - \varepsilon(\tilde{\psi}v)_x + \varepsilon(\tilde{\psi}v)_x - \hat{\varepsilon}(\tilde{\psi}v)_x\|_X \\
&\leq \|\,\varepsilon(\tilde{\psi}(u-v))_x\|_X + \|\,(\varepsilon - \hat{\varepsilon})(\tilde{\psi}v)_x\|_X \\
&\leq \|\varepsilon\|_{\mathbb{R}} \left(\|\,\tilde{\psi}_x(u-v)\|_X + \|\,\tilde{\psi}(u-v)_x\|_X\right) + \|\,\tilde{\psi}v\|_V \|\,\varepsilon - \hat{\varepsilon}\|_{\mathbb{R}} \\
&\leq \sqrt{2}\,\|\varepsilon\|_{\mathbb{R}} \left(\|\,\tilde{\psi}\|_V + \|\,\tilde{\psi}\|_{L^\infty}\right) \|u-v\|_V + \|\,\tilde{\psi}v\|_V \|\,\varepsilon - \hat{\varepsilon}\|_{\mathbb{R}}.
\end{aligned}$$

For the third term, a straightforward computation using the definition of $f(\varepsilon)$ in (4.21) gives

$$\|f(\varepsilon) - f(\hat{\varepsilon})\|_X \leq \|\varepsilon - \hat{\varepsilon}\|_{\mathbb{R}} \left(\|\,h\,\tilde{\psi}\|_V + \|\varepsilon + \hat{\varepsilon}\|_{\mathbb{R}}\,\|\,\tilde{\psi}\,\tilde{\psi}_x\|_X\right).$$

Letting $\|u - v\|_V$ and $\|\varepsilon - \hat{\varepsilon}\|_{\mathbb{R}}$ tend to zero shows that $\mathcal{F}(\cdot,\cdot)$ is continuous over $V \times \mathbb{R}$.

Next, consider the Fréchet differentiability of $\mathcal{F}(\cdot,\cdot)$ with respect to each of its arguments. For a fixed $\varepsilon \in \mathbb{R}$, $\mathcal{F}$ maps V to X and for v fixed in V, $\mathcal{F}$ maps $\mathbb{R}$ to X. Therefore, the Fréchet derivatives will be defined on the domains

$$D_v\mathcal{F}(v;\varepsilon) : V \subset X \to X, \quad D_\varepsilon\mathcal{F}(v;\varepsilon) : \mathbb{R} \to X.$$

It will be shown that the Fréchet derivatives are given by

$$[D_v\mathcal{F}(v;\varepsilon)]\,r = -(vr)_x - (\psi(\varepsilon)r)_x, \quad [D_\varepsilon\mathcal{F}(v;\varepsilon)]\,\hat{\varepsilon} = \left[-(\tilde{\psi}v)_x - (\tilde{\psi}h)_x - \varepsilon\tilde{\psi}\right]\hat{\varepsilon}.$$

First, it is easily seen that both of these operators are continuous on their respective domains of definition. Showing that these linear operators are actually the appropriate Fréchet derivatives is also straightforward. For the v derivative, let ε be fixed in $\mathbb{R}$. A direct computation shows

$$\begin{aligned}\|\mathcal{F}(r;\varepsilon) - \mathcal{F}(v,\varepsilon) - [D_v\mathcal{F}(v;\varepsilon)](r-v)\|_X &= \|-(r-v)_x(r-v)\|_X \\ &\leq \|r-v\|_{L^\infty}\|(r-v)_x\|_X \leq \sqrt{2}\,\|r-v\|_V^2\end{aligned}$$

which is $o(\|r-v\|_V)$ as $\|r-v\|_V \to 0$. Therefore, $D_v\mathcal{F}(v;\varepsilon)$ is the Fréchet derivative of $\mathcal{F}$ with respect to v. The other follows in a similar fashion. Also, recall that $v_0(x;\varepsilon) = w_0(x) - \psi(x;\varepsilon)$ (see 4.20). Since $\psi(x;\varepsilon) = \varepsilon\tilde{\psi}(x) = \varepsilon(x+1)/2$, v_0 is clearly differentiable with respect to ε over all of $\mathbb{R}$ and the derivative is given by $D_\varepsilon v_0(\varepsilon) = -\tilde{\psi}$.

All of the requirements of Corollary 4.2.1 are now satisfied. Since the solution to $v(t;0)$ to the undisturbed problem exists on $(0,T)$, it follows that the sensitivity defined in (4.27) exists on $(0,T)$ and satisfies the abstract linear initial value problem

$$\dot{r}(t) = \mathcal{A}r(t) + [D_v\mathcal{F}(v;0)]\,r(t) + [D_\varepsilon\mathcal{F}(v;0)], \quad r(0) = D_\varepsilon v_0(0),$$

on $(0,T)$. Substituting the exact form of the operators into the above expression shows that $r = r(t,x)$ must satisfy the linear partial differential equation given by (4.28)-(4.30). □

Note that the sensitivity equation for the transformed state is precisely what one obtains by differentiating the transformed NLCD equation (4.18)-(4.20) with respect to ε, using the chain rule and setting $\varepsilon = 0$. The abstract framework has made this procedure rigorous.

The above result can be used to prove that the sensitivities for the untransformed NLCD equation satisfy the formally derived sensitivity equation presented in the beginning of this section.

Corollary 4.3.2 *Let $w(t,x;\varepsilon)$ be the solution of the NLCD equation (4.10)-(4.12) on $(0,T)$ for some $T > 0$. Then $w(t,x;\varepsilon)$ is continuously differentiable with respect to ε so that the sensitivity defined in (4.14) exists on $(0,T)$ and satisfies the linear sensitivity equation (4.15)-(4.17).*

Proof: Let $w(t,x;\varepsilon)$ and $v(t,x;\varepsilon)$ be the solutions of the untransformed and transformed NLCD equations, respectively. Also let $r(t,x)$ be the sensitivity of the transformed state v defined in the above theorem in (4.27). The transformation was given by $w(t,x;\varepsilon) = v(t,x;\varepsilon) + \psi(x;\varepsilon)$, where $\psi(x;\varepsilon) = \varepsilon\tilde{\psi}(x) = \varepsilon(x+1)/2$. Since v and ψ are both differentiable with respect to ε, so is w. Therefore, $s(t,x)$, the sensitivity of the untransformed state defined in (4.14), is given by

$$s(t,x) = \frac{\partial}{\partial\varepsilon}w(t,x;\varepsilon)\Big|_{\varepsilon=0} = \frac{\partial}{\partial\varepsilon}v(t,x;\varepsilon)\Big|_{\varepsilon=0} + \frac{\partial}{\partial\varepsilon}\psi(x;\varepsilon)\Big|_{\varepsilon=0} = r(t,x) + \tilde{\psi}(x)$$

Since the sensitivity $r(t,x)$ exists on $(0,T)$, so does $s(t,x)$. Also, since $r(t,x)$ satisfies the linear partial differential equation (4.28)-(4.30), a substitution shows that the $s(t,x)$ satisfies the linear sensitivity equation (4.15)-(4.17). □

Here, we make some observations about the sensitivities $s(t,x)$ for the untransformed NLCD equation. The above corollary shows that $s(t,x)$ satisfies the sensitivity equation given by

$$\begin{gathered} s_t = \mu s_{xx} - (hs)_x - (ws)_x \\ s(t,-1) = 0, \quad s(t,1) = 1 \\ s(0,x) = 0. \end{gathered}$$

By Proposition 4.3.1, solutions of the unperturbed NLCD equation will tend to zero if the initial data is small and smooth. In this case, if the sensitivity does not grow without bound, one might expect the term $(ws)_x$ in the sensitivity equation to become negligible as $t \to \infty$. Therefore, in certain cases the asymptotic behavior of the sensitivity $s(t,x)$ can possibly be determined by the linear steady problem

$$\mu s_{xx}(x) - (h(x)\, s(x))_x = 0, \quad s(t,-1) = 0, \;\; s(t,1) = 1.$$

This equation can be transformed ($r = s + \tilde{\psi}$) to yield an equation with homogeneous boundary conditions given by

$$\mu r_{xx}(x) - (h(x)\, r(x))_x = (h(x)\, \tilde{\psi}(x))_x, \quad r(-1) = 0, \;\; r(1) = 0.$$

Theorem 4.3.2 guarantees that the linear operator $\mathcal{A}$ given by (4.23) is invertible and therefore this equation has a unique solution. Inverting the transformation leads to a unique solution for the steady equation for s.

We have not proved here that these steady equations actually determine the long time behavior of the sensitivities, but they still provide insight into the sensitivity of solutions with respect to the disturbance ε. In particular, we note that due to the non-normality of the linear operator appearing in the steady (and time dependent) sensitivity equations, there is the possibility that the forcing terms will cause the sensitivities to be large. Therefore, these steady equations will be investigated numerically in the next chapter.

4.4 Sensitivities for a 2D Burgers' Equation

Now we return to our motivating problem, a two dimensional scalar Burgers' equation over the rectangular domain $\Omega = (0,1) \times (0,1) \subset \mathbb{R}^2$. The partial differential equation is given by

$$w_t(t,x,y) + w(t,x,y)w_x(t,x,y) + w(t,x,y)w_y(t,x,y) = \mu \nabla^2 w(t,x,y), \tag{4.31}$$

with μ a positive constant, and is accompanied by periodic boundary conditions in the x direction,

$$w(t,0,y) = w(t,1,y), \quad w_x(t,0,y) = w_x(t,1,y) \quad \text{for all } y, \tag{4.32}$$

nonhomogeneous Dirichlet boundary conditions on the top and bottom walls of Ω,

$$w(t,x,0) = 1, \quad w(t,x,1) = -1, \tag{4.33}$$

and initial condition

$$w(0,x,y) = w_0(x,y). \tag{4.34}$$

As discussed in the introduction to this chapter, we will not directly study this problem but rather we investigate the fluctuations about an equilibrium state. Specifically, we investigate the sensitivity of the fluctuations with respect to a simplified form of small wall roughness. Therefore, we consider a *parameter dependent domain* Ω_q that is in some sense close to the original domain Ω and consider sensitivities of the solution with respect to the shape parameters q. The fluctuation problem is transformed from the parameter dependent domain to a fixed domain that is more convenient for analysis and computations.

Some of the details for the sensitivity equation derivation are similar to the 1D nonlinear convection diffusion (NLCD) equation considered in the previous section. Therefore, the full details of the derivation will not be presented here. However, in spite of the many similarities between the problems, there is one main difference. Namely, the 1D problem holds over a fixed domain while the domain for the 2D problem moves with the parameters. Treating sensitivities with respect to a shape parameter can cause some challenging theoretical and computational issues. First, some simple model problems examined in [33] and [130] show that solutions and sensitivities can have different regularities, or the regularity of each may change with respect to the shape parameter. Also, different techniques to transform the problem to a "computational domain" can also lead to differences in regularity for computed sensitivities [33]. We will comment more on the numerical challenges in the next chapter.

4.4.1 Problem Formulation

The following result guarantees the existence of a specific equilibrium state for the above problem.

Lemma 4.4.1 *The two dimensional Burgers' equation given by (4.31)-(4.34) has at least one equilibrium state. In particular, there exists a unique equilibrium h of the form $h = h(y)$ that is given by the unique solution of the one dimensional boundary value problem*

$$h(y)h_y(y) = \mu h_{yy}(y), \quad h(0) = 1, \quad h(1) = -1. \tag{4.35}$$

Specifically, $h(\cdot)$ is a hyperbolic tangent profile of the form

$$h(y) = c \tanh\left(-\frac{c}{2\mu}(y - 1/2)\right), \tag{4.36}$$

where c is chosen so that this function satisfies the Dirichlet boundary conditions.

Proof: An equilibrium state h must satisfy the steady PDE

$$h(x,y)h_x(x,y) + h(x,y)h_y(x,y) = \mu\left(h_{xx}(x,y) + h_{yy}(x,y)\right),$$

with the x periodic boundary conditions (4.32) and the Dirichlet boundary conditions (4.33). Note that a solution of the form $h(x,y) = h(y)$ will automatically satisfy the x periodic boundary conditions. Making this simplification yields the 1D steady state Burgers' equation with nonhomogeneous Dirichlet boundary conditions given by (4.35). Corollary 3.3.1 shows that this problem has a unique solution given by (4.36). □

No other equilibrium states have been (numerically) observed for this problem. Although it is unknown whether this equilibrium is unique, this is plausible due to the similarity of this 2D problem to the 1D Burgers' equation. This is an open question. Define the fluctuations z about the hyperbolic tangent equilibrium h by $z(t,x,y) = w(t,x,y) - h(y)$. The function z then satisfies the 2D NLCD equation

$$z_t + zz_x + zz_y = \mu\nabla^2 z - (hz)_x - (hz)_y, \tag{4.37}$$

with periodic boundary conditions in the x direction

$$z(t,0,y) = z(t,1,y), \quad z_x(t,0,y) = z_x(t,1,y), \tag{4.38}$$

homogeneous Dirichlet boundary conditions on the top and bottom walls

$$z(t,x,0) = 0, \quad z(t,x,1) = 0, \tag{4.39}$$

and initial data

$$z(0,x,y) = z_0(x,y) := w_0(x,y) - h(y). \tag{4.40}$$

This equation holds on the rectangular domain $\Omega = (0,1)\times(0,1)$. Below, we investigate the sensitivity of solutions to this equation with respect to a simplified form of small wall roughness.

First, we present the weak form of the problem. Let the state space X be $L^2(\Omega)$ with the standard inner product and norm. Also define $V \subset X$ by

$$V = \left\{ v \in H^1(\Omega) \,:\, v(0,y) = v(1,y),\ 0 < y < 1;\ v(x,0) = 0 = v(x,1),\ 0 < x < 1 \right\},$$

with inner product $\langle u, v\rangle_V = \langle u_x, v_x\rangle_X + \langle u_y, v_y\rangle_X$ and corresponding norm. In a similar manner to the previous section, the weak problem is to find $z \in V$ such that

$$\frac{\partial}{\partial t}\langle z, \varphi\rangle_X = -\mu\langle z, \varphi\rangle_V - \langle h(z_x + z_y), \varphi\rangle_X - \langle h_x z, \varphi\rangle_X - \langle z(z_x + z_y), \varphi\rangle_X + \langle f, \varphi\rangle_X$$

for all $\varphi \in V$. A bilinear form $a : V \times V \to X$ can be defined by

$$a(u, v) = -\mu \langle z, \varphi \rangle_V - \langle h(z_x + z_y), \varphi \rangle_X - \langle h_x z, \varphi \rangle_X .$$

As in the previous section, this leads to the linear operator $\mathcal{A} : \mathcal{D}(\mathcal{A}) \subset X \to X$ given by

$$\mathcal{A}v = \mu \nabla^2 v - (hv)_x - (hv)_y$$

on the domain

$$\mathcal{D}(\mathcal{A}) = \{ v \in V \, : \, \mathcal{A}v \in X \} .$$

Here, the derivatives hold in the distributional sense. As before, we can show that $\mathcal{A}$ is sectorial and generates an analytic semigroup.

Lemma 4.4.2 *Let $\Omega = (0, 1) \times (0, 1)$ and $h(\cdot) \in C^1(\mathrm{cl}(\Omega))$. Then for the spaces X and V and the linear operator $\mathcal{A}$ defined above, $X^{1/2} = V$, the spectrum of $\mathcal{A}$ is discrete and $\mathcal{A}$ is sectorial and generates an analytic semigroup.*

Proof: The proof is similar to the analogous result for the one dimensional NLCD problem in the previous section and is omitted. □

Unlike the one dimensional case, we do not know if $\mathcal{A}$ has all of its eigenvalues bounded away from the imaginary axis in the left half plane. Therefore, we cannot conclude that $\mathcal{A}$ generates an exponentially stable semigroup. However, due to the similarity of this problem with the 1D NLCD equation, it is likely that $\mathcal{A}$ does generate an exponentially stable semigroup. Also, numerical approximations (using finite elements, see section 5.2.4) of the spectrum of $\mathcal{A}$ and also of solution trajectories indicate that the zero state is asymptotically stable. These questions are open.

Define the nonlinear operator $\mathcal{F} : V \subset X \to X$ by $\mathcal{F}(v) = -vv_x - vv_y$. Then the NLCD equation (4.37)-(4.40) can be written as the abstract initial value problem over X given by

$$\dot{z}(t) = \mathcal{A}z(t) + \mathcal{F}(z(t)), \quad z(0) = z_0 \in X.$$

With the abstract formulation of the problem on the smooth domain completed, we now examine the fluctuation equation over the rough walled domain. The details of the abstract formulation are similar to the smooth domain case and so are not presented here.

Consider the NLCD equation (4.37)-(4.40) on the pseudo-rectangular domain

$$\Omega(\alpha, \beta) = \left\{ (x, y) \in \mathbb{R}^2 \, : \, 0 < x < 1, \, b(x; \alpha, \beta) < y < t(x; \alpha, \beta) \right\},$$

where

$$b(x; \alpha, \beta) = \alpha \sin(\beta x), \quad t(x; \alpha, \beta) = 1 + b(x; \alpha, \beta) = 1 + \alpha \sin(\beta x).$$

Here, $y = b(x; \alpha, \beta)$ and $y = t(x; \alpha, \beta)$ are the equations for the bottom and top wall of the domain. If α is small, the perturbed domain $\Omega(\alpha, \beta)$ is, in a sense, close to the smooth domain $\Omega(0, 0) = (0, 1) \times (0, 1)$. Therefore, the perturbation to the domain can be viewed as a simplified form of wall roughness. The constant α measures the height of the wall roughness

while β can be thought of as a degree of roughness. See figure 4.1 in the introduction to this chapter for a comparison of the smooth and rough domains.

The perturbation to the domain clearly alters the formulation of the above PDE. In particular, the Dirichlet boundary conditions (4.39) become

$$z(t,x,b(x;\alpha,\beta);\alpha,\beta)=0, \quad z(t,x,t(x;\alpha,\beta);\alpha,\beta)=0. \tag{4.41}$$

This follows from directly substituting in the equations $y=b$ and $y=t$ for the bottom and top walls, respectively. A more subtle effect of the perturbation of the domain is on the x periodic boundary conditions. Note that the left wall of the domain is given by

$$\{\,(x,y)\,:\,x=0,\ b(0;\alpha,\beta)<y<t(0;\alpha,\beta)\}$$

while the right wall is now given by

$$\{\,(x,y)\,:\,x=1,\ b(1;\alpha,\beta)<y<t(1;\alpha,\beta)\}\,.$$

This is due to the form of the wall roughness. Now $b(0;\alpha,\beta)=0$ and so the left wall is not perturbed. However, $b(1;\alpha,\beta)$ is not necessarily zero and so the right wall may be "moved". Due to the simple forms of b and t, the restriction on y can be written as $0<y-b(1;\alpha,\beta)<1$. Since for the x periodic boundary conditions the function values and x partial derivatives should be equal on the left and right walls of the perturbed domain, a natural reformulation of the x periodic boundary conditions (4.38) is given by

$$z(t,0,y)=z(t,1,y-b(1;\alpha,\beta)), \quad z_x(t,0,y)=z_x(t,1,y-b(1;\alpha,\beta)) \quad \text{for all } y. \tag{4.42}$$

If the perturbation to the domain had been more complex, it may have been even more difficult, if not impossible, to formulate reasonable boundary conditions on the rough walled domain.

4.4.2 Sensitivities and the Transformed State Equation

We now investigate the sensitivity of the solution z with respect to the height of the wall roughness α. Denote the dependence of the solution on the shape parameters α and β by writing $z=z(t,x,y;\alpha,\beta)$. Then define the sensitivity of the solution to the perturbation of the domain as

$$s(t,x,y)=\frac{\partial z}{\partial \alpha}(t,x,y;\alpha,\beta)\Big|_{\alpha=0,\ \beta=\beta_0}.$$

Here, β_0 is chosen to indicate the degree of wall roughness. Since the domain is parameter dependent, there are two natural ways to formulate sensitivity equations. The first method will lead to an equation that is not practical due to the periodic boundary conditions. For the second method, the nonlinear convection-diffusion equation is transformed from the parameter dependent domain back to the original smooth domain. The sensitivities are then formulated in a similar way to the 1D NLCD equation considered in the previous section.

We now briefly summarize two different methods to formulate a sensitivity equation to solve for $s(t,x,y)$. For a more complete discussion and comparison of these methods, see [33]. The first method is known as the **hybrid-sensitivity equation method** (HSEM) and it proceeds as follows.

1. Derive the sensitivity equation on the parameter dependent domain.
2. Transform the state equation and the sensitivity equation to a fixed "computational domain".
3. Solve the transformed equations and invert the transformation to recover the sensitivity.

Here, a computational domain is a domain that does not depend on the sensitivity parameters and should also be relatively easy to compute on. An alternate strategy is known as the **abstract semi-analytical method** (ASAM).

1. Transform the state equation to a fixed computational domain.
2. Derive the sensitivity equation for the transformed state on the computational domain.
3. Solve for the transformed state and its sensitivity.
4. Recover the original sensitivity by inverting the transformation and using the chain rule.

In this method, the last step requires the sensitivity of the transformation with respect to the parameter of interest. This can often be very complicated.

For the HSEM, formally differentiate the 2D Burgers' fluctuation equation (4.37) with respect to α to obtain a linear PDE for the sensitivity given by

$$s_t = \mu\nabla^2 s - ((h+z)\,s)_x - ((h+z)\,s)_y.$$

For the boundary conditions on the parameter dependent domain, one must use the chain rule since the boundary of the domain and the solution depend on the parameter α. In particular, for the Dirichlet boundary conditions (4.41), differentiating with respect to α and setting $\alpha = 0$ yields Dirichlet boundary conditions for the sensitivity given by

$$\begin{aligned} s(t,x,0) &= -z_y(t,x,0;0,\beta_0)\,b_\alpha(x;0,\beta_0), \\ s(t,x,1) &= -z_y(t,x,1;0,\beta_0)\,t_\alpha(x;0,\beta_0). \end{aligned}$$

(As with all other subscripts, the subscripts on b and t denote partial derivatives.) For the periodic boundary conditions (4.42), we obtain

$$\begin{aligned} s(t,0,y) &= -z_y(t,1,y;0,\beta_0)\,b_\alpha(x;0,\beta_0) + s(t,1,y), \\ s(t,x,1) &= -z_{yx}(t,1,y;0,\beta_0)\,t_\alpha(x;0,\beta_0) + s_x(t,1,y). \end{aligned}$$

The second derivative term in the second condition is undesirable for numerical computation. Therefore, the HSEM is not practical for this problem.

For the ASAM, one must specify a fixed "computational domain" and a transformation. In this case, the natural computational domain is the smooth domain $\Omega(0,0) = (0,1)\times(0,1)$. For simplicity, we refer to this domain as Ω. A transformation between the rough walled domain and the smooth domain is easily found due to the simplicity of the wall roughness. Define $T : \Omega(\alpha,\beta) \to \Omega$ by

$$\begin{bmatrix} \xi \\ \eta \end{bmatrix} = T(x,y;\alpha,\beta) = \begin{bmatrix} x \\ y - b(x;\alpha,\beta) \end{bmatrix}.$$

To avoid confusion, we use (x,y) coordinates in $\Omega(\alpha,\beta)$ and (ξ,η) coordinates for Ω. It is clear that T is invertible and $T^{-1} : \Omega \to \Omega(\alpha,\beta)$ is given by

$$\begin{bmatrix} x \\ y \end{bmatrix} = T^{-1}(\xi,\eta;\alpha,\beta) = \begin{bmatrix} \xi \\ \eta + b(\xi;\alpha,\beta) \end{bmatrix}.$$

Below, we transform the NLCD equation (4.37), (4.40), (4.41), (4.42) on $\Omega(\alpha,\beta)$ to an equation on Ω.

For ease of notation, momentarily suppress the dependence of all functions on the parameters α and β. Define $\phi(\xi,\eta)$ and $g(\xi,\eta)$ to be the transformations of the fluctuations $z(t,x,y)$ and the equilibrium state $h(x,y) = h(y)$ (4.36) to the smooth rectangle. Specifically,

$$\begin{aligned} \phi(\xi,\eta) &:= z(t,\xi,\eta+b(\xi)) = z(t,x(\xi),y(\xi,\eta)), \\ g(\xi,\eta) &:= h(\eta+b(\xi)) = h(y(\xi,\eta)). \end{aligned}$$

Since $z(t,x,y) = \phi(t,\xi(x),\eta(x,y))$ and $h(y) = g(\xi(x),\eta(x,y))$, the derivatives z_x, z_y, h_y, etc., can be computed using the chain rule to give

$$\begin{aligned} z_x(t,x,y) &= \phi_\xi(t,\xi(x),\eta(x,y)) + \eta_x(x,y)\,\phi_\eta(t,\xi(x),\eta(x,y)), \\ z_y(t,x,y) &= \phi_\eta(t,\xi(x),\eta(x,y)), \\ z_{xx}(t,x,y) &= \phi_{\xi\xi} + 2\eta_x\,\phi_{\xi\eta} + \eta_{xx}\,\phi_\eta + (\eta_x)^2\,\phi_{\eta\eta}, \\ z_{yy}(t,x,y) &= \phi_{\eta\eta}, \\ h_y(y) &= g_\eta, \\ h_{yy}(y) &= g_{\eta\eta}, \end{aligned}$$

since $\xi_x = 1$, $\xi_y = 0$, $\eta_y = 1$ and $\eta_{yy} = 0$.

To complete the transformation of all of the functions from $\Omega(\alpha,\beta)$ to Ω, we use the inverse transformation to change all variables from $(x,y) \in \Omega(\alpha,\beta)$ to $(\xi,\eta) \in \Omega$. Define the transformed derivative functions

$$A(\xi) := \eta_x(\,\xi,\eta - b(\xi)\,) = \eta_x(x,y) = -b_\xi(\xi) = -\alpha\beta\cos(\beta\xi),$$

$$B(\xi) \;:=\; \eta_{xx}(\,\xi, \eta - b(\xi)\,) \;=\; \eta_{xx}(x,y) \;=\; -b_{\xi\xi}(\xi) \;=\; \alpha\beta^2 \sin(\beta\xi).$$

Applying the transformation to the NLCD equation (4.37) on $\Omega(\alpha,\beta)$ yields an equation on Ω for $\phi(\xi,\eta;\alpha,\beta) = z(t,x(\xi),y(\xi,\eta);\alpha,\beta)$ given by

$$\begin{aligned}\phi_t + \phi\phi_\xi + (A+1)\phi\phi_\eta \;&=\; \mu\phi_{\xi\xi} + 2\mu A\phi_{\xi\eta} + \mu\left(A^2+1\right)\phi_{\eta\eta} - g\phi_\xi \\ &\quad + (\mu B - (A+1)g)\,\phi_\eta - g_\eta\phi.\end{aligned}$$

For the computations in the next chapter, it is useful to rewrite this equation in divergence form as

$$\begin{aligned}\phi_t + \phi\phi_\xi + (A+1)\phi\phi_\eta \;&=\; \mu\left(\frac{\partial}{\partial\xi}\left(\phi_\xi + A\phi_\eta\right) + \frac{\partial}{\partial\eta}\left(A\phi_\xi + \left(A^2+1\right)\phi_\eta\right)\right) \\ &\quad + (\mu B - (A+1)g - \mu A_\xi)\,\phi_\eta - g\phi_\xi - g_\eta\phi.\end{aligned}$$

Since $B = A_\xi$, this simplifies to

$$\begin{aligned}\phi_t + \phi\phi_\xi + (A+1)\phi\phi_\eta \;&=\; \mu\left(\frac{\partial}{\partial\xi}\left(\phi_\xi + A\phi_\eta\right) + \frac{\partial}{\partial\eta}\left(A\phi_\xi + \left(A^2+1\right)\phi_\eta\right)\right) \\ &\quad -(A+1)g\phi_\eta - g\phi_\xi - g_\eta\phi. \qquad (4.43)\end{aligned}$$

Applying the transformation to the boundary conditions (4.41), (4.42) and initial condition (4.40) on $\Omega(\alpha,\beta)$ gives

$$\phi(t,0,\eta) = \phi(t,1,\eta), \quad \phi_\xi(t,0,\eta) = \phi_\xi(t,1,\eta) \quad \text{for all } \eta, \qquad (4.44)$$

$$\phi(t,\xi,0) = 0, \quad \phi(t,\xi,1) = 0 \quad \text{for all } \xi, \qquad (4.45)$$

$$\phi(0,\xi,\eta) = \phi_0(\xi,\eta) := z_0(\xi,\eta + b(\xi)). \qquad (4.46)$$

The system (4.43)-(4.46) is the transformation of the fluctuation equations on $\Omega(\alpha,\beta)$ onto Ω. Notice that setting $\alpha = 0$ causes $A = 0$ and $g = h$ which reduces the transformed equations to the original fluctuation equations.

The transformed equation can be written as an abstract differential equation over $X = L^2(\Omega)$ as

$$\dot{\phi}(t) = \mathcal{A}\phi(t) + \hat{\mathcal{A}}(\alpha,\beta)\phi + \mathcal{F}(\phi(t)) + \hat{\mathcal{F}}(\phi(t);\alpha,\beta),$$

Here, $\mathcal{A}$ and $\mathcal{F}(\cdot)$ are the linear and nonlinear operators defined above for the problem on the smooth domain while $\hat{\mathcal{A}}(\alpha,\beta)$ and $\hat{\mathcal{F}}(\,\cdot\,;\alpha,\beta)$ are linear and nonlinear parameter dependent perturbations to these operators. Therefore, the simple form of wall roughness causes a perturbation of the original equation in both the linear and nonlinear terms. The perturbed nonlinear term $\mathcal{F}(\cdot) + \hat{\mathcal{F}}(\,\cdot\,;\alpha,\beta)$ is still conservative. This follows directly by changing variables in the integration back to the rough walled domain.

Since the boundary conditions hold on a parameter independent domain, one can derive an equation for the sensitivity of the transformed state ϕ with respect to α at $\alpha = 0$. Since

this follows in a similar manner to the 1D NLCD equation in the previous section, the details will not be presented here. We mention that the solution of the original undisturbed fluctuation equation would appear explicitly in the sensitivity equation. This follows since a substitution of $\alpha = 0$ into the transformed state equation yields the original NLCD equation. Therefore, the transformed equations would never have to be solved to compute the sensitivities. After solving for the sensitivity of the transformed state, one would then use the chain rule to recover the sensitivity of the fluctuations z with respect to α, i.e., $s = \partial z/\partial\alpha$. For further details on this last step, see [33].

There is a great potential for the sensitivity of the fluctuations with respect to the wall roughness to be large. This is due to the non-normality of the linear operator. However, unlike the ODE model problems and the 1D NLCD equation, the sensitivity equation will not contain a forcing function. Therefore, the sensitivity can only be driven by the non-normality of the linear operator and by the solution of the fluctuation equations.

4.5 Discussion

In this chapter, we focused on formulating the continuous sensitivity method to examine the change in solutions to certain model problems with respect to small disturbance to the equations. The derivative of the solution with respect to a parameter is a measure of the sensitivity of the solution with respect to the small disturbance. To find this sensitivity, the equations are formally differentiated with respect to the parameter leading to a linear equation for the sensitivity. A classical result from ODE theory makes this procedure rigorous for ODEs, however for a general infinite dimensional system it is not clear that the sensitivities exist or satisfy the formally derived equation. However, for a class of abstract semilinear parabolic equations it is known that the formal derivations can be made rigorous. We presented a one dimensional nonlinear convection-diffusion equation as an example to illustrate the ideas.

Our motivation for examining the sensitivity of solutions to the model problems with respect to small disturbances comes from the new scenarios for transition to turbulence discussed in section 2.4.2. These theories indicate that small disturbances play a large role in the transition process. However, the effects of the small disturbances have only been studied for non-normal linear systems. The CSEM allows one to examine the sensitivity of a fully nonlinear problem with respect to a small disturbance.

As a starting point, we examined three model problems under various types of small disturbances. Through various transformations, it was seen that both the linear and nonlinear terms in an equation can be perturbed by a small disturbance. Also, conservative nonlinearities can cease to be conservative in the perturbed system. These properties of the disturbed system cannot be deduced by a linear investigation into the stability or sensitivity of a system. However, using the CSEM, one can study the affects of the perturbed nonlinear terms on solutions. For the model problems, the linear sensitivity equations arising from each problem are governed by non-normal linear operators. As discussed in section 2.4.2, this non-normality can cause substantial transient growth of solutions. Also, the sensitivity

equations are all driven by the solution to the undisturbed problem and can be accompanied by a forcing function. These forces combined with the non-normality of the linear operator show that the sensitivities have the potential to be large even if the disturbances to the problem are small.

Chapter 5

Numerical Results

In this chapter, we present numerical results for the model problems outlined in the previous chapter. We begin with a description of the finite element method used in this thesis to approximate the solutions of the partial differential equation model problems. Specifically, we focus on the group finite element formulation used on the nonlinear problems. We apply this method to the 1D and 2D nonlinear convection diffusion (NLCD) equations and compare the approximate solutions of the undisturbed and disturbed problems. We show that a small disturbance can have a great impact on the solution and also indicate why classical linear analysis cannot predict this behavior. The computed sensitivity for the one dimensional NLCD equation shows that the continuous sensitivity equation method (CSEM) can provide insight into the disturbed problem. Next, a sensitivity analysis is performed for the ODE model problems. We also consider the control problem and show that a linear feedback control can decrease the sensitivity with respect to small disturbances. In particular, we demonstrate how a linear control can delay transition or even relaminarize a fully chaotic system.

5.1 Finite Element Formulation

We briefly review the finite element scheme used for our numerical experiments. Specifically, we focus on the use of the group finite element method to approximate the solutions of 1D and 2D NLCD equations and briefly compare this method to the standard Galerkin finite element method. The main motivation for using the group method is that, when applicable, it is more efficient than the standard finite element method and also retains accuracy. Although we do not discuss the standard finite element method in great detail (a standard references is Fix and Strang's text [54]), we carefully describe the group finite element method for the model problems. For a more general description of the group method, see [40] (where the group method is called "product approximation") and the references in section 5.1.2 below.

It should be noted that the nonlinear convection-diffusion equation become especially difficult to simulate when the first derivative convection terms dominate the second derivative diffusion terms. This naturally occurs when the viscosity coefficient μ of the diffusion term

is small. This is analogous to the large Reynolds number case. Standard numerical methods for simulation become increasingly unreliable the more convection dominates diffusion in such problems. Therefore, many modified and more advanced numerical schemes have been developed to treat such difficulties. Upwinded finite differences and finite elements [57], stabilized finite elements [24] and least squares finite elements [23] have been utilized for convection dominated problems. However, this numerical issue is not a focus of this work and hence we limit our study to relatively moderate values of the diffusion parameter μ.

Matlab's `ode23s` is used to solve the nonlinear ODE systems that resulted from the finite element approximations. The routine `ode23s` is an implicit 2^{nd}-3^{rd} order solver with adaptive time stepping. The latter feature is especially important for the model problems considered here since some of the solutions change slowly over very long time intervals. Thus, `ode23s` combined with the group finite element method provides an effective computational algorithm for the model problems. With few exceptions, most computations required less than a minute on a single Pentium 4 processor.

5.1.1 Standard Finite Element Formulation for the 1D Model Problem

Here, we describe the standard Galerkin finite element method for the transformed nonlinear convection-diffusion model problem (4.18)-(4.20) that was discussed in section 4.3. The system takes the general form

$$w_t(t,x) + w(t,x)w_x(t,x) = \mu w_{xx}(t,x) - (g(x)\, w(t,x))_x + f(x), \tag{5.1}$$

with Dirichlet boundary conditions

$$w(t,-1) = 0, \quad w(t,1) = 0, \tag{5.2}$$

and initial condition

$$w(0,x) = w_0(x). \tag{5.3}$$

We assume μ is a positive constant, $g \in C^1(-1,1)$ and the forcing function as well as the initial condition are both in $L^2(-1,1)$. Let $X = L^2(-1,1)$ with the standard inner product and norm. Throughout this section, we denote the L^2 inner product by $\langle \cdot, \cdot \rangle$. Also let $V = H_0^1(-1,1)$. Recall that the weak form of the equation is given by

$$\frac{\partial}{\partial t} \langle w, \varphi \rangle = -\mu \langle w_x, \varphi_x \rangle + \langle gw, \varphi_x \rangle - \langle ww_x, \varphi \rangle + \langle f, \varphi \rangle, \tag{5.4}$$

where $\varphi(\cdot) \in V$. Once an approximate solution is computed for this system, the transformation is inverted to yield an approximate solution to the original nonlinear convection-diffusion equation (4.10)-(4.12).

We search for an approximate solution w^N in a finite dimensional subspace V^N of V. To form V^N, partition the solution interval $[-1,1]$ into $x_0 = -1 < x_1 < \cdots < x_N < x_{N+1} = 1$

(the "mesh") and define the piecewise linear basis functions by

$$\varphi_j(x) = \begin{cases} (x - x_{j-1})/(x_j - x_{j-1}), & x \in [x_{j-1}, x_j] \\ (x - x_{j+1})/(x_j - x_{j+1}), & x \in [x_j, x_{j+1}] \\ 0, & \text{otherwise} \end{cases}. \tag{5.5}$$

These functions are all contained in V except for $\varphi_0(\cdot)$ and $\varphi_{N+1}(\cdot)$. These functions are not required and so we define V^N by $V^N = \text{span}\{\varphi_1(\cdot), \ldots, \varphi_N(\cdot)\} \subset V$. The approximate solution $w^N(t, \cdot) \in V^N$ is defined by

$$w^N(t, x) = \sum_{j=1}^{N} w_j(t)\varphi_j(x), \tag{5.6}$$

where the functions $w_j(\cdot)$ are unknown.

Substituting the trial solution into the weak form (5.4) and choosing the test function $\varphi = \varphi_i$, for $i = 1, \ldots, N$, yields the standard finite element ordinary differential equations

$$\sum_j \langle \varphi_i, \varphi_j \rangle \dot{w}_j(t) = \sum_j \left(-\mu \left\langle \varphi_i', \varphi_j' \right\rangle + \langle g\, \varphi_i', \varphi_j \rangle \right) w_j(t) - \left\langle w^N w_x^N, \varphi_i \right\rangle + \langle f, \varphi_j \rangle, \tag{5.7}$$

These equations simplify to

$$\mathbf{M}\dot{\mathbf{w}}(t) = \mathbf{A}\mathbf{w}(t) + F(\mathbf{w}(t)) + \mathbf{f}, \tag{5.8}$$

where $\mathbf{w}(t) = [w_1(t), \ldots, w_N(t)]^T$ and the entries of $\mathbf{M}$, $\mathbf{A}$, $F(\cdot)$ and $\mathbf{f}$ are given by

$$M_{ij} = \langle \varphi_i, \varphi_j \rangle, \tag{5.9}$$

$$A_{ij} = -\mu \left\langle \varphi_i', \varphi_j' \right\rangle + \langle g\, \varphi_i', \varphi_j \rangle, \tag{5.10}$$

$$F_i(w) = -\left\langle w^N w_x^N, \varphi_i \right\rangle, \quad \text{and} \tag{5.11}$$

$$f_i = \langle f, \varphi_i \rangle. \tag{5.12}$$

The mass matrix $\mathbf{M}$ is well known to be invertible. Due to the simple form of the piecewise linear shape functions, $F_i(w)$ can be computed explicitly with an equally spaced mesh as

$$F_i(w) = \frac{1}{6}\left(w_{i-1}^2 + w_{i-1}w_i - w_i w_{i+1} - w_{i+1}^2 \right). \tag{5.13}$$

To obtain the initial condition for the finite element ODE (5.8), project the initial condition (5.3) of the NLCD equation onto V^N, the span of the linear basis functions. That requires one to find a function of the form

$$v_0(\cdot) = \sum_{j=1}^{N} a_j\, \varphi_j(\cdot),$$

that minimizes the distance, $\|v_0 - w_0\|_{L^2}$, to the initial condition $w_0(\cdot)$. It is well known (see [82, section 3.3]) that this minimization problem is equivalent to solving $\langle v_0 - w_0, \varphi_i \rangle_{L^2} = 0$ for each φ_i in V^N. Expanding the sum yields the linear system $\mathbf{Ma} = \mathbf{b}$, where $b_i = \langle w_0, \varphi_i \rangle_{L^2}$, and $\mathbf{M}$ is the mass matrix given above. The vector $\mathbf{a}$ is then the initial condition for the finite element ODE.

5.1.2 The Group Finite Element Formulation and a Comparison with the Standard Formulation

Here, we describe the group finite element method for the one dimensional model NLCD equation (5.1)-(5.3) and contrast it with the standard finite element method. First, rewrite the Burgers' equation (5.1) in so called conservation form as

$$w_t(t,x) + \frac{1}{2}\left(w^2(t,x)\right)_x = \mu w_{xx}(t,x) - (g(x)\, w(t,x))_x + f(x)$$

and introduce the weak form

$$\frac{\partial}{\partial t}\langle w, \varphi \rangle = -\mu \langle w_x, \varphi_x \rangle + \langle gw, \varphi_x \rangle - \left\langle (w^2/2)_x, \varphi \right\rangle + \langle f, \varphi \rangle .$$

As before, we use a piecewise linear approximation (5.6) to the solution $w(t,x)$ but we also introduce a separate approximation for the nonlinear term, w^2, given by

$$w^2(t,x) \approx \sum_{j=1}^{N} w_j^2(t)\varphi_j(x).$$

As before, substituting these approximations into the weak form yields the group finite element ordinary differential equations

$$\sum_j \langle \varphi_i, \varphi_j \rangle \dot{w}_j(t) = \sum_j \left(-\mu \left\langle \varphi_i', \varphi_j' \right\rangle + \langle g\, \varphi_i', \varphi_j \rangle\right) w_j(t) - \frac{1}{2}\sum_j \left\langle \varphi_i, \varphi_j' \right\rangle w_j^2(t) + \langle f, \varphi_i \rangle . \tag{5.14}$$

Thus one obtains

$$\mathbf{M}\dot{\mathbf{w}}(t) = \mathbf{A}\mathbf{w}(t) + \mathbf{A}_c\mathbf{w}^{\wedge 2}(t) + \mathbf{f}, \tag{5.15}$$

where again $\mathbf{w}(t) = [w_1(t), \ldots, w_N(t)]^T$ and now $\mathbf{w}^{\wedge 2}$ is defined by

$$\mathbf{w}^{\wedge 2}(t) = [w_1^2(t), \ldots, w_N^2(t)]^T.$$

The matrices $\mathbf{A}$ and $\mathbf{M}$ and the vector $\mathbf{f}$ are again given by (5.9), (5.10) and (5.12) respectively and the matrix $\mathbf{A}_c$ is defined by

$$[A_c]_{ij} = -\frac{1}{2}\left\langle \varphi_i, \varphi_j' \right\rangle .$$

The initial condition for the ODE is computed in the same manner as for the standard finite element approximation. Once the approximate solution is computed, the transformation is inverted to yield an approximate solution to the original NLCD equation (4.10)-(4.12).

The computational advantages of the group formulation come from the simple form of the group finite element ODE (5.15). Note that the inner products only need to be evaluated once to form the matrices. This contrasts with the Galerkin finite element scheme where the inner products and the Jacobian are normally recomputed at each time step. For the group scheme, the Jacobian is easily computed from the matrix ODE. These advantages are important on fine meshes and when integrating over long time periods (as we will require in later computations).

The group finite element formulation is not without drawbacks. First, the group formulation cannot be used on an arbitrary nonlinearity. A nonlinear term must appear as a "group", i.e., it must be of the form $\mathcal{L}f(w(t,x))$, where $\mathcal{L}$ is a (formal) differential operator. For the NLCD equation above, $f(w) = w^2/2$ and $\mathcal{L} = \partial/\partial x$. The group method approximates this term by

$$\sum_{j=1}^{N} f(w_j(t))\mathcal{L}\varphi_j(x).$$

Although this type of nonlinearity is very general, certain types of nonlinearities cannot be treated with the group method. For example, the group formulation would not directly apply to a nonlinearity of the form $f(\mathcal{L}w(t,x))$. Also, since the the main advantage of the group method comes from the evaluation of a nonlinearity by a matrix/vector multiplication, the group formulation offers less advantage if the matrices are too large to be stored. Furthermore, the convergence theory is not complete.

However, there are some cases where theory has been developed. Convergence is known for certain semilinear elliptic problems ([1], [40], [103]), specific quasilinear parabolic problems [47], the nonlinear heat equation [137] and the nonlinear (hyperbolic) Klein-Gordon equation [137]. The above theory provides error estimates that are similar to the standard finite element formulation for these problems. Also, in certain cases one can prove superconvergence.

Computational studies show the performance of the group finite element method equals, or exceeds, the standard approach (see the papers cited above and the references therein). Of particular interest in this thesis is the group method's performance on Burgers' equation. Computational studies suggest that the group formulation is a convergent scheme for Burgers' type equations ([40], [56], [57, Section10.3], [99], [108], and [127]). In light of these findings and the major computational savings of the group formulation, we use the group finite element method for the spatial discretizations in this thesis.

5.1.3 Finite Element Formulation for the 1D Sensitivity Equation

Now, we describe the finite element formulation for the sensitivity equation discussed in section 4.3. In particular, consider the sensitivity equation of the transformed system (4.28)-

(4.30) given by

$$r_t(t,x) = \mu r_{xx}(t,x) - (h(x)\, r(t,x))_x - (w(t,x)\, r(t,x))_x - (h(x)\, \tilde{\psi}(x))_x - (\tilde{\psi}(x)\, w(t,x))_x$$
$$r(t,-1) = 0, \quad r(t,1) = 0$$
$$r(0,x) = -\tilde{\psi}.$$

Here, $w(t,x) = w(t,x;0)$ is the solution to the undisturbed Burgers' fluctuation problem (4.10)-(4.12) with $\varepsilon = 0$. The functions $h(\cdot)$ and $\tilde{\psi}(\cdot)$ may be treated as general functions. The weak form of this problem is to find $r \in V = H_0^1$ such that

$$\frac{\partial}{\partial t} \langle r, \varphi \rangle = -\mu \langle r_x, \varphi_x \rangle + \langle hr, \varphi_x \rangle + \langle wr, \varphi_x \rangle + \langle h\tilde{\psi}, \varphi_x \rangle$$

for all $\varphi \in V$. As above, once an approximate solution to this equation is obtained, the transformation is inverted to recover an approximate solution to the sensitivity equation (4.31)-(4.31) for the untransformed system.

Introduce the approximate solution $r^N(t,\cdot) \in V^N$ defined by

$$r^N(t,x) = \sum_{j=1}^{N} r_j(t)\varphi_j(x),$$

where again the functions $r_j(\cdot)$ are unknown. Also, suppose that an approximation $w^N(t_j,x)$ for $w(t_j,x)$ has been computed at a discrete set of time values given by $0 = t_1 < \cdots < t_M = T$. For simplicity, in the computations presented below $w^N(t,x)$ was computed using the group finite element method described above with the same set of basis functions for the sensitivity calculations. Note that the same numerical scheme (or even the same mesh) need not be used for both computations. Substituting the trial solution into the weak form and choosing the test function $\varphi = \varphi_i$, for $i = 1, \ldots, N$, yields the linear finite element ordinary differential equations

$$\mathbf{M}\dot{\mathbf{r}}(t) = \mathbf{A}(t)\mathbf{r}(t) + \mathbf{f}(t),$$

where $\mathbf{r}(t) = [r_1(t), \ldots, r_N(t)]^T$, $\mathbf{M}$ is given by (5.9) and the entries of $\mathbf{A}(t)$ and $\mathbf{f}(t)$ are given by

$$A_{ij}(t) = -\mu \left\langle \varphi_i', \varphi_j' \right\rangle + \langle h\varphi_i', \varphi_j \rangle + \left\langle w^N(t,\cdot)\varphi_i', \varphi_j \right\rangle$$

and

$$f_i(t) = \langle h\tilde{\psi}, \varphi_i' \rangle + \left\langle w^N(t,\cdot)\, \tilde{\psi}, \varphi_i' \right\rangle,$$

respectively.

The initial condition is projected onto the finite element space V^N as above to give the initial condition $\mathbf{r}(0) = \mathbf{r}_0$ for the finite element ODE. Since the values of $w(t,x)$ are only given at certain t values, we did not use Matlab's `ode23s` solver in this case. Instead, we use

the trapezoid rule for the time stepping so that the solution update takes the form

$$\Big(\mathbf{M} - \frac{\Delta t_j}{2}\mathbf{A}(t_{j+1})\Big)\,\mathbf{r}(t_{j+1}) = \Big(\mathbf{M} + \frac{\Delta t_j}{2}\mathbf{A}(t_j)\Big)\,\mathbf{r}(t_j) + \frac{\Delta t_j}{2}\Big(\mathbf{f}(t_{j+1}) + \mathbf{f}(t_j)\Big),$$

where t_j are the discrete set of time values mentioned above and $\Delta t_j = t_{j+1} - t_j$.

Also, as discussed in section 4.3, we are interested in the solution of the boundary value problem

$$\mu r_{xx}(x) - (h(x)\,r(x))_x - (h(x)\,\tilde{\psi}(x))_x = 0, \quad r(-1) = 0, \quad r(1) = 0.$$

It is possible that the solution to this problem is the steady state solution of the above sensitivity equation whenever $w(t,x)$ tends to zero as $t \to \infty$. Again, this is an open problem. We will approximate the solution to this equation to see if it numerically predicts the long time behavior of the sensitivities. The weak form is given by

$$-\mu\,\langle r_x, \varphi_x\rangle + \langle hr, \varphi_x\rangle = -\langle h\tilde{\psi}, \varphi_x\rangle.$$

Proceeding as usual shows that the entries of the finite element matrix $\mathbf{A}$ and vector $\mathbf{f}$ are given by

$$A_{ij} = -\mu\,\left\langle \varphi_i', \varphi_j' \right\rangle + \langle h\,\varphi_i', \varphi_j\rangle$$

and

$$f_i = -\langle h\tilde{\psi}, \varphi_i'\rangle.$$

The coefficients $\mathbf{r}_{ss}$ of the approximate solution are given as the solution of the linear system $\mathbf{A}\mathbf{r}_{ss} = \mathbf{f}$.

Note that if the first order linear terms had not been integrated by parts, then the gradient $w_x(t,x)$ would have appeared in the finite element formulation. The finite element approximation $w_x^N(t,x)$ of $w_x(t,x)$ is one order less accurate than the finite element approximation $w^N(t,x)$ of $w(t,x)$. Therefore, if this approximate gradient had appeared in the finite element formulation, one would expect to lose an order of accuracy in the sensitivity approximations. This difficulty can be treated rather cheaply employing projection methods similar to those employed in a-posteriori error estimators in finite elements (see, [34], [131]). However, since we can avoid this difficulty and our emphasis is not on the numerical methods, we do not treat these issues here.

5.1.4 Group Finite Element Formulation for the 2D Model Problem

Finally, we describe the group finite element formulation for the transformed two dimensional model Burgers' equation (4.43)-(4.46) considered in section 4.4 which is of the general form

$$w_t + \frac{a_1}{2}\left(w^2\right)_x + \frac{a_2}{2}\left(w^2\right)_y \;=\; \mu\left(\frac{\partial}{\partial x}(\,b_{11}w_x + b_{12}w_y\,) + \frac{\partial}{\partial y}(\,b_{21}w_x + b_{22}w_y\,)\right)$$

$$+ c_1 w_x + c_2 w_y + c_0 w + f, \tag{5.16}$$

with constant viscosity $\mu > 0$, and with the coefficient functions, a_i, b_{ij} and c_i, and forcing function, f, all in L^2. This equation is defined over the rectangular domain $\Omega = (0,1)\times(0,1)$ with periodic boundary conditions in the x direction,

$$w(t,0,y) = w(t,1,y), \quad w_x(t,0,y) = w_x(t,1,y) \quad \text{for all } y, \tag{5.17}$$

zero Dirichlet boundary conditions on the top and bottom walls,

$$w(t,x,0) = 0 = w(t,x,1) \quad \text{for all } x, \tag{5.18}$$

and initial condition

$$w(0,x,y) = f_0(x,y). \tag{5.19}$$

Once an approximate solution is found, it will not be transformed back to the rough walled domain $\Omega(\alpha,\beta)$ for simplicity.

Let $X = L^2(\Omega)$ and define

$$V = \Big\{ v \in H^1(\Omega) \,:\, v(0,y) = v(1,y),\ 0 < y < 1;\ v(x,0) = 0 = v(x,1),\ 0 < x < 1 \Big\}.$$

The weak formulation is to find $w \in V$ such that

$$\begin{aligned} \frac{\partial}{\partial t}\langle w, \varphi\rangle &= -\mu\Big(\langle b_{11}w_x + b_{12}w_y, \varphi_x\rangle + \langle b_{21}w_x + b_{22}w_y, \varphi_y\rangle \Big) \\ &\quad + \langle c_1 w_x, \varphi\rangle + \langle c_2 w_y, \varphi\rangle + \langle c_0 w, \varphi\rangle + \langle f, \varphi\rangle \end{aligned}$$

for all $\varphi \in V$. Partition the x interval $[0,1]$ by $0 = x_1 < \cdots < x_{m+1} = 1$ and the y interval $[0,1]$ by $0 = y_0 < \cdots < y_{n+1} = 1$. This yields a rectangular mesh on Ω with nodes $\{(x_i, y_j)\}$. We construct 1D piecewise linear basis functions (5.5) in each coordinate direction with appropriate modifications for the boundary conditions. This will yield piecewise continuous bilinear functions contained in V.

For the y direction, the piecewise linear functions must satisfy zero Dirichlet boundary conditions and so they can be constructed as in the 1D case above. Therefore, define the piecewise linear functions $\{\psi_j(y)\}$ for $j = 1, \ldots n$ which take in values of y in $[0,1]$ and satisfy the zero Dirichlet boundary conditions imposed by V. For the x direction, the piecewise linear functions must have a common value at the endpoints of $[0,1]$ and so the construction must proceed in a slightly different manner. First, for $i = 2, \ldots, m$, define the piecewise linear basis functions $\{\phi_j(y)\}$ as above. Note that these basis functions automatically satisfy $\phi_j(0) = \phi_j(1)$. For the nodes on the boundary (x_1 and x_{m+1}) construct the single piecewise linear function (see figure 5.1) given by

$$\phi_1(x) = \begin{cases} (x - x_2)/(x_1 - x_2), & x \in [x_1, x_2] \\ (x - x_m)/(x_{m+1} - x_m), & x \in [x_m, x_{m+1}] \\ 0, & \text{otherwise} \end{cases}.$$

Observe that this function satisfies $\phi_1(0) = \phi_1(1)$ and completes the set of x periodic basis functions.

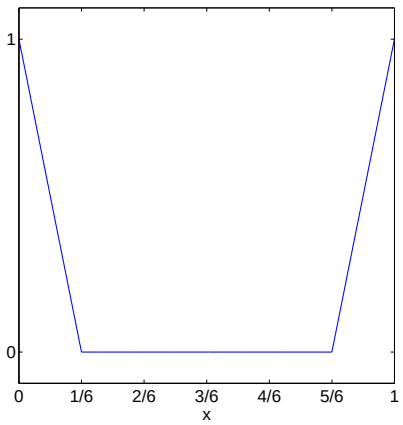

Figure 5.1: The 1D x periodic basis function $\phi_1(x)$ over 7 equally spaced nodes

The global continuous piecewise bilinear basis functions in V are given as products of the 1D basis functions defined above. For $i = 1, \ldots, m$ and $j = 1, \ldots, n$ define the functions

$$\varphi_k(x, y) = \phi_i(x)\psi_j(y), \quad \text{where} \quad k = i + (j-1)m.$$

Since the piecewise linear functions in each coordinate direction satisfy the appropriate boundary conditions imposed by V, the products of these functions lie in V. Therefore, define $V^N = \text{span}\{\varphi_1, \ldots, \varphi_N\}$, where $N = n \times m$ is the total number of basis functions. Define the group finite element approximations by

$$w(t, x, y) \approx \sum_{j=1}^{N} w_j(t)\varphi_j(x, y), \quad \text{and} \quad w^2(t, x, y) \approx \sum_{j=1}^{N} w_j^2(t)\varphi_j(x, y),$$

Substituting the approximations into the above weak form and choosing $\varphi = \varphi_i$ for $i = 1, \ldots, N$ yields the group finite element ordinary differential equations

$$\mathbf{M}\dot{\mathbf{w}}(t) = \mathbf{A}\mathbf{w}(t) + \mathbf{A}_c\mathbf{w}^{\wedge 2}(t) + \mathbf{f},$$

where $\mathbf{w}(t) = [w_1(t), \ldots, w_N(t)]^T$ and $\mathbf{w}^{\wedge 2}(t) = [w_1^2(t), \ldots, w_N^2(t)]^T$. The entries of the finite element matrices and vectors are given by

$$\begin{aligned} M_{ij} &= \langle \varphi_i, \varphi_j \rangle, \\ A_{ij} &= -\mu \left\langle \frac{\partial \varphi_i}{\partial x}, b_{11}\frac{\partial \varphi_j}{\partial x} + b_{12}\frac{\partial \varphi_j}{\partial y} \right\rangle - \mu \left\langle \frac{\partial \varphi_i}{\partial y}, b_{21}\frac{\partial \varphi_j}{\partial x} + b_{22}\frac{\partial \varphi_j}{\partial y} \right\rangle \end{aligned}$$

$$
\begin{aligned}
&+\left\langle c_1\,\varphi_i\,,\,\frac{\partial\varphi_j}{\partial x}\right\rangle+\left\langle c_2\,\varphi_i\,,\,\frac{\partial\varphi_j}{\partial y}\right\rangle+\langle c_0\,\varphi_i,\varphi_j\rangle\,,\\
[A_c]_{ij} &= -\frac{1}{2}\left\langle \varphi_i\,,\,a_1\frac{\partial\varphi_j}{\partial x}\right\rangle-\frac{1}{2}\left\langle \varphi_i\,,\,a_2\frac{\partial\varphi_j}{\partial y}\right\rangle,\quad \text{and}\\
f_i &= \langle f,\varphi_i\rangle\,,
\end{aligned}
$$

where $\langle\cdot,\cdot\rangle$ is the standard L^2 inner product over the rectangular domain Ω. The mass matrix $\mathbf{M}$ is invertible and the initial condition to the ODE is constructed in the same way as in the 1D formulation above.

5.2 Sensitivity Analysis of Burgers' Equation

As discussed in section 3.3.2, solutions to the one dimensional nonlinear convection diffusion (NLCD) equation can display extreme sensitivity to small disturbances in the equations and boundary conditions. We investigate the cause of this sensitivity in order to gain insight into the role that small disturbances can play in the transition process. Specifically, we examine a transformed version of the problem to see how the small disturbance "enters" the equation. Also, we use the continuous sensitivity equation method to compute the sensitivity of solutions with respect this small disturbance. Then we turn to the two dimensional NLCD equation considered in the previous chapter. Here, we briefly examine the impact of a simplified form of wall roughness on the solutions.

5.2.1 Comparison of the 1D Undisturbed and Disturbed Problems

We begin with the 1D NLCD equation studied in the previous chapter given by

$$z_t + zz_x = \mu z_{xx} - (hz)_x \tag{5.20}$$

with Dirichlet boundary conditions

$$z(t,-1) = 0, \quad z(t,1) = \varepsilon \tag{5.21}$$

and initial condition

$$z(0,x) = z_0(x). \tag{5.22}$$

As before, μ is a positive constant and $h(\cdot)$ is the hyperbolic tangent profile given by (4.13). We focus on the sensitivity of the solutions with respect to the parameter ε.

In the previous chapter, the origin for the undisturbed system (i.e., with $\varepsilon = 0$) was shown to be asymptotically stable with respect to the H^1 norm. Therefore, if the initial condition is near to the origin, the solution must converge to the zero state. Figure 5.2 shows the numerical solution (using 64 equally spaced nodes) quickly approach the zero state with $\mu = .05$ and initial condition $z_0(x) = \sin(\pi x)$. Kreiss and Kreiss showed that the

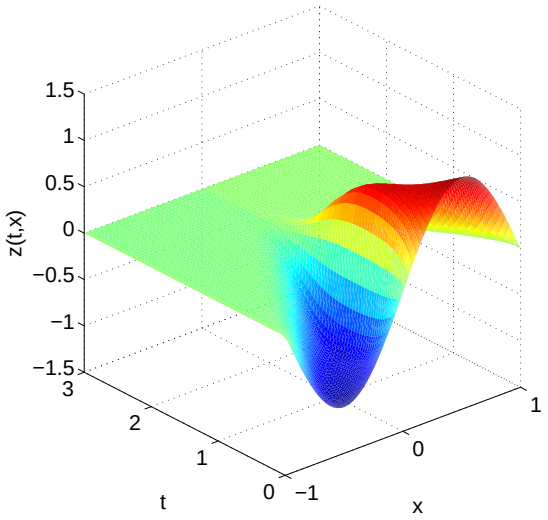

Figure 5.2: Approximate solution of the NLCD equation (5.20)-(5.22) over the time interval $[0, 3]$ with $\mu = .1$ and $z_0(x) = \sin(\pi x)$.

linear operator associated with the NLCD equation given by

$$\mathcal{A}_0 v(t) = \mu v_{xx} - (hv)_x, \tag{5.23}$$

on the domain $\mathcal{D}(\mathcal{A}_0) = H^2 \cap H_0^1$, has an eigenvalue exponentially close to zero [80]. Therefore, we expect that some solutions will tend to zero very slowly. This phenomenon is observed numerically. For instance, computations with the initial condition $z_0(x) = (1-x)(1+x)^3$ and $\mu = .05$ show the solution converging to the zero state in over 10^8 time units.

For $\varepsilon \neq 0$, the solutions behave much differently. For example, if $z_0 = 0$ and $\varepsilon = 0$, then the solution would stay at zero for all time. However, with $\varepsilon \neq 0$ the zero function is no longer an equilibrium. Figure 5.3 shows time snapshots of the approximate solution computed with 64 equally spaced nodes, $\mu = .1$, $\varepsilon = 10^{-5}$ and initial condition $z_0 = 0$. The steady state solution is reached after a long time ($t \approx 1000$) and is nearly zero. Therefore, the small boundary perturbation with $\varepsilon = 10^{-5}$ has little impact on the long time behavior of the solution. However, when $\varepsilon = 10^{-3}$ the solution "transitions" to an order one steady state (see figure 5.4). Decreasing μ causes the situation to become worse as expected. Figure 5.5 shows the solution with $z_0 = 0$, $\mu = .05$ and $\varepsilon = 10^{-4}$. An even smaller disturbance has caused the "transition". Similar behavior has been observed for a wide variety of initial data. If we let $\mu = 1/R$, then these examples suggest that a boundary disturbance $\varepsilon = O(R^{-3})$ will cause the solution to transition to an order one steady state. This is similar to the results concerning disturbances to the Orr-Sommerfeld equations discussed in section 2.4.2.

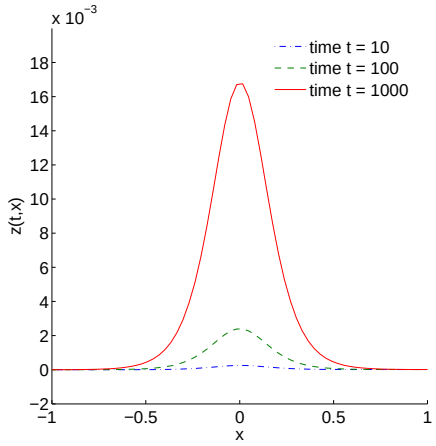

Figure 5.3: Approximate solution of the NLCD equation (5.20)-(5.22) with $\mu = .1$, $z_0(x) = 0$ and $\varepsilon = 10^{-5}$.

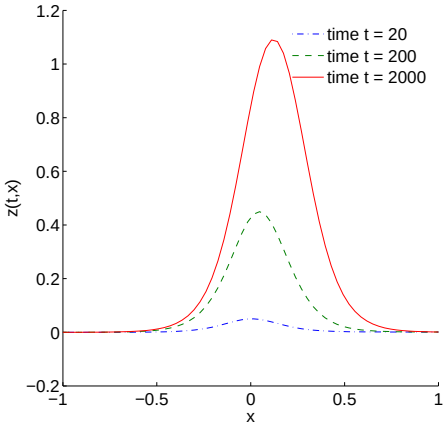

Figure 5.4: Approximate solution of the NLCD equation (5.20)-(5.22) with $\mu = .1$, $z_0(x) = 0$ and $\varepsilon = 10^{-3}$.

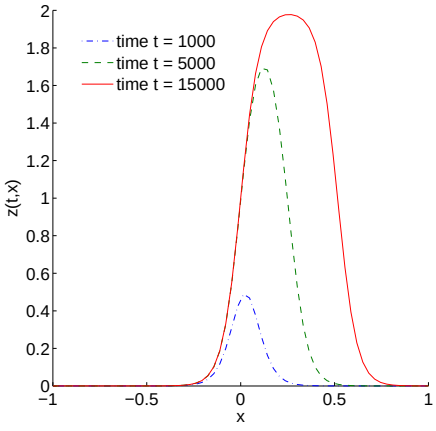

Figure 5.5: Approximate solution of the NLCD equation (5.20)-(5.22) with $\mu = .05$, $z_0(x) = 0$ and $\varepsilon = 10^{-4}$.

5.2.2 A Transformation of the 1D Disturbed Problem

As discussed in section 3.3.2, this "supersensitivity" of solutions to Burgers' equation with respect to small disturbances in the boundary is well known. For the most part, this phenomenon has been studied using asymptotic analysis. However, we examine this problem from a different point of view. As in the previous chapter, we transform the disturbed nonlinear convection-diffusion equations (5.20)-(5.22) to a PDE with homogeneous boundary conditions. This allows us to make a direct comparison between the undisturbed and disturbed problems. Let

$$v(t,x) = z(t,x) - \psi(x), \quad \text{where} \quad \psi(x) = \varepsilon(x+1)/2.$$

It follows that $v(t,x)$ satisfies the partial differential equation

$$v_t + vv_x = \mu v_{xx} - \left((h+\psi)v \right)_x - \left(\psi\psi_x + (\psi h)_x \right) \tag{5.24}$$

with Dirichlet boundary conditions

$$v(t,-1) = 0, \quad v(t,1) = 0 \tag{5.25}$$

and initial condition

$$v(0,x) = v_0(x) := z_0(x) + \psi(x). \tag{5.26}$$

Note that the small disturbance in the boundary condition is transformed into a perturbation of the linear operator and also produces a small forcing function.

This small forcing function seems to be essential for the solution to "transition" to an order one steady state. Figure 5.6 shows the steady state solution of the fluctuation equation (5.20)-(5.22) with $\mu = .05$ and $\varepsilon = 10^{-4}$ computed using the transformed fluctuation equation (5.24)-(5.26) with $f(\varepsilon) = -\psi\psi_x - (\psi h)_x$ set to zero. The solution does not transition when this seemingly negligible forcing function is removed. This is in contrast to Figure 5.5 which shows a transition to a large steady state solution to the same problem computed in the same manner without setting $f(\varepsilon)$ equal to 0. The small forcing function is triggering the drastic change in the dynamics of the system. Observe that the forcing function is small. For $\varepsilon = 10^{-4}$, the L^2 norm of $f(\varepsilon)$ is given by

$$\|f(\varepsilon)\|_{L^2} \approx 1.9606 \times 10^{-4}.$$

The natural linear operator associated with the transformed NLCD equation (5.24) is given by

$$\mathcal{A}_\varepsilon v(t) = \mu v_{xx} - \left((h + \psi(\varepsilon))v \right)_x,$$

over the domain $\mathcal{D}(\mathcal{A}_\varepsilon) = H^2 \cap H_0^1$. This linear operator can be treated with the techniques described in section 4.3. In particular, Theorem 4.3.1 applies and so $\mathcal{A}_\varepsilon$ generates an exponentially stable C_0-semigroup. When $f = 0$, the zero function, $z = 0$, is an asymptotically stable equilibrium. Therefore, the small forcing function is an essential term necessary to trigger "transition" to an order one steady state.

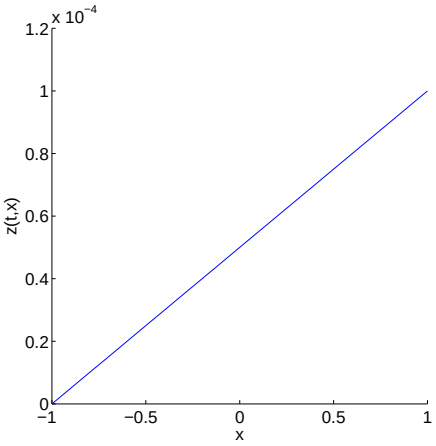

Figure 5.6: Steady state solution of the NLCD equation (5.20)-(5.22) computed via the transformed system (5.24)-(5.26) with $z_0(x) = 0$, $\mu = .05$, $\varepsilon = 10^{-4}$ and without the small forcing function (see text for details).

This phenomenon is quite interesting since, as mentioned in section 2.4.2, many researchers are investigating the sensitivity of flow problems with respect to small disturbances by examining the sensitivity of the underlying linear operator. The natural linear operator $\mathcal{A}_0$ for the undisturbed NLCD equation (5.20)-(5.22) is defined by $\mathcal{A}_0 z = \mu z_{xx} - (hz)_x$ on the domain $\mathcal{D}(\mathcal{A}_0) = H^2 \cap H_0^1$. As mentioned above, this operator generates an exponentially stable C_0-semigroup, yet it has an eigenvalue exponentially close to the imaginary axis. With the spectrum so close to the imaginary axis, it is possible that a small disturbance in the boundary could cause the linear operator $\mathcal{A}_0$ to become unstable. Solutions starting near the zero state would then grow and "transition". However, in this case, even when $\varepsilon \neq 0$ the operator $\mathcal{A}_\varepsilon$ still generates an exponentially stable C_0-semigroup.

Therefore, despite the fact that the linear operator $\mathcal{A}_0$ has an eigenvalue exponentially close to the imaginary axis, the linear operator is quite stable with respect to certain perturbations in the boundary. Theorem 4.3.1 shows that any C^1 perturbation to $h(\cdot)$ in the first derivative term of $\mathcal{A}_0$ (no matter how large) will not cause the linear operator to become unstable. The pseudospectra of finite element approximations to the operator provides insight into how the spectrum of the operator behaves changes under arbitrary small bounded perturbations to the operator (see section 2.4.1). We do not know if the pseudospectra of the matrix approximations of $\mathcal{A}_0$ converge to the *actual* pseudospectra of $\mathcal{A}_0$. This convergence issue requires a careful analysis that is beyond the scope of this paper. However, the numerical results presented in Figure 5.7 provide some evidence to support convergence in this special case. In this figure, μ is fixed at .1 and the number of finite element nodes is increased. It is clear that the pseudospectra of the approximations are converging on a fixed region in $\mathbb{C}$. Thus, it is plausible that the pseudospectra of the approximate operators are converging to the pseudospectra of $\mathcal{A}_0$. Therefore, we study the pseudospectra of the approximations

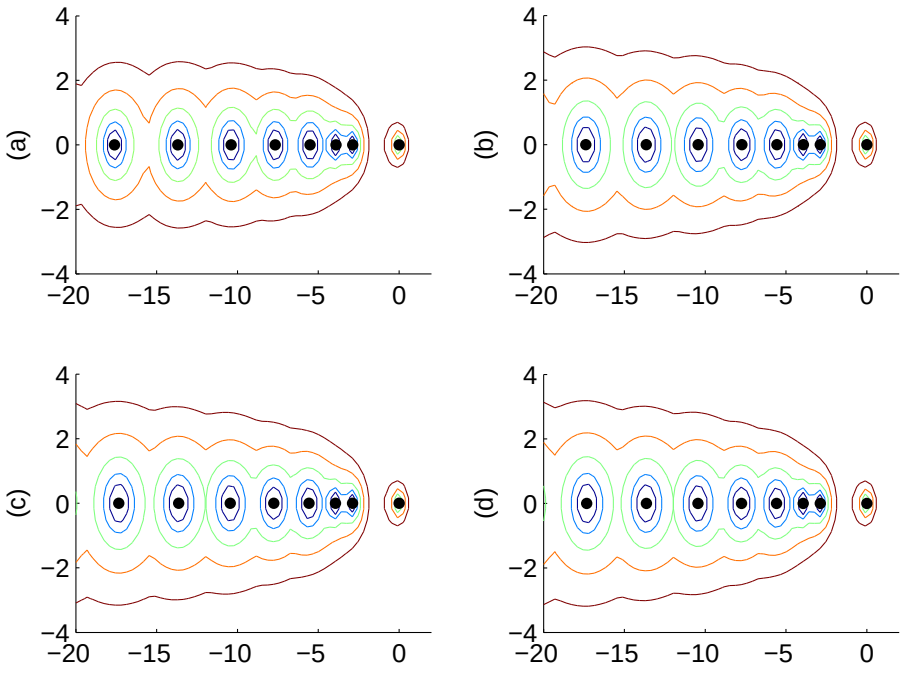

Figure 5.7: Pseudospectra of a finite element approximation to the linear operator $\mathcal{A}_0$ with $\mu = .1$ and (a) 32, (b) 64, (c) 128 and (d) 256 equally spaced finite element nodes. The contours of the ε pseudospectra are for $\varepsilon = 10^{-1.2}, 10^{-1}, \ldots, 10^{-.4}$ from inside to outside.

to investigate the sensitivity of the operator $\mathcal{A}_0$ with respect to small bounded disturbances. Figures 5.8 and 5.9 show pseudospectra plots of finite element approximations of $\mathcal{A}_0$ with $\mu = .05$ and 64 equally spaced nodes, and $\mu = .025$ and 128 with equally spaced nodes, respectively. An arbitrary small perturbation to the (approximate) operator can cause the eigenvalues to drastically shift locations. However, the pseudospectra generally stays well away from the imaginary axis. In particular, the pseudospectra demonstrates that arbitrary small perturbations to the (approximate) operator barely affect the location of the eigenvalue closest to the imaginary axis. Therefore, the exponentially small eigenvalue of the actual operator $\mathcal{A}$ appears to be fairly robust with respect to arbitrary small perturbations.

To summarize, in this example, the stability of the zero equilibrium is not sensitive with respect to arbitrary small disturbances in the boundary. Rather, it is the *location* of the equilibrium that is extremely sensitive. A small perturbation to the zero Dirichlet boundary conditions causes the zero equilibrium to move an order of magnitude. If this type of scenario occurs for the Navier-Stokes equations, small boundary disturbances would not cause a laminar flow state to become unstable, but instead would cause the laminar flow to change shape or possibly disappear entirely. It would then be impossible for the

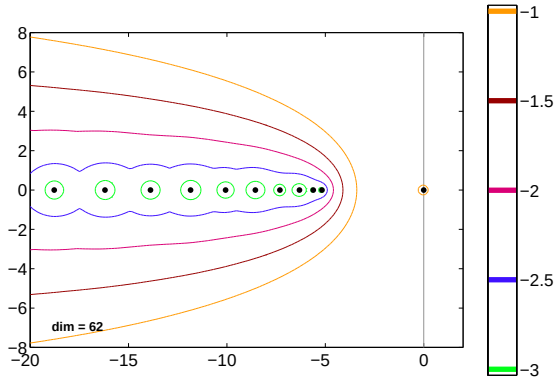

Figure 5.8: Pseudospectra of a finite element approximation to the linear operator $\mathcal{A}_0$ with $\mu = .05$ and 64 equally spaced finite element nodes. The vertical line is the imaginary axis. The dot near the line is an eigenvalue in the left half plane. The contours are on a log 10 scale.

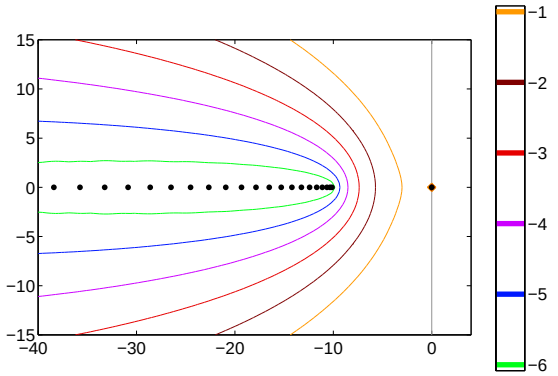

Figure 5.9: Pseudospectra of a finite element approximation to the linear operator $\mathcal{A}_0$ with $\mu = .025$ and 128 equally spaced finite element nodes. The vertical line is the imaginary axis. The dot near the line is an eigenvalue in the left half plane. The contours are on a log 10 scale.

flow to relaminarize and the flow could transition to turbulence. This provides a potential explanation of why classical stability analysis fails to predict the accepted experimental values for the critical Reynolds number.

5.2.3 1D Sensitivity Computations

Next, we examine the sensitivity of the solution with respect to ε using the continuous sensitivity equation method outlined in the previous chapter. In particular, denote the dependence of the solution z to the nonlinear convection-diffusion equation (5.20)-(5.22) on ε by writing $z = z(t, x; \varepsilon)$ and define the sensitivity of z at $\varepsilon = 0$ by

$$s(t, x) = \frac{\partial z}{\partial \varepsilon}(t, x; \varepsilon)\Big|_{\varepsilon=0}. \tag{5.27}$$

Corollary 4.3.2 guarantees that $s(t, x)$ exists and satisfies the linear partial differential equation

$$s_t(t, x) = \mu s_{xx}(t, x) - (h(x)s(t, x))_x - (z(t, x; 0)s(t, x))_x, \tag{5.28}$$

with boundary conditions

$$s(t, -1) = 0, \quad s(t, 1) = 1 \tag{5.29}$$

and initial condition

$$s(0, x) = 0. \tag{5.30}$$

Since the sensitivity is evaluated at $\varepsilon = 0$, the solution $z(t, x; 0)$ of the undisturbed problem enters the sensitivity equation. We also consider the steady equation given by (see section 4.3)

$$\mu s_{xx}(x) - (h(x)\, s(x))_x = 0, \quad s(t, -1) = 0, \;\; s(t, 1) = 1. \tag{5.31}$$

Again, it is not known whether the solution to this equation determines the long time behavior of the sensitivity.

We begin by computing the sensitivity of the zero state with respect to ε. Since in this case the zero state is the solution for all time to the undisturbed problem (i.e., $z(t, x; 0) = 0$), the sensitivity equation is linear and time does not appear explicitly in the equation. Therefore, the only driving force in the sensitivity equation is the nonhomogeneous Dirichlet boundary condition $s(t, 1) = 1$. As discussed earlier, the linear operator is non-normal in this case and so a moderate sized force has the potential to have a great impact on the sensitivity. As discussed above, the computations of the disturbed NLCD equation did not stay near zero but moved an order of magnitude away after a long period of time. Therefore, we expect that the zero state is very sensitive and that the sensitivity increases as time increases.

Figure 5.10 shows the finite element approximation to the sensitivity with $N = 64$ equally spaced nodes and $\mu = .1$ over the time interval $[0, 4]$. The sensitivity is increasing and is already fairly large at $t = 4$. This shows that the solution to the disturbed NLCD equation could undergo a large change. Integrating further in time shows that the computed sensitivity continues to increase and it eventually becomes exceptionally large, especially near $x = 0$

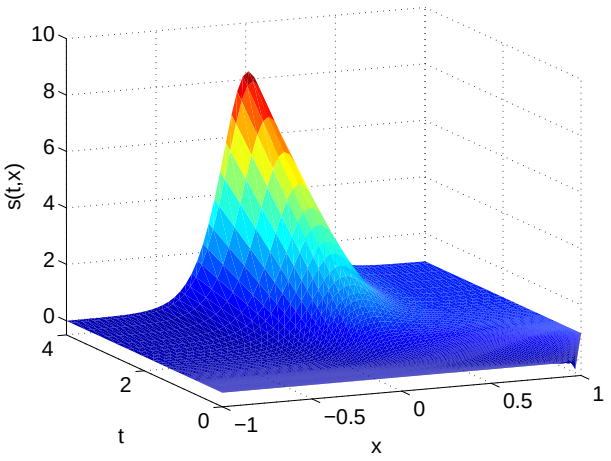

Figure 5.10: The sensitivity of the zero solution of the NLCD equation with respect to ε over the time interval $[0, 4]$. The sensitivity is computed using the sensitivity equation (5.28)-(5.30) with $\mu = .1$, $N = 64$, $z_0(x) = 0$.

(see figure 5.11). The size of the sensitivity for $\mu = .01$ is much more dramatic. Figure 5.12 shows that as time increases, the sensitivity slowly increases until reaching a steady state of height approximately 10^{14}. Note also that the main support of the sensitivity is over the small interval $[-.1, .1]$. The sensitivity is similar to a delta function centered at $x = 0$. This behavior indicates that the solution of the disturbed NLCD equation with zero initial data will change drastically near $x = 0$. Also, in both cases the time dependent sensitivity reaches the same steady state predicted by the steady sensitivity equation although the time taken to reach the steady state can be large. For the sensitivity computations with $\mu = .01$, figure 5.12 shows the approximate solution with $N = 1028$ equally spaced nodes and it is not clear even at this level of refinement that the solutions have numerically converged. This is due to the sharp gradient in the solution. To produce truly accurate approximations for such a problem, one could resort to special numerical techniques such as adaptive mesh refinement and stabilized finite element schemes.

Next, we present sensitivity computations for a solution of the undisturbed NLCD equation that displays slow motion. A moderate value of μ was used in order to avoid the numerical issues we encountered above. For initial data $z_0(x) = (1 - x)(1 + x)^3$ and $\mu = .1$, the solution to the undisturbed NLCD equation (5.20)-(5.22) experiences a small growth and then settles into a long decay to the zero state which is reached at approximately $t = 10000$. Figures 5.13 and 5.14 show group finite element approximations to the solution at various times with $N = 64$ equally spaced nodes. Figures 5.15 and 5.16 show the sensitivity computed from the sensitivity equation (5.28)-(5.30) at various values of t. As in the previous example, the sensitivity starts off small but increases as time becomes large. It reaches a large steady state approximately centered over $x = 0$ at about $t = 10000$. Also, the sensitiv-

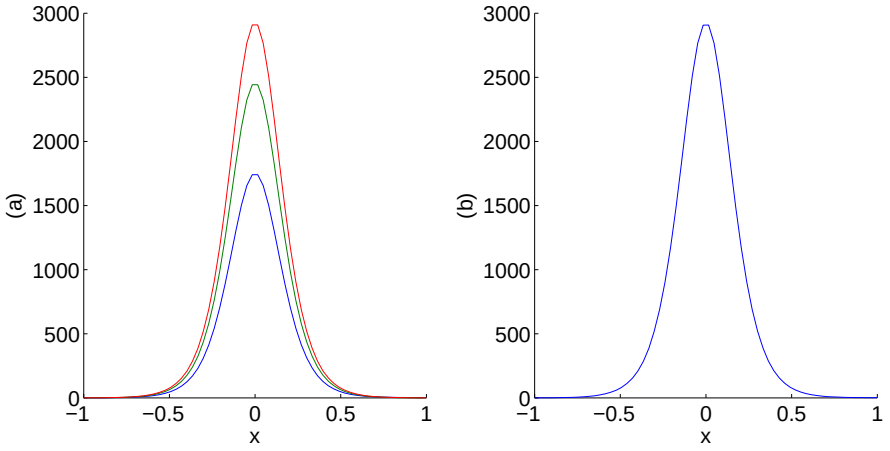

Figure 5.11: (a) The sensitivity of the zero solution of the NLCD equation with respect to ε. The sensitivity is computed using the sensitivity equation (5.28)-(5.30) at $t = 1000, 2000, 10000$. (b) Approximate solution of steady sensitivity equation (5.31). Here, $\mu = .1$, $N = 64$, $z_0(x) = 0$ and the sensitivity is monotonically increasing in time. The steady state is reached at $t = 10000$.

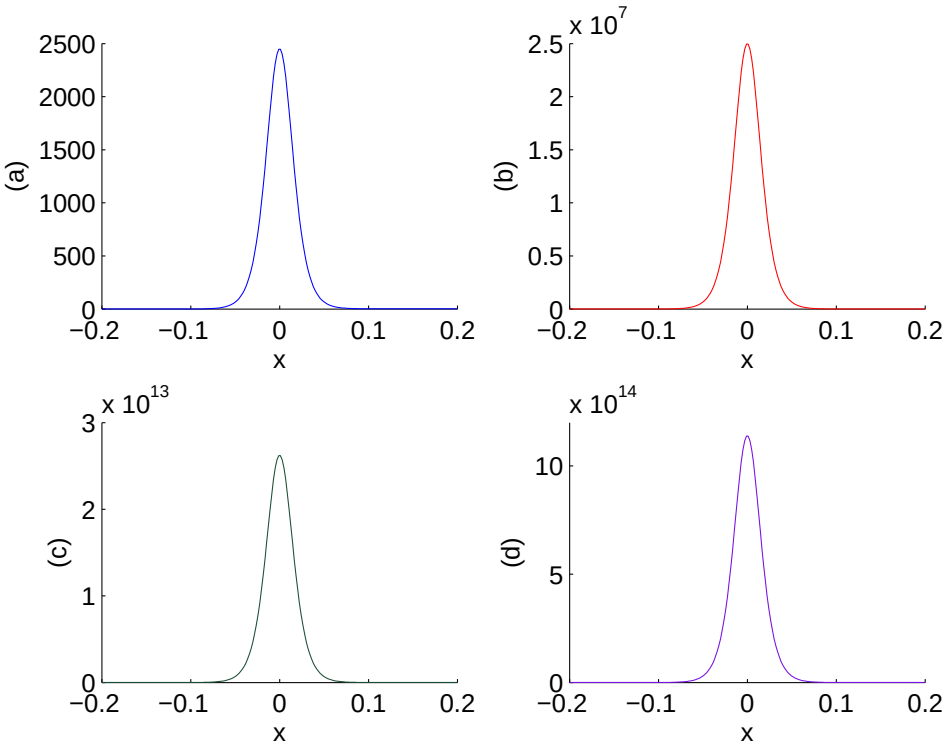

Figure 5.12: The sensitivity of the zero solution of the NLCD equation with respect to ε. The sensitivity is computed using the sensitivity equation (5.28)-(5.30) at (a) $t = 100$, (b) $t = 10^6$, (c) $t = 10^{12}$. (d) Approximate solution of steady sensitivity equation (5.31). Here, $\mu = .01$, $N = 1028$ and $z_0(x) = 0$. Note the scale on the vertical axis.

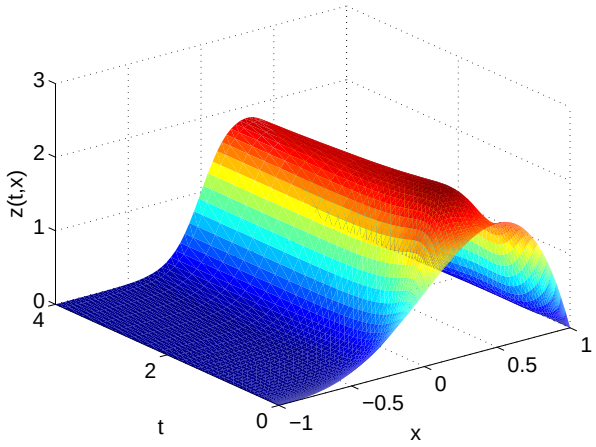

Figure 5.13: Numerical solution of the undisturbed NLCD equation (5.20)-(5.22) over the time interval $[0, 4]$ with $\mu = .1$, $\varepsilon = 0$, $N = 64$, $z_0(x) = (1-x)(1+x)^3$.

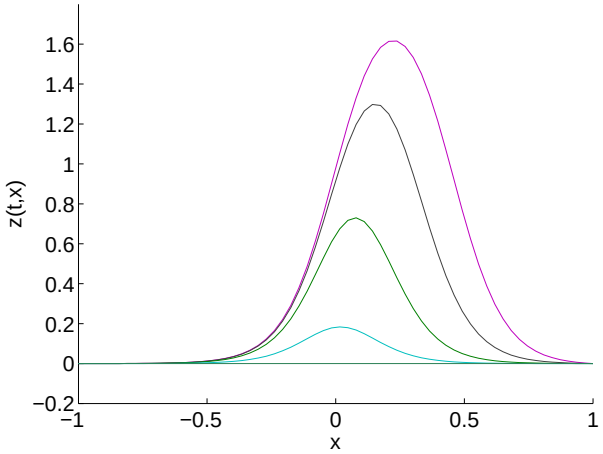

Figure 5.14: Numerical solution of the undisturbed NLCD equation (5.20)-(5.22) at $t = 25, 100, 500, 2000, 10000$. Here, $\mu = .1$, $\varepsilon = 0$, $N = 64$, $z_0(x) = (1-x)(1+x)^3$ and the solution is monotonically decreasing in time. The solution remains nearly zero after $t = 10000$.

ity displays a *spatial region* where the sensitivity is the largest. Notice that the peak value of the sensitivity is near $x = 1$ when t is small and moves toward $x = 0$ as time increases.

Remark: Observe that the sensitivity provides valuable information indicating the possibility of transition and it shows precisely *where* the solution is sensitive. This observation could have ramifications for sensor and actuator placement in control applications. For example, suppose that solutions to a certain problem are sensitive to a specific type of disturbance and that this sensitivity is undesirable. If sensitivity computations show there is a particular region where solutions are more sensitive, this region has the potential to be a good area to place sensors to measure the disturbance and actuators to control the disturbed solution.

This example also shows that the sensitivities can provide information about the solution of the perturbed problem. Recall that the sensitivity is the derivative of the solution to the nonlinear convection-diffusion equation (5.20)-(5.22) with respect to ε evaluated at $\varepsilon = 0$ (5.27). If the solution to the undisturbed problem and the corresponding sensitivity have been computed, one can use a first order Taylor series expansion to get a rough approximation of the solution to the disturbed problem. The approximation is given by

$$z(t, x; \varepsilon) \approx z_{TA}(t, x; \varepsilon) := z(t, x; 0) + \varepsilon s(t, x). \tag{5.32}$$

Figure 5.17 shows a reasonable agreement for this example between this rough approximation and the actual solution of the disturbed NLCD equation with $\varepsilon = 10^{-4}$ for the NLCD equation. However, when ε is larger, the agreement breaks down as seen in figure 5.18 where $\varepsilon = 10^{-3}$. This shows that the sensitivity is only guaranteed to give accurate information about the solution to the perturbed problem when ε is small enough. This is precisely due to the fact that the definition of the sensitivity involves taking a limit as $\varepsilon \to 0$. However, this example shows that even though the sensitivity does not necessarily provide precise information about the solution of the disturbed problem, it still can be used as a rough guide as to the degree and location of the change in the solution due to the disturbance. Therefore, if solving the disturbed problem is computationally demanding, this rough Taylor approximation using the sensitivity could be used to gain some qualitative information about the nature of the disturbed solution with minor computational effort.

The above examples demonstrate that the computed sensitivities give an accurate picture of the change in the solution with respect to ε for small of ε. This property has the potential to be useful in realistic applications where the size of disturbances could be extremely small. For example, it may be difficult or impossible to simulate the disturbed state for a small enough perturbation to the problem. However, we have shown how the sensitivity can be used to give a rough approximation to the disturbed state. This approximation can be quite accurate when the disturbance is small. Also, as seen above, one can find exactly where (spatially) the sensitivity will be the greatest. This has the potential to be useful for sensor and actuator placement in control problems. None of this information can be obtained through a purely linear analysis of the problem. As discussed above, a linear spectral analysis of this problem shows that the zero state is asymptotically stable, while only a slight perturbation to the problem causes this equilibrium to move by an order of

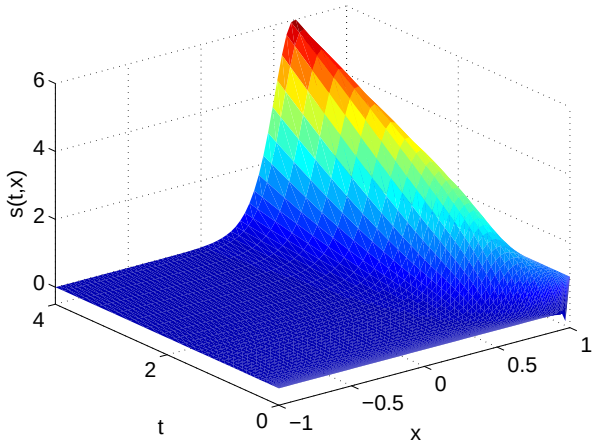

Figure 5.15: Numerical solution of the sensitivity equation (5.28)-(5.30) over the time interval $[0, 4]$ with $\mu = .1$, $\varepsilon = 0$, $N = 64$, $z_0(x) = (1-x)(1+x)^3$.

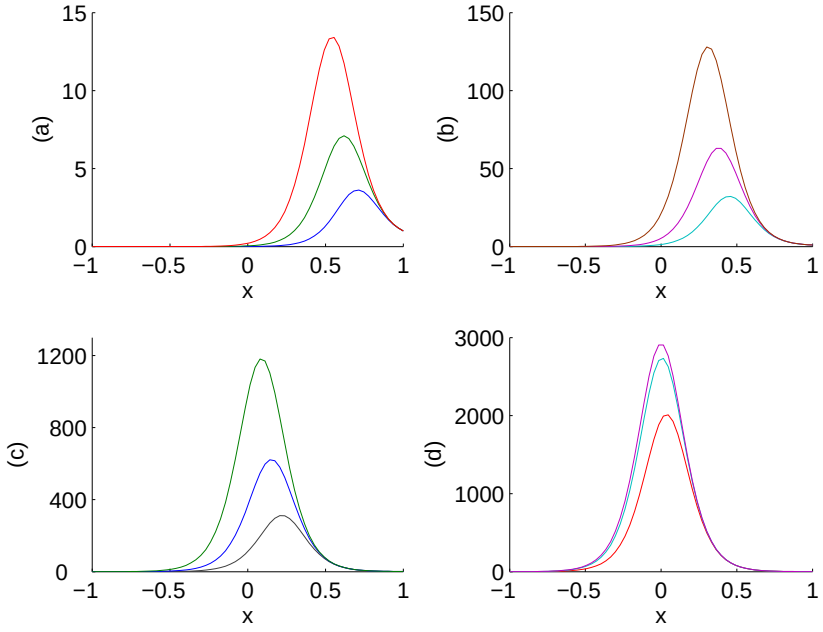

Figure 5.16: Numerical solution of the sensitivity equation (5.28)-(5.30) at various time values: (a) $t = 2, 5, 10$ (b) $t = 25, 50, 100$ (c) $t = 250, 500, 1000$ (d) $t = 2000, 4000, 10000$. Here, $\mu = .1$, $N = 64$, $z_0(x) = (1-x)(1+x)^3$ and the sensitivity is monotonically increasing in time. The steady state is reached at $t \approx 10000$.

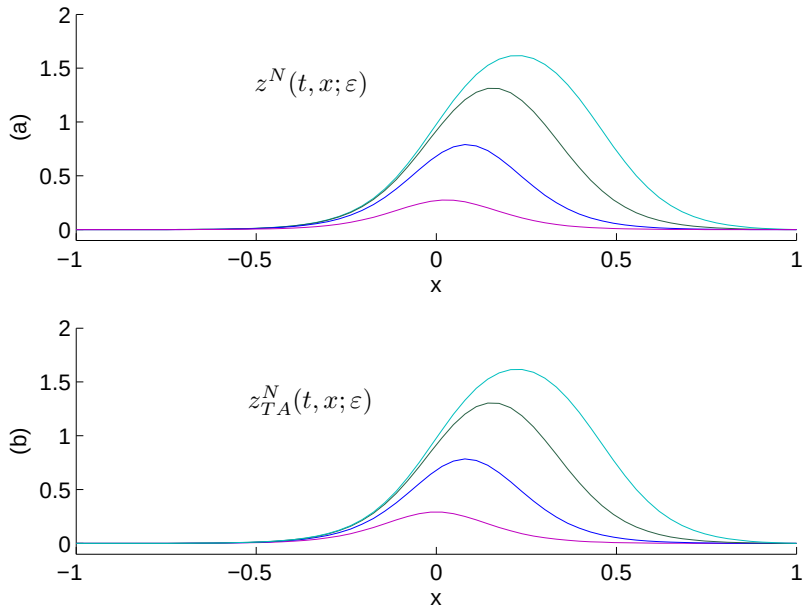

Figure 5.17: Comparison of (a) numerical solution $z^N(t,x;\varepsilon)$ of the disturbed NLCD equation (5.20)-(5.22) and (b) first order Taylor series approximation $z^N_{TA}(t,x;\varepsilon)$ defined in (5.32) to the solution of disturbed NLCD equation. Here, $\mu = .1$, $\varepsilon = 10^{-4}$, $N = 64$, $z_0(x) = (1-x)(1+x)^3$ and $t = 25, 100, 500, 10000$ and both solutions are monotonically decreasing in time. The nonzero steady state is reached at $t = 10000$.

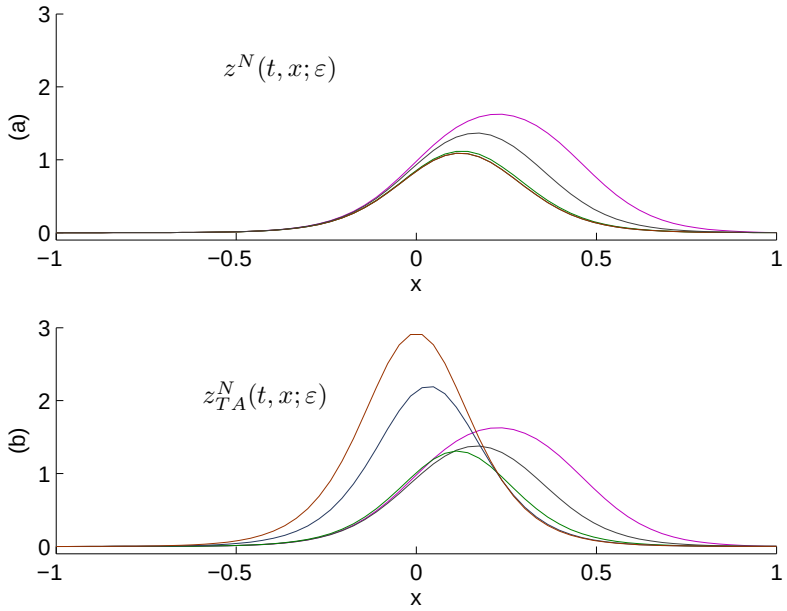

Figure 5.18: Figures (a) and (b) are analogous to figure 5.17. Here, $\varepsilon = 10^{-3}$ and $t = 25, 100, 500, 2000, 10000$. The numerical solution $z^N(t,x;\varepsilon)$ in (a) monotonically decreases to the steady state while the rough Taylor approximation $z^N_{TA}(t,x;\varepsilon)$ in (b) first decreases and then increases up to a different steady state.

magnitude, drastically changing the dynamics of the system. The continuous sensitivity method yields this information for the relatively minor cost of solving a linear sensitivity equation.

5.2.4 Comparison of the 2D Undisturbed and Disturbed Problems

In the previous chapter, we studied the two dimensional scalar nonlinear convection-diffusion equation given by

$$z_t + zz_x + zz_y = \mu\nabla^2 z - (hz)_x - (hz)_y, \tag{5.33}$$

with boundary conditions

$$z(t,0,y) = z(t,1,y), \quad z_x(t,0,y) = z_x(t,1,y), \tag{5.34}$$

$$z(t,x,0) = 0, \quad z(t,x,1) = 0, \tag{5.35}$$

and initial condition

$$z(0,x,y) = z_0(x,y). \tag{5.36}$$

The spatial domain is the rectangle $\Omega = (0,1) \times (0,1)$. Again, μ is a positive constant and $h = h(y)$ is the hyperbolic tangent profile given by (4.36). Here, we examine the sensitivity of solutions with respect to a simplified form of wall roughness. Specifically, the equation is taken to hold over the "rough walled" domain

$$\Omega(\alpha,\beta) = \left\{ (x,y) \in \mathbb{R}^2 \,:\, 0 < x < 1,\ b(x;\alpha,\beta) < y < t(x;\alpha,\beta) \right\},$$

where

$$b(x;\alpha,\beta) = \alpha\sin(\beta x), \quad t(x;\alpha,\beta) = 1 + b(x;\alpha,\beta) = 1 + \alpha\sin(\beta x).$$

Here, $y = b(x;\alpha,\beta)$ and $y = t(x;\alpha,\beta)$ are the equations for the bottom and top wall of the domain and α is assumed to be small so that the walls are nearly flat.

As mentioned in section 4.4, the linear operator for the undisturbed problem is given by

$$\mathcal{A}z = \mu\nabla^2 z - (hz)_x - (hz)_y.$$

for all z in the domain of $\mathcal{A}$ defined by

$$\mathcal{D}(\mathcal{A}) = \left\{ z \in H^1(\Omega) \,:\, \mathcal{A}z \in L^2(\Omega),\ z(0,y) = z(1,y),\ z(x,0) = 0 = z(x,1) \right\}$$

Lemma 4.4.2 guarantees that $\mathcal{A}$ generates an analytic semigroup. Therefore, if the spectrum of this operator lies in the left half plane (and is bounded away from the imaginary axis), then one could easily apply Theorem 2.2.3 to show that the the zero state is asymptotically stable with respect to the H^1 norm. Unfortunately, it is not known if this operator has its spectrum contained entirely in the left half plane. However, finite element approximations to the linear operator suggest that the spectrum of $\mathcal{A}$ does indeed lie in the left half plane. Table 5.1 shows the real part of the rightmost eigenvalue of the approximations for various

Table 5.1: Largest eigenvalue of the finite element approximation to the linear operator $\mathcal{A}$ in the 2D NLCD equation for various values of μ. N is the total number of basis functions used in the approximation and n is the number of equally spaced finite element nodes placed in each coordinate direction.

	N = 210	N = 930	N = 3906
μ	n = 16	n =32	n = 64
.1	$-.1293$	$-.1383$	$-.1403$
.05	-4.405×10^{-4}	-1.403×10^{-3}	-1.712×10^{-3}

values μ and n, the number of equally spaced nodes in each coordinate direction. It appears that the leading eigenvalue has negative real part and is not approaching the imaginary axis as n increases. Therefore, it is plausible that the zero state is an asymptotically stable equilibrium for this system in the H^1 norm. This has been computationally observed for a wide variety of initial data, see Figure 5.19 for a typical simulation. In fact, it appears that, like the 1D nonlinear convection-diffusion equation, most solutions converge to the zero state as $t \to \infty$.

For the disturbed problem, in section 4.4 the fluctuation equation was transformed from the rough domain $\Omega(\alpha, \beta)$ to the smooth domain Ω. If the transformed state is denoted by $\phi(\xi, \eta)$, then the transformed equation is given by

$$\begin{aligned} \phi_t + \phi\phi_\xi + (A+1)\phi\phi_\eta &= \mu\left(\frac{\partial}{\partial\xi}\left(\phi_\xi + A\phi_\eta\right) + \frac{\partial}{\partial\eta}\left(A\phi_\xi + \left(A^2+1\right)\phi_\eta\right)\right) \\ &\quad -(A+1)g\phi_\eta - g\phi_\xi - g_\eta\phi, \end{aligned} \tag{5.37}$$

with boundary conditions and initial condition

$$\phi(t,0,\eta) = \phi(t,1,\eta), \quad \phi_\xi(t,0,\eta) = \phi_\xi(t,1,\eta) \quad \text{for all } \eta, \tag{5.38}$$

$$\phi(t,\xi,0) = 0, \quad \phi(t,\xi,1) = 0 \quad \text{for all } \xi, \tag{5.39}$$

$$\phi(0,\xi,\eta) = \phi_0(\xi,\eta) := z_0(\xi, \eta + b(\xi)). \tag{5.40}$$

Here, g is the transformation of h and $A = A(\xi;\alpha,\beta)$ is also a byproduct of the transformation. In this case, unlike the 1D transformed NLCD equation, there is no forcing function to drive the solution of this transformed system. Also, the zero state is still an equilibrium. However, it now appears that the zero function is unstable for certain values of α and β. Table 5.2 shows the real part of the largest eigenvalue of finite element approximations to the perturbed linear operator for various values μ, α, β and n, the number of equally spaced nodes in each coordinate direction. This data suggests that the zero state is still asymptotically stable if the wall roughness isn't large enough (i.e., α is small) or rough enough (i.e., β is small).

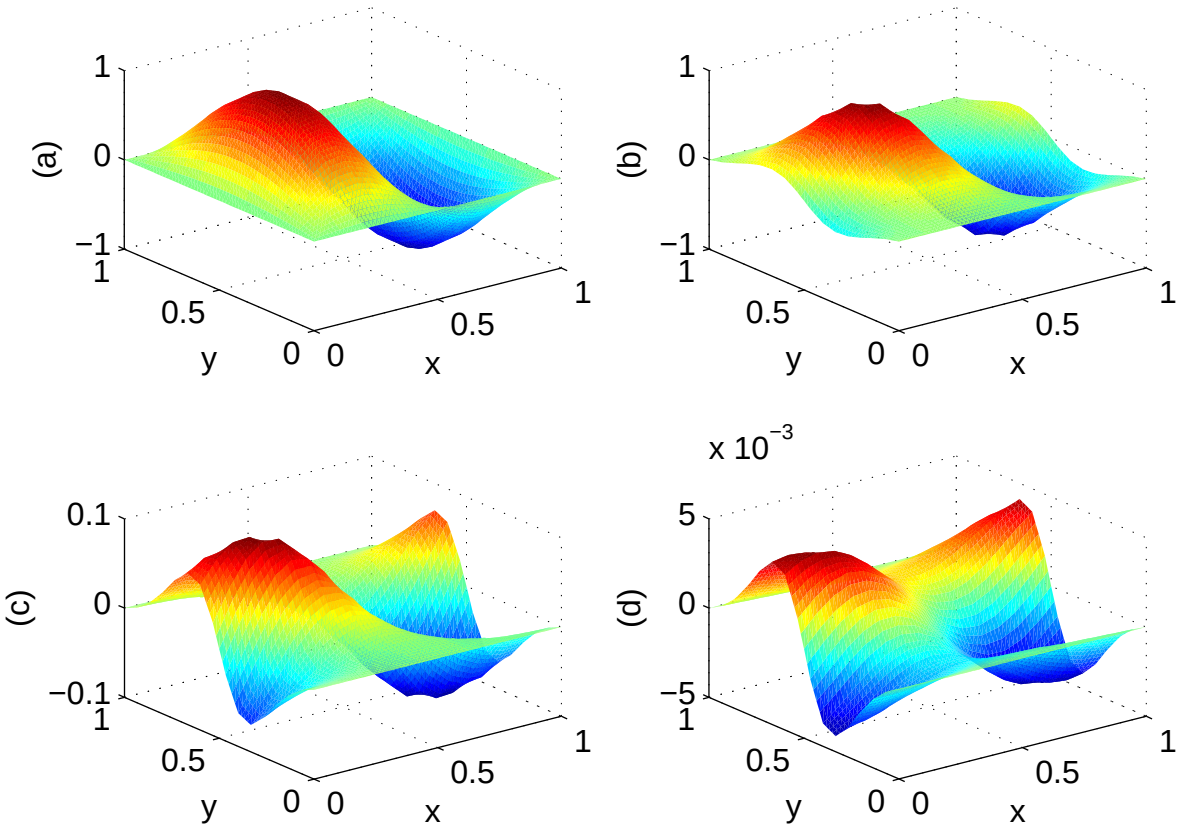

Figure 5.19: Numerical solution of the 2D NLCD equation (5.33)-(5.36) at times (a) $t = 0$, (b) $t = .1$, (c) $t = .5$ and (d) $t = 1$. Here, $\mu = .1$, $z_0(x, y) = \sin(2\pi x)\sin(\pi y)$ and $n = 16$ equally spaced nodes are used in each coordinate direction.

Computational experiments show that whenever α and β are small enough, numerical solutions to the transformed 2D nonlinear convection-diffusion equation tend to the zero state in a similar manner as numerical solutions to the undisturbed problem (compare figure 5.19). Therefore, the solution is not sensitive if the wall roughness is not too large or too rough. However, increasing these values eventually causes a great change in the solutions. Figure 5.20 shows a numerical solution with $\mu = .05$, $\alpha = .001$ and $\beta = 75$ at various time values. The solution quickly decays but then begins a *slow* ascent to an order one steady state solution. Figures 5.21 shows a similar order one numerical steady state solution obtained with $\mu = .05$, $\alpha = .001$, and $\beta = 100$. The very small wall roughness has caused the solutions to move an order of magnitude away from the origin. As with the 1D NLCD equation, decreasing μ only increases the change in the solution. Figure 5.22(b) shows the much larger steady state with $\mu = .025$, $\alpha = .0005$ and $\beta = 75$. The small form of simplified wall roughness causes solutions to "transition" where otherwise solutions would decay to

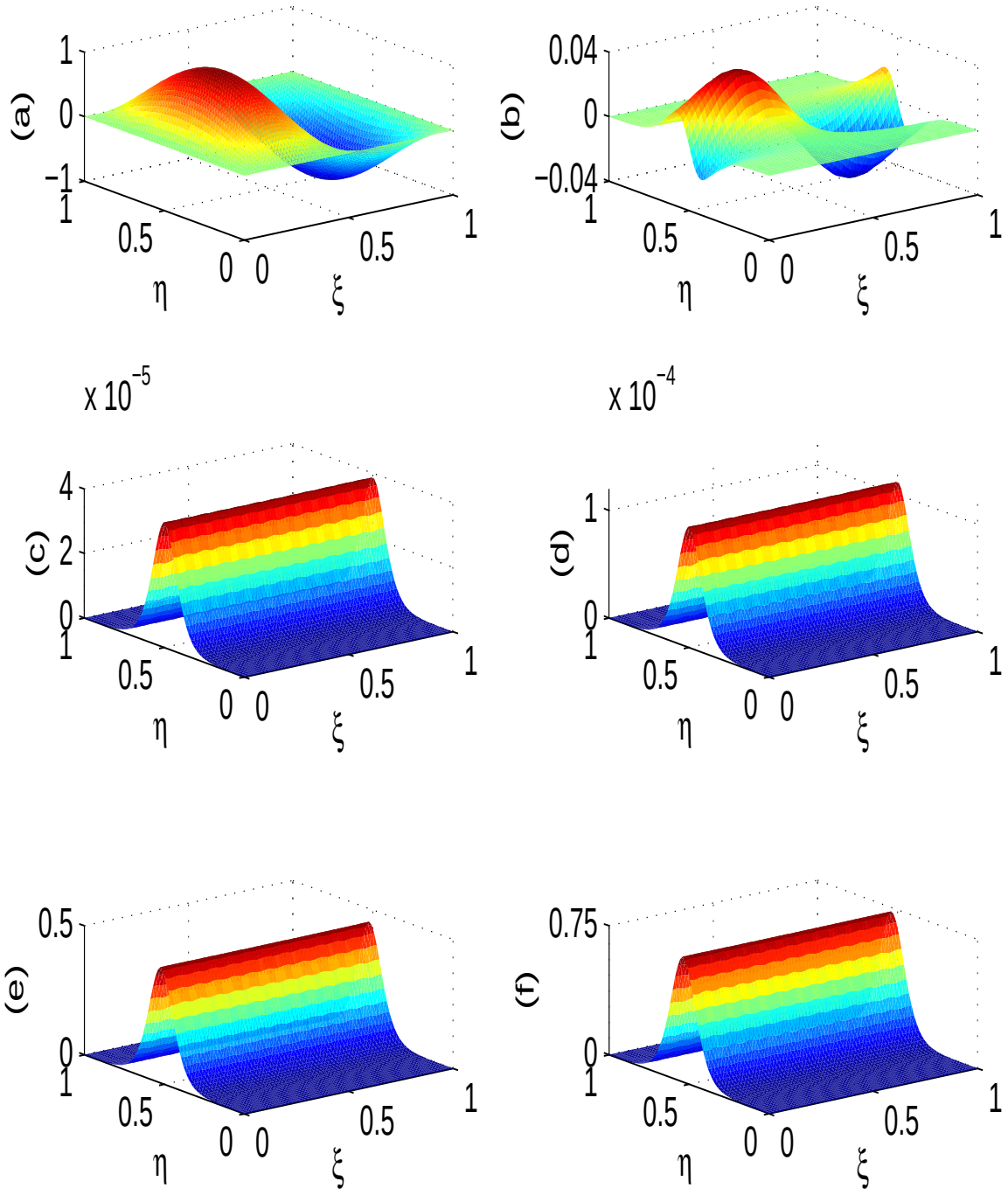

Figure 5.20: Numerical solution of transformed 2D NLCD equation (5.37)-(5.40) at (a) $t = 0$, (b) $t = 1$, (c) $t = 10$, (d) $t = 1000$, (e) $t = 10000$ and (f) $= 15000$. Here, $\phi_0(x, y) = \sin(2\pi\xi)\sin(\pi\eta)$, $\mu = .05$, $\alpha = .001$, $\beta = 75$ and $n = 64$ equally spaced nodes are used in each coordinate direction.

Table 5.2: Largest eigenvalue of the finite element approximation to the linear operator of the transformed 2D NLCD equation for various values of μ. N is the total number of basis functions used in the approximation and n is the number of equally spaced finite element nodes placed in each coordinate direction.

			N = 210	N = 930	N = 3906
μ	α	β	n = 16	n =32	n = 64
.05	.0001	75	-1.838×10^{-4}	-1.144×10^{-3}	-1.1452×10^{-3}
.05	.001	75	2.188×10^{-3}	1.346×10^{-3}	9.549×10^{-4}
.05	.001	100	2.869×10^{-3}	2.104×10^{-3}	1.757×10^{-3}

zero.

An interesting difference between the 1D and 2D problems is that the small wall roughness appears to create new equilibria in the 2D problem. The nonzero steady state solutions of the transformed fluctuation equation appear to be constant in ξ, i.e., $\psi_{ss}(\xi, \eta) = \psi_{ss}(\eta) = z_{ss}(y - b(x; \alpha, \beta))$. However the "nearby" function $z_{ss}(y)$ is not an equilibrium of the original fluctuation equation (5.33)-(5.36). Recall in section 4.4 we considered the 2D NLCD equation

$$w_t + ww_x + ww_y = \mu \nabla^2 w, \quad w(t, x, 0) = 1, \quad w(t, x, 1) = -1$$

with periodic boundary conditions in the x direction. Lemma 4.4.1 implies that any equilibrium of the form $h = h(y)$ to this problem is necessarily unique. The change of variable $z(t, x, y) = w(t, x, y) - h(y)$ was then made to arrive at the fluctuation equation. Therefore, if there were to exist another equilibrium $z_{ss} = z_{ss}(y)$ to the fluctuation problem, that would imply the existence of another equilibrium of the form $w = w(y) \neq h(y)$ to the original 2D NLCD equation above. Since this is impossible, there cannot be an equilibrium to the fluctuation problem of the form $z = z(y)$. Therefore, we conjecture that the nonzero steady state solutions of the transformed fluctuation equation are "new" equilibria, i.e., they are not transformations of equilibria to the original fluctuation equation. Including a small wall roughness causes these equilibria to appear.

This experiment uses a very simple approximation of wall roughness. In reality, actual wall roughness is three dimensional and most likely not smooth. A transformation to a smooth region would be impossible. It is then difficult to tell what influence "real" wall roughness has on an actual flow system. However, this simple example here provides some insight. When the wall roughness is large enough, solutions "transitioned" to an order one steady state when they should have decayed to zero. The linear operator became unstable and new equilibria appeared. Also, for a fixed roughness size, one sees transition as μ approaches zero. This is what one observes in experimental fluid flow. These observations provide a possible explanation of the failure of classical linear stability analysis to predict transition to turbulence in certain fluid flows (such as Couette or pipe flows). Including some form of wall roughness or small disturbances in flow models would give a more accurate

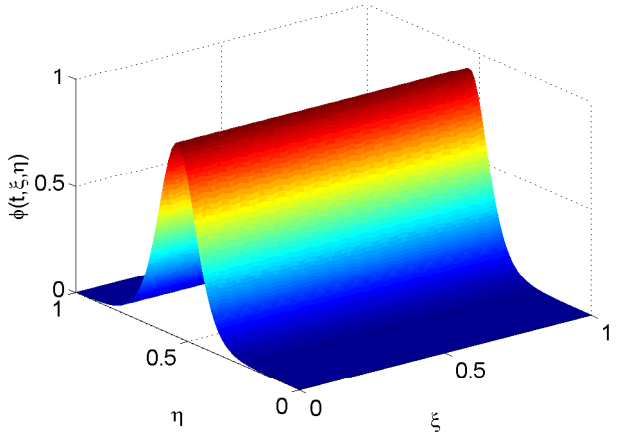

Figure 5.21: Numerical steady state solution of the transformed 2D NLCD equation (5.37)-(5.40) at $t \approx 7000$, with $\mu = .05$, $\alpha = .001$, $\beta = 100$, $\phi_0(\xi, \eta) = \sin(2\pi\xi)\sin(\pi\eta)$ and $n = 64$ equally spaced nodes used in each coordinate direction.

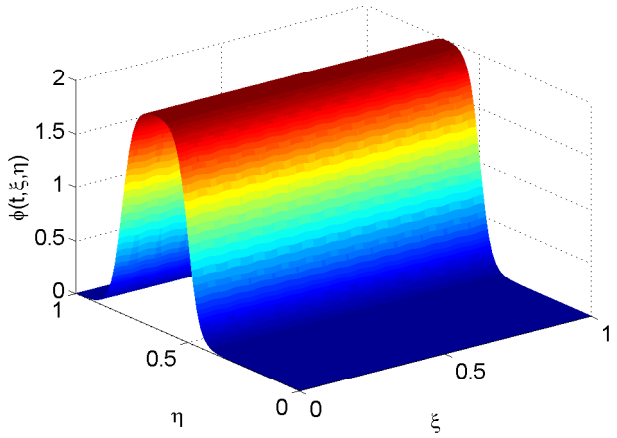

Figure 5.22: Numerical steady state solution of the transformed 2D NLCD equation (5.37)-(5.40) at $t \approx 5000$, with $\mu = .025$, $\alpha = .0005$, $\beta = 75$, $\phi_0(\xi, \eta) = \sin(2\pi\xi)\sin(\pi\eta)$ and $n = 64$ equally spaced nodes used in each coordinate direction.

picture of transition.

5.3 Sensitivity Analysis of ODE Model Problems

Here we focus on the ODE model problems introduced in section 4.1 given by

$$\dot{x}(t) = \mathbf{A}x(t) + \|x(t)\| \mathbf{S}x(t) + \varepsilon d, \quad x(0) = x_0 \in \mathbb{R}^n, \tag{5.41}$$

where $\mathbf{A}$ is a constant stable matrix, $\mathbf{S}$ is a constant skew-symmetric matrix, $\|\cdot\|$ is the standard Euclidean norm and $\mathbf{d}$ is a constant vector. Recall that ODEs of this form with $\varepsilon = 0$ are known to be very sensitive with respect to initial data. The origin is asymptotically stable, but if the initial data is not extremely close to zero then solutions can transition to another state. Therefore, these systems have been used as model problems for flow systems which show extreme sensitivity to disturbances in the laminar flow. We focus here on sensitivity with respect to the forcing term εd only. Considerable work on the sensitivity to initial data may be found in the references [5], [6] and [143].

In section 4.1 the sensitivity of the solutions with respect to the small disturbance ε at $\varepsilon = 0$ was defined by

$$s(t) = \frac{\partial x}{\partial \varepsilon}(t; \varepsilon) \Big|_{\varepsilon=0}.$$

Corollary 4.1.1 shows that this sensitivity satisfies the linear differential equation

$$\dot{s}(t) = \mathbf{A}s(t) + D_x F(x(t;0))s(t) + d, \quad s(0) = 0 \in \mathbb{R}^n, \tag{5.42}$$

where $x(t;0)$ is the solution to the undisturbed problem and $D_x F(\cdot)$ is the Jacobian of the nonlinear term $F(x) = \|x\| \mathbf{S}x$ given by

$$D_x F(x) = \begin{cases} \|x\| \mathbf{S} + \mathbf{S}\, xx^T / \|x\|, & \text{if } x \neq 0 \\ 0, & \text{if } x = 0. \end{cases} \tag{5.43}$$

As discussed earlier, since the matrix $\mathbf{A}$ is non-normal, the solution to the sensitivity equation can exhibit large transient growth for certain initial data. We will show that the sensitivity can predict time intervals where solutions are rapidly changing.

We also consider the control problem to illustrate that linear feedback control has the potential to suppress the sensitivity of the solution. We examine the ability of the control in these model problems to delay transition and even relaminarize fully developed chaotic flows. Although there are several control design methodologies, we limit our presentation to LQR control. Recall the optimal LQR controller minimizes the cost

$$J(u, x_0) = \int_0^\infty \langle \mathbf{Q}x(t), x(t) \rangle_{\mathbb{R}^n} + \langle \mathbf{R}u(t), u(t) \rangle_{\mathbb{R}} \, dt$$

subject to the linearized initial value problem

$$\dot{x}(t) = \mathbf{A}x(t) + \mathbf{B}u(t), \quad x(0) = x_0, \tag{5.44}$$

with $\mathbf{Q}$ positive semidefinite and $\mathbf{R}$ positive definite. Since in the example systems $\mathbf{A}$ is a stable matrix, it is well known that there is a unique solution to the LQR problem. The optimal control is given by the linear feedback law $u(t) = -\mathbf{K}x(t)$, where $\mathbf{K} = \mathbf{R}^{-1}\mathbf{B}^T\mathbf{\Pi}$ and $\mathbf{\Pi}$ is the unique symmetric non-negative definite solution of the matrix algebraic Riccati equation

$$\mathbf{A}^T\mathbf{\Pi} + \mathbf{\Pi}\mathbf{A} + \mathbf{\Pi}\mathbf{B}\mathbf{R}^{-1}\mathbf{B}^T\mathbf{\Pi} + \mathbf{Q} = \mathbf{0}.$$

We conduct a numerical study of how the control impacts the nonlinear perturbed system

$$\dot{x}(t) = \mathbf{A}x(t) + \|x(t)\|\,\mathbf{S}x(t) + \mathbf{B}u(t) + \varepsilon d, \quad x(0) = x_0. \tag{5.45}$$

5.3.1 The Two Dimensional System

The two dimensional system takes the specific form

$$\mathbf{A} = \begin{bmatrix} -1/R & 1 \\ 0 & -2/R \end{bmatrix}, \quad \mathbf{S} = \begin{bmatrix} 0 & -1 \\ 1 & 0 \end{bmatrix}, \quad d = \begin{bmatrix} 1 \\ 1 \end{bmatrix}, \tag{5.46}$$

The positive constant R plays the role of a Reynolds number. Figure 5.23 shows the phase portrait of the undisturbed system with $R = 5$. There are five equilibria. The red are unstable while the blue are stable. The light lines are the stable manifolds and the dark lines are the unstable manifolds for the unstable hyperbolic points. If the initial data lies inside the light lines, then $\|x(t)\| \to 0$. If the initial data lies outside of this band, then the solution converges to one of the other two equilibria. One can show that the system is dissipative. There is a global compact attractor defined by the five equilibria and the unstable manifolds of the hyperbolic points. Observe that the largest ball absorbing ball about zero shrinks as R increases. In fact, this ball has radius on the order of R^{-2}. In figure 5.23, we set $R = 5$ so that the basin of attraction for the origin is clearly visible. In figure 5.24, we set $R = 8$ to illustrate the shrinking of the domain.

Define the vector $x_{TS} = [1, 0]^T$ to be the eigenvector corresponding to the eigenvalue $-1/R$ which is closest to the imaginary axis. Also, define the vector $x_{OB} = [1, 1]^T$. The energy in the initial condition x_0 is given by the norm $\|x_0\|$. It is clear from the above phase portrait that for initial data in each of these directions, the solution with initial data in the x_{OB} direction will transition at a lower energy than an initial data in the x_{TS} direction. For example, if $R = 10$, then x_{OB} will transition when $\|x_{OB}\| > .0087$ while x_{TS} will transition when $\|x_{OB}\| > .02$. These initial states are analogous to the Tollmien-Schlichting (TS) and oblique (OB) waves for plane Poiseuille flow. The Tollmien-Schlichting state corresponds to the eigenvalue that is closest to the imaginary axis, yet transition occurs at a smaller energy for the oblique state. This is consistent with observations in [123].

For the disturbed problem, if $R = 6$ and $\varepsilon = 10^{-3}$, Figure 5.25 shows the phase portrait

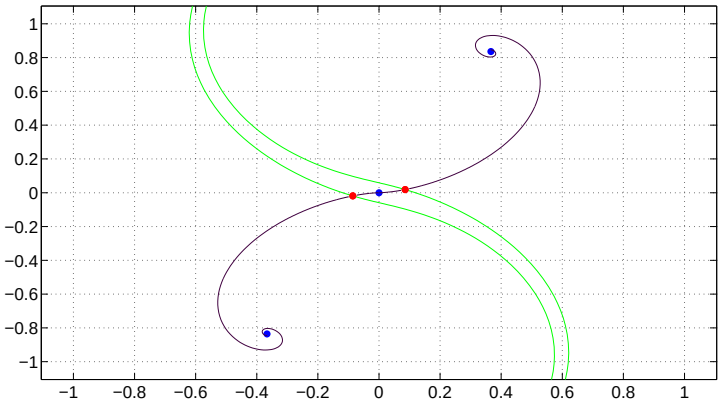

Figure 5.23: Phase portrait for the undisturbed 2D system (5.41), (5.46) with $R = 5$ and $\varepsilon = 0$.

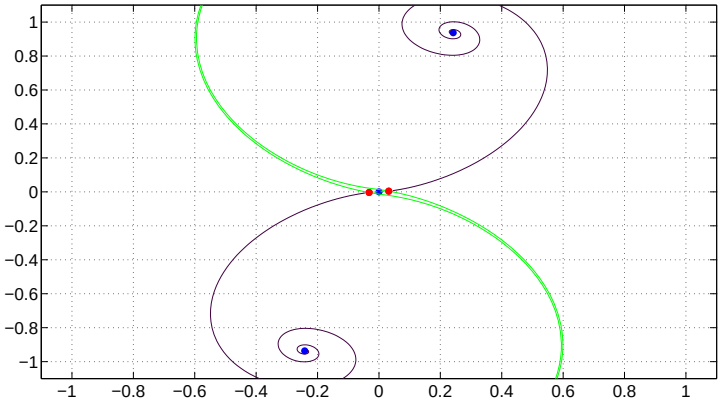

Figure 5.24: Phase portrait for the undisturbed 2D system (5.41), (5.46) with $R = 8$ and $\varepsilon = 0$.

change dramatically. The equilibria experience a subcritical bifurcation and the zero state, which was an asymptotically stable equilibrium, is no longer an equilibrium. The light line and the dark line are the stable and unstable manifolds for the one remaining unstable equilibrium. Now, any initial data near zero will transition to one of the two remaining stable equilibria. Also, for larger values of R, ε can be very small and still cause the bifurcation of equilibria. This is the same structure observed in the nonlinear convection diffusion equation.

The continuous sensitivity equation method is able to predict this phenomenon for this model problem. Let $x_0 = .02\, x_{TS}$ and $x_0 = .005\, x_{OB}$ so that the solutions of the undisturbed

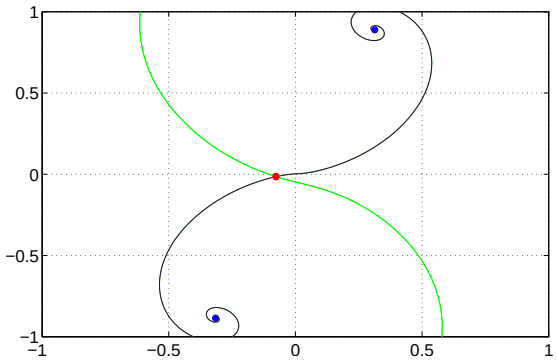

Figure 5.25: Phase portrait for the 2D disturbed system (5.41), (5.46) with $R = 6$ and $\varepsilon = 10^{-3}$.

problem with these initial conditions are in the basin of attraction and will converge to the zero state. Figure 5.26 shows the sensitivity of the solution with the TS initial data computed using the sensitivity equation (5.42), (5.43), (5.46) in comparison with the solution of the disturbed problem with $\varepsilon = 5 \times 10^{-4}$. Note that the sensitivity peaks almost at the same time that the solution of the disturbed problem "transitions". Although changing the initial condition and the value of ε yields different transition times, the sensitivity still provides a a rough precursor to the transition time. Figure 5.27 shows the analogous computations with the oblique initial state and the smaller disturbance $\varepsilon = 10^{-4}$. The sensitivities are much larger which implies the solution is more sensitive than the solution with the TS initial data. This is observed for Poiseuille flow. Also, the transition time is again matched by the peak of the sensitivity. More importantly, the sensitivities show a rapid growth long before the transition occurs. Hence, the sensitivities might provide useful information for a feedback controller.

Consider the LQR control problem described above. We set $R = 10$ to demonstrate the effectiveness of the LQR linear feedback control on a sensitive problem. Choose the state weight $\mathbf{Q} = \mathbf{I}$, the control weight $\mathbf{R} = 10$ and $\mathbf{B} = [0, 1]^T$ so that the control only enters into the second component of the state equation. In this case, the optimal LQR feedback gain $\mathbf{K}$ is given by $\mathbf{K} = [0.2397, 0.5871]$ and the closed loop system with $\varepsilon = 0$ has the phase portrait shown in Figure 5.28. Again, there are five equilibria. The red are unstable and the blue stable. The lighter and darker lines are the stable and unstable manifolds for the unstable hyperbolic points. Notice that the basin of attraction for the origin is now quite large. The largest absorbing ball for the origin has radius of approximately .34. In contrast, the radius of the ball for the uncontrolled system is approximately .005. If $\varepsilon \neq 0$ so that the small disturbance enters to the controlled problem, the phase portrait of the resulting system is almost identical. Therefore, the control has drastically reduced the sensitivity of the problem to the disturbance εd. We note that different choices for the state and control weights $\mathbf{Q}$ and $\mathbf{R}$ as well as the control input matrix $\mathbf{B}$ can have a great impact on the nonlinear dynamics of the closed loop system. For instance, allowing less control by

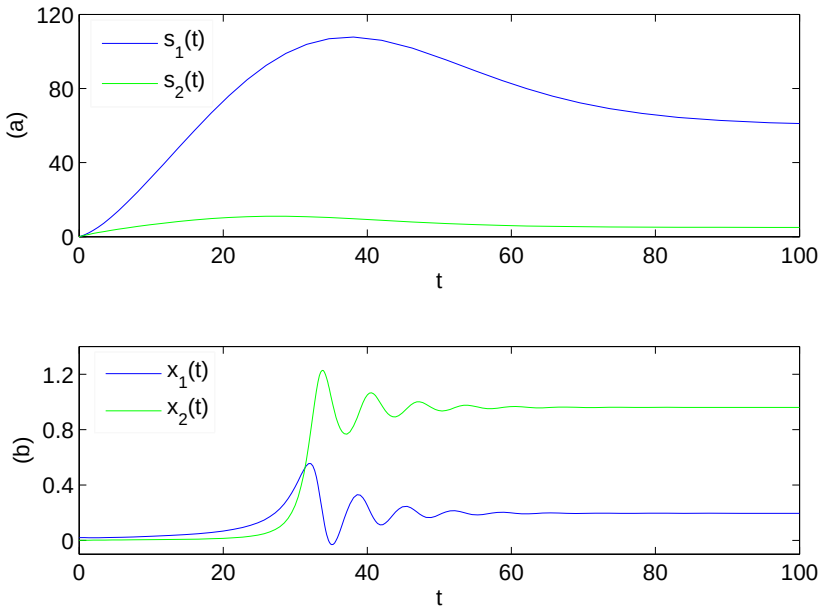

Figure 5.26: (a) Computed sensitivity of the solution of the 2D system with respect to ε at $\varepsilon = 0$ (b) Numerical solution of 2D disturbed problem. In both figures, $R = 10$, $x_0 = .02\, x_{TS}$, $\varepsilon = 5 \times 10^{-4}$.

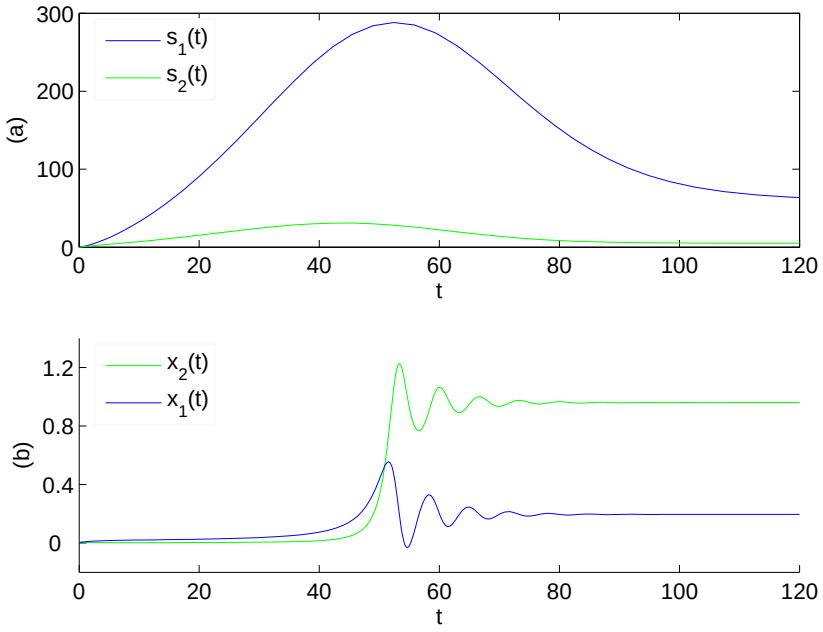

Figure 5.27: (a) Computed sensitivity of the solution of the 2D system with respect to ε at $\varepsilon = 0$ (b) Numerical solution of 2D disturbed problem. In both figures, $R = 10$, $x_0 = .005\, x_{OB}$, $\varepsilon = 10^{-4}$.

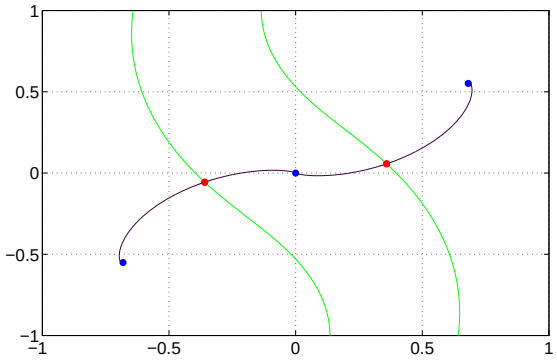

Figure 5.28: Phase portrait for the closed loop system (5.45), (5.46) with $\mathbf{Q} = \mathbf{I}$, $\mathbf{R} = 10$, $\mathbf{B} = [0, 1]^T$, $R = 10$ and $\varepsilon = 0$. The control $u(t)$ is the optimal LQR control for the linearized system (5.44).

increasing the control weight $\mathbf{R}$ shrinks the size of the largest attracting ball for the origin. However, allowing more control by decreasing $\mathbf{R}$ to 4 eliminates all of the equilibrium except the origin which becomes globally attracting. In this case, although the open and closed loop systems are both dissipative, the global attractors are very different. It is important to note that *linear* feedback can dramatically alter the nature of the global attractor for a *nonlinear* system. This example shows that linear feedback has the potential to decrease the sensitivity of flows with respect to small disturbances and alter the global dynamics. In particular, feedback may be able to enlarge the domain of attraction for a laminar flow and thus delay transition or even eliminate chaotic/turbulent flow.

5.3.2 The Three Dimensional System

Although the simple 2D model problem above captures the essential ideas, we present a 3D model to illustrate the points for a chaotic system. Define the matrices by

$$\mathbf{A} = \begin{bmatrix} -.5/R & 1 & 0 \\ 0 & -.75/R & 1 \\ 0 & 0 & -1/R \end{bmatrix}, \quad \mathbf{S} = \begin{bmatrix} 0 & -1 & -.5 \\ 1 & 0 & .25 \\ .5 & -.25 & 0 \end{bmatrix}, \quad d = \begin{bmatrix} 1 \\ 1 \\ 1 \end{bmatrix}, \tag{5.47}$$

and consider the initial value problem (5.41). The 3D system exhibits a wide variety of behaviors, depending on the value of R. When $R < 4$, at least one of the nonzero equilibria is stable and all solutions converge to a stable equilibrium. If R is larger than 4, all of the nonzero equilibria are unstable and solutions can tend to either a periodic, quasi-periodic, or chaotic orbit. In particular, chaotic solutions are observed in the approximate range $9.5 < R < 23$. Figure 5.29 shows a chaotic orbit for the above system with $R = 10$. Also, for large enough initial data, solutions will spiral out to infinity. Recall from Corollary 4.1.1 that the zero state is always an asymptotically stable equilibrium. However, like the 2D model,

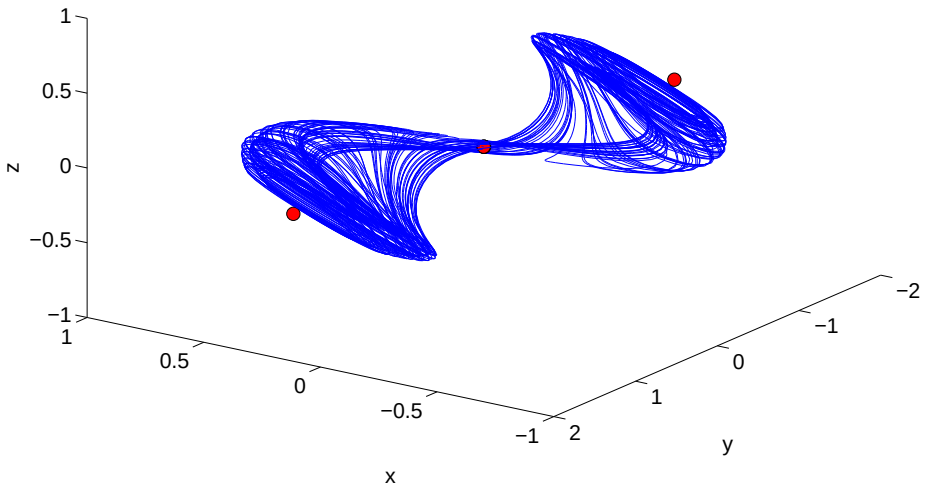

Figure 5.29: Representative numerical solution of the 3D system at $R = 10$. The red circles are unstable equilibria. The origin is a stable equilibrium and there are two unstable equilibria very near the origin.

there are two unstable equilibria near the origin which rapidly approach the zero state as R increases. Thus, the largest attracting ball for the origin is quite small and decreases with radius on the order of R^{-2} as R increases.

Again define the Tollmien-Schlichting (TS) state $x_{TS} = [1, 0, 0]^T$ as the eigenvector corresponding to the eigenvalue $-.5/R$ which is closest to the imaginary axis. Also define the oblique state $x_{OB} = [1, 1, 1]^T$. In the same manner as the 2D problem, the oblique state will transition at a lower energy than the TS state. For $R = 10$, the oblique initial state transitions whenever $\|x_{OB}\| > 1.7 \times 10^{-5}$ while the TS state transitions when $\|x_{TS}\| > 10^{-3}$. Again, this mirrors the behavior of the TS and oblique waves in plane Poiseuille flow. For the perturbed problem with $\varepsilon = 10^{-7}$, the zero state is no longer an equilibrium and the TS state also transitions.

The sensitivities of solutions to the 3D problem with respect to ε are similar to the sensitivities the 2D problem. In particular, the sensitivities can again predict the transition and approximate transition times. To illustrate, let $R = 10$ and choose initial data for both the TS and oblique states of $x_0 = 10^{-3} x_{TS}$ and $x_0 = 9 \times 10^{-6}$, respectively. Figure 5.30 compares the sensitivity with the solution of the disturbed problem with $\varepsilon = 10^{-7}$ for the TS initial state. Figure 5.30 shows the same comparison for the oblique initial state with $\varepsilon = 5 \times 10^{-8}$. The peaks of the sensitivities again correspond with the transition times of the solutions of the disturbed problems. Again, the sensitivity provides a rough estimate of the transition time for the disturbed system.

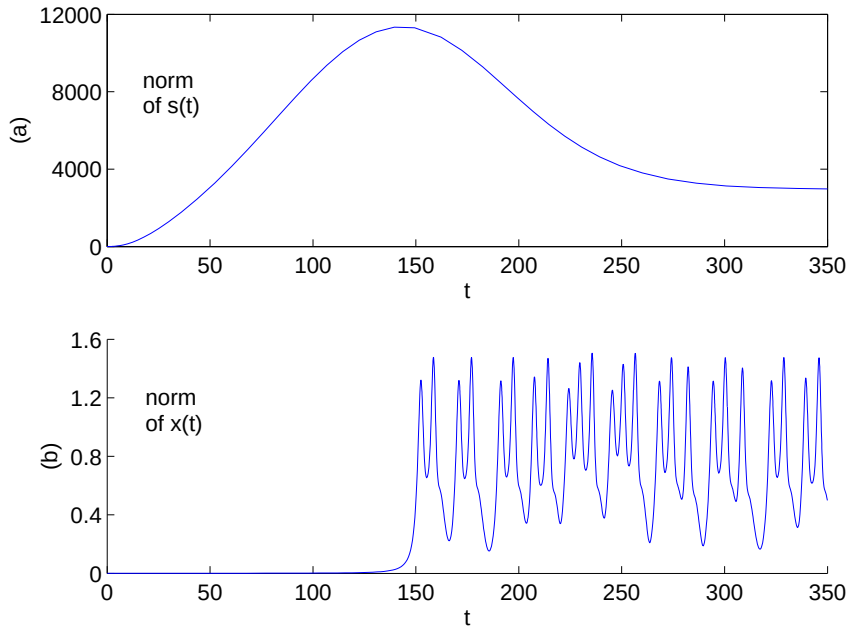

Figure 5.30: (a) Norm of the computed sensitivity $s(t)$ of the solution of the 3D system with respect to ε at $\varepsilon = 0$ (b) Norm of the solution $x(t;\varepsilon)$ of the 3D disturbed problem. In both figures, $R = 10$, $x_0 = 10^{-3}\, x_{TS}$, $\varepsilon = 10^{-7}$.

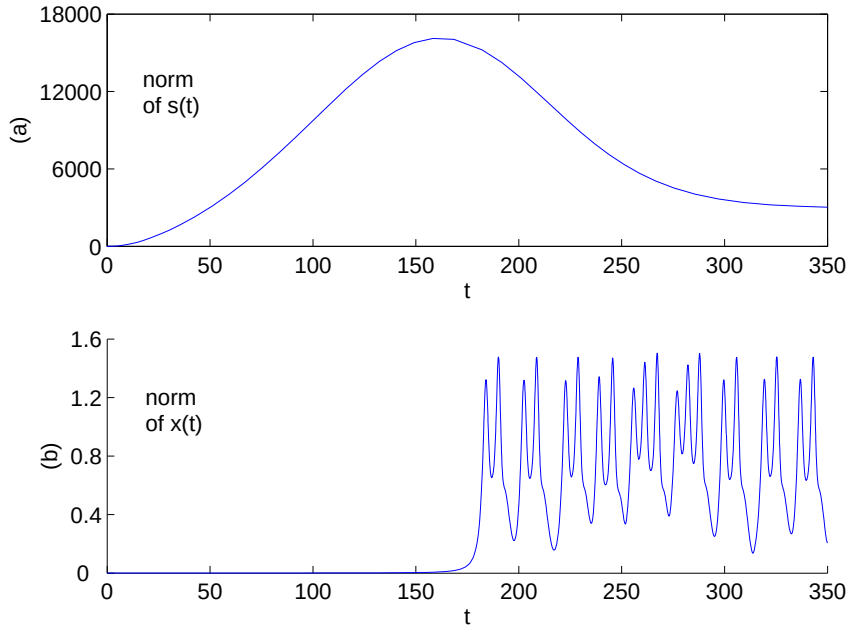

Figure 5.31: (a) Norm of the computed sensitivity $s(t)$ of the solution of the 3D system with respect to ε at $\varepsilon = 0$ (b) Norm of the solution $x(t;\varepsilon)$ of the 3D disturbed problem. In both figures, $R = 10$, $x_0 = 9 \times 10^{-6}\, x_{OB}$, $\varepsilon = 5 \times 10^{-8}$.

Finally, we show that an LQR controller has the potential to stabilize a fully developed chaotic flow. The main idea is to turn on the control when the chaotic flow enters the domain of attraction of the origin for the closed loop system. This method is based on the capturing ideas presented by Yorke and colleagues in [124] and [125]. As a test case, consider the LQR controller with state weight $\mathbf{Q} = \mathbf{I}$, control weight $\mathbf{R} = 1$ and $\mathbf{B} = [0, 0, 1]^T$ so that the control enters through the last component of the system. Computing the feedback gain as described above yields $\mathbf{K} = [0.8862, 2.1290, 2.1952]$. The closed loop system is obtained by setting $u(t) = -\mathbf{K}x(t)$. We first apply the capturing control to the undisturbed system with $\varepsilon = 0$. The location of the equilibria of the closed loop system provide an approximation to the domain of attraction for the zero state. There are two unstable equilibria of distance of about .3358 away from the origin. Therefore, a reasonable guess is that the largest ball of attraction for the origin has a radius of about .33. For the oblique initial data $x_0 = 10^{-4}x_{OB}$, the solution transitions to a chaotic attractor at $t = 150$. Thus, we wait until the solution has transitioned and do not turn on the control until the norm of the solution is less than .33. In this numerical experiment, the controller turned on at $t = 154$ and almost instantly stabilized the solution. For other initial data, the control would turn on at different times, but the flow was always stabilized to the zero state. This method was also successful when the disturbance εd was allowed to enter the system. This example suggests that this capturing method has potential for relaminarizing fully developed chaotic flow even in the presence of disturbances.

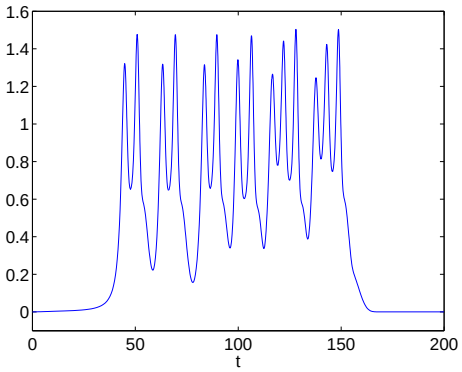

Figure 5.32: Norm of the numerical solution of the 3D closed loop system with $R = 10$, $\varepsilon = 0$, $x_0 = 10^{-4}x_{OB}$. The control is turned on at $t = 154$.

5.4 Discussion

It is clear from the examples presented in this chapter that small disturbances entering through forcing or a boundary condition can greatly affect the dynamics of a system. Classical stability analysis of the linearized part of the system may not be able to detect these

changes. In particular, the zero state may be an asymptotically stable equilibrium for the nonlinear problem, yet a small disturbance to the equation can cause a solution starting near the origin to transition to another state. As seen above, this phenomenon can be caused by a bifurcation of equilibria due to small perturbations. The zero equilibrium can move an order of magnitude or even disappear entirely. None of this can be seen by examining the spectrum of the linear part of the equations.

In contrast, the sensitivity equation method formulated in the previous chapter can provide considerable useful information about the disturbed system. The sensitivity can predict regions of space where the solution will undergo the largest change due to a particular disturbance. This information may be valuable for sensor and actuator placement for the control problem. Also, sensitivities can predict regions in time where the solution will be the most sensitive to the small disturbance. In particular, the sensitivity can predict possible transitions and give a rough prediction of a transition time. Therefore, sensitivity analysis can prove useful in control design. Also, sensitivity analysis is a useful tool to analyze the role of a specific perturbation in the transition process.

A non-normal linear operator can cause the solution of a nonlinear system to be extremely sensitive with respect to small disturbances. Since the non-normality of the linear operator is a crucial feature that increases sensitivity, one has hope that linear feedback might be sufficient to control transition. We explored these idea for low order ODE model problems and have shown how a linear control can drastically decrease the sensitivity of a system to small disturbances. Specifically, the control can enlarge the domain of attraction for an equilibrium state which reduces the possibility that a small disturbance will cause a bifurcation and transition. This property demonstrates that feedback control has the potential to delay transition or even relaminarize a fully developed turbulent flow.

Chapter 6

Conclusion and Summary of Main Results

The main focus of this thesis has been to investigate the effects of small disturbances on the solutions of dynamical systems with non-normal linear part. Our motivation comes from the Navier-Stokes equations and the unsolved problem of accurately predicting transition to turbulence in certain fluid flows. Recent work on the transition problem indicates that small disturbances play an important role in transition. To try to more completely identify the role of small disturbances in the transition process, we explored certain model problems that share a similar mathematical framework with the Navier-Stokes equations. Specifically, we studied how certain boundary and forcing disturbances affected the equations. We formulated the continuous sensitivity equation method to investigate the change in solutions with respect to a small disturbance. We also explored the use of a linear feedback controller to reduce the sensitivity of a problem to small disturbances.

In considering these problems, we are led to the following conclusions.

1. Small forcing or boundary disturbances can cause bifurcation of equilibria which can lead to transition.

2. Small wall roughness can cause an equilibrium to become unstable and also create new equilibria leading to transition.

3. Sensitivity analysis can predict if solutions are sensitive to a specific type of small disturbance. The sensitivities can predict regions in space and time where the solutions will be sensitive and they can provide a precursor to transition.

4. Linear feedback control can reduce the sensitivity of a nonlinear system by changing the global dynamics. Therefore, linear feedback has the potential to delay transition and even stabilize fully chaotic flows.

All of these results center around the fact that nonlinear systems with a non-normal linear operator can be sensitive to small disturbances.

In the course of this work, we have encountered many important problems that require further investigation.

1. The relationship between the linearized Navier-Stokes operator and the Orr-Sommerfeld operator needs to be closely examined.

2. A stronger theory for stability of equilibria is needed for infinite dimensional dynamical systems. In particular, it would be beneficial to have a stability theory that does not require the small perturbation to the initial condition to be smooth.

3. Work needs to be done on representing realistic disturbances in flow systems. Good representations would lead to better algorithms for sensitivity analysis and control.

4. Sensitivity analysis needs to be explored further in predicting transition for flow systems. Also, the benefits of sensitivity analysis in control problems needs to be thoroughly investigated.

5. The concept of a capturing control needs to be investigated for controllers that only have access to partial state information. Also, the relationship between the control weights and the sensitivity of the system should be thoroughly examined.

We mention an alternate flow model known as the Bipolar fluid equations (see [13] for an overview) that may provide insight into the problem of representing realistic wall roughness. The equations are more complex than the Navier-Stokes equations, but they have many theoretical advantages including global existence and uniqueness of solutions and compact global attractors in both bounded domains and unbounded channels (see [14], [15], [20], [21]). More importantly, solutions to the Bipolar fluid equations are known to exhibit sensitivity with respect to wall roughness [16]. In fact, in a certain case, infinitesimal wall roughness can be represented by a particular Neumann boundary condition. Results such as this are not known for the Navier-Stokes equations. Since the Bipolar fluid equations display sensitivity to wall roughness, it is possible that these equations are a more accurate flow model for predicting transition.

Finally, we note that the recent theoretical results in [11] and [12] on boundary control for the Navier-Stokes equations also support the conjecture of using linear feedback control to stabilize turbulent flow. Barbu et. al show that on bounded domains it is possible to stabilize an unstable laminar flow by linear feedback on the boundary. Moreover, in two dimensions this can be done with a finite number of controllers. It would be useful to develop numerical tools to test the usefulness of this theory.

Bibliography

[1] L. Abia and J. M. Sanz-Serna, *Interpolation of the coefficients in nonlinear elliptic Galerkin procedures*, SIAM Journal on Numerical Analysis, 21 (1984), pp. 77–83.

[2] E. Allen, J. A. Burns, D. S. Gilliam, J. Hill, and V. I. Shubov, *The impact of finite precision arithmetic and sensitivity on the numerical solution of partial differential equations*, Journal of Mathematical and Computer Modeling, 35 (2004), pp. 1165–1195.

[3] J. A. Atwell, J. T. Borggaard, and B. B. King, *Reduced order controllers for Burgers' equation with a nonlinear observer*, International Journal of Applied Mathematics and Computer Science, 11 (2001), pp. 1311–1330.

[4] J. D. Avrin, *Large-eigenvalue global existence and regularity results for the Navier-Stokes equation*, Journal of Differential Equations, 127 (1996), pp. 365–390.

[5] J. S. Baggett, T. A. Driscoll, and L. N. Trefethen, *A mostly linear model of transition to turbulence*, Physics of Fluids, 7 (1995), pp. 833–838.

[6] J. S. Baggett and L. N. Trefethen, *Low-dimensional models of subcritical transition to turbulence*, Physics of Fluids, 9 (1997), pp. 1043–1053.

[7] A. Bahadir, *A fully implicit finite-difference scheme for two-dimensional Burgers equations*, Applied Mathematics and Computation, 137 (2003), pp. 131–137.

[8] A. Balogh, D. S. Gilliam, and V. I. Shubov, *Stationary solutions for a boundary controlled Burgers' equation*, Mathematical and Computer Modelling, 33 (2001), pp. 21–37.

[9] B. Bamieh and M. Dahleh, *Disturbance energy amplification in three-dimensional channel flows*, in Proceedings of the American Control Conference, San Diego, California, 1999, pp. 4532–4537.

[10] ——, *Energy amplification in channel flows with stochastic excitation*, Physics of Fluids, 13 (2001), pp. 3258–3269.

[11] V. Barbu, I. Lasiecka, and R. Triggiani, *Boundary stabilization of Navier-Stokes equations*, Memoires of the AMS, 2005, to appear.

[12] V. Barbu and R. Triggiani, *Internal stabilization of Navier-Stokes equations with finite dimensional controllers*, Indiana University Mathematics Journal, 53 (2004), pp. 1443–1494.

[13] H. Bellout, F. Bloom, and J. Nečas, *Phenomenological behavior of multipolar viscous fluids*, Quarterly of Applied Mathematics, L (1992), pp. 559–583.

[14] ——, *Bounds for the dimensions of the attractors of non-linear bipolar viscous fluids*, Asymptotic Analysis, 11 (1995), pp. 131–167.

[15] ——, *Existence, uniqueness, and stability of solutions to the initial-boundary value problem for bipolar viscous fluids*, Differential Integral Equations, 8 (1995), pp. 453–464.

[16] H. Bellout and S. L. Wills, *Perturbation of the domain and regularity of the solutions of the bipolar fluid flow equations in polygonal domains*, International Journal of Non-Linear Mechanics, 30 (1995), pp. 235–262.

[17] A. Bensoussan, G. Da Prato, M. C. Delfour, and S. K. Mitter, *Representation and Control of Infinite Dimensional Systems: Volumes I and II*, Birkhäuser, Boston, 1992.

[18] T. R. Bewley, *Flow control: new challenges for a new Renaissance*, Progress in Aerospace Sciences, 37 (2001), pp. 21–58.

[19] A. Biryuk, *Note on the transformation that reduces the Burgers equation to the heat equation*. preprint, available at http://www.ma.hw.ac.uk/˜kuksin/students.html, 2003.

[20] F. Bloom and W. Hao, *Regularization of a non-Newtonian system in an unbounded channel: existence and uniqueness of solutions*, Nonlinear Analysis, 44 (2001), pp. 281–309.

[21] ——, *Regularization of a non-Newtonian system in an unbounded channel: existence of a maximal compact attractor*, Nonlinear Analysis, 43 (2001), pp. 743–766.

[22] L. Boberg and U. Brosa, *Onset of turbulence in a pipe*, Zeitschrift Fur Naturforschung Section A-A Journal of Physical Sciences, 43 (1988), pp. 697–726.

[23] P. B. Bochev and M. D. Gunzburger, *Finite element methods of least-squares type*, SIAM Review, 40 (1998), pp. 789–837.

[24] P. B. Bochev, M. D. Gunzburger, and J. N. Shadid, *Stability of the SUPG finite element method for transient advection-diffusion problems*, Computer Methods in Applied Mechanics and Engineering, 193 (2004), pp. 2301–2323.

[25] A. Bohé, *Free layers in a singularly perturbed boundary value problem*, SIAM Journal on Mathematical Analysis, 21 (1990), pp. 1264–1280.

[26] J. Borggaard and J. Burns, *A PDE sensitivity equation method for optimal aerodynamic design*, Journal of Computational Physics, 136 (1997), pp. 366–384.

[27] P. Braz e Silva, *Resolvent estimates for plane Couette flow*, SIAM Journal on Applied Mathematics, 65 (2005), pp. 667–683.

[28] J. M. Burgers, *A mathematical model illustrating the theory of turbulence*, Advances in Applied Mechanics, 1 (1948), pp. 171–199.

[29] J. Burns, A. Balogh, D. S. Gilliam, and V. I. Shubov, *Numerical stationary solutions for a viscous Burgers' equation*, Journal of Mathematical Systems, Estimation, and Control, 8 (1998), pp. 1–16.

[30] J. A. Burns, *Nonlinear distributed parameter control systems with non-normal linearizations: Applications and approximations*, in Research Directions in Distributed Parameter Systems, Frontiers in Applied Mathematics, 27, SIAM, Philadelphia, PA, 2003, pp. 17–53.

[31] J. A. Burns and S. Kang, *A control problem for Burgers' equation with bounded input/output*, Nonlinear Dynamics, 2 (1991), pp. 235–262.

[32] ——, *A stabilization problem for Burgers' equation with unbounded control and observation*, in Estimation and Control of Distributed Parameter Systems, International Series of Numerical Mathematics, 100, Birkhäuser, 1991, pp. 51–72.

[33] J. A. Burns and L. G. Stanley, *A note on the use of transformations in sensitivity computations for elliptic systems*, Mathematical and Computer Modelling, 33 (2001), pp. 101–114.

[34] J. A. Burns, L. G. Stanley, and D. L. Stewart, *A projection method for accurate computation of design sensitivities*, in Optimal Control: Theory, Algorithms and Applications, W. Hager and P. Pardalos, eds., vol. 15 of Applied Optimization, Conference on Optimal Control: Theory, Algorithms and Applications, Kluwer Academic Publishers, 1998, pp. 40–66.

[35] K. M. Butler and B. F. Farrell, *Three-dimensional optimal perturbations in viscous shear flow*, Physics of Fluids A, 4 (1992), pp. 1637–1650.

[36] C. I. Byrnes, D. S. Gilliam, and V. I. Shubov, *On the global dynamics of a controlled viscous Burgers' equation*, Journal of Dynamical and Control Systems, 4 (1998), pp. 457–519.

[37] F. Calogero and S. De Lillo, *The Burgers equation on the semi-infinite and finite intervals*, Nonlinearity, 2 (1989), pp. 37–43.

[38] C. Cao and E. S. Titi, *Asymptotic behavior of viscous 1–D scalar conservation laws with Neumann boundary conditions*, in Mathematics & Mathematics Education, S. Elaydi, E. S. Titi, M. Saleh, S. K. Jain, and R. A. Saris, eds., Third Palestinian Mathematics Conference, Bethlehem University, West Bank, World Scientific, 2002, pp. 206–224.

[39] S. J. Chapman, *Subcritical transition in channel flows*, Journal of Fluid Mechanics, 451 (2002), pp. 35–97.

[40] I. Christie, D. F. Griffiths, A. R. Mitchell, and J. M. Sanz-Serna, *Product approximation for nonlinear problems in the finite element method*, IMA Journal of Numerical Analysis, 1 (1981), pp. 253–266.

[41] E. A. Coddington and N. Levinson, *Theory of Ordinary Differential Equations*, Krieger Publishing Co., Malabar, Florida, reprint of 1955 ed., 1984.

[42] J. D. Cole, *On a quasi-linear parabolic equation occurring in aerodynamics*, Quarterly of Applied Mathematics, 9 (1951), pp. 225–236.

[43] P. Constantin and C. Foias, *Navier-Stokes Equations*, University of Chicago Press, Chicago, IL, 1988.

[44] R. F. Curtain and H. J. Zwart, *An Introduction to Infinite-Dimensional Linear System Theory*, no. 21 in Texts in Applied Mathematics, Springer-Verlag, New York, 1995.

[45] S. De Lillo, *Burgers equation on the finite interval*, Inverse Problems, 6 (1990), pp. L17–L20.

[46] A. Dogan, *A Galerkin finite element approach to Burgers equation*, Applied Mathematics and Computation, 157 (2004), pp. 331–246.

[47] J. Douglas and T. Dupont, *The effect of interpolating the coefficients in nonlinear parabolic Galerkin procedures*, Mathematics of Computation, 29 (1975), pp. 360–389.

[48] J. Doyle, *Guaranteed margins for LQG regulators*, IEEE Transactions on Automatic Control, AC-23 (1978), pp. 756–757.

[49] P. G. Drazin and W. H. Reid, *Hydrodynamic Stability*, Cambridge University Press, New York, 1981.

[50] M. Efe and H. Özbay, *Low dimensional modeling and Dirichlét boundary controller design for Burgers equation*, International Journal of Control, 77 (2004), pp. 895–906.

[51] M. Embree and L. N. Trefethen, *Pseudospectra gateway.* Web site: http://www.comlab.ox.ac.uk/pseudospectra.

[52] B. F. Farrell and P. J. Ioannou, *Stochastic forcing of the linearized Navier-Stokes equations*, Physics of Fluids A, 5 (1993), pp. 2600–2609.

[53] ——, *Variance maintained by stochastic forcing of non-normal dynamical systems associated with linearly stable shear flows*, Physical Review Letters, 72 (1994), pp. 1188–1191.

[54] G. J. Fix and G. Strang, *An Analysis of the Finite Element Method*, Prentice-Hall, Englewood Cliffs, N.J., 1973.

[55] C. A. J. Fletcher, *Burgers' equation: A model for all reasons*, in Numerical Solutions of Partial Differential Equations, J. Noyle, ed., North-Holland, Amsterdam-New York, 1982, pp. 139–225.

[56] ——, *The group finite element formulation*, Computer Methods in Applied Mechanics and Engineering, 37 (1983), pp. 225–244.

[57] ——, *Computational Techniques for Fluid Dynamics I*, Springer-Verlag, Berlin, 1991.

[58] G. P. Galdi, *An Introduction to the Mathematical Theory of the Navier-Stokes Equations I and II*, Springer-Verlag, New York, 1994.

[59] E. Gallestey, D. Hinrichsen, and A. J. Pritchard, *Spectral value sets of closed linear operators*, Proceedings of the Royal Society of London A, 456 (2000), pp. 1397–1418.

[60] M. Garbey and H. G. Kaper, *Asymptotic-numerical study of supersensitivity for generalized Burgers' equations*, SIAM Journal on Scientific Computing, 22 (2000), pp. 368–385.

[61] T. Gebhardt and S. Grossmann, *Chaos transition despite linear stability*, Physical Review E, 50 (1994), pp. 3705–3711.

[62] S. K. Godunov, *Modern Aspects of Linear Algebra*, vol. 175 of Translations of Mathematical Monographs, American Mathematical Society, Providence, RI, 1998.

[63] L. H. Gustavsson, *Energy growth of three-dimensional disturbances in plane Poiseuille flow*, Journal of Fluid Mechanics, 224 (1991), pp. 241–260.

[64] T. Hagen and J. Turi, *A semigroup approach to a class of semilinear parabolic differential equations*, Nonlinear Analysis, 34 (1998), pp. 17–35.

[65] W. Hahn, *Stability of Motion*, Springer-Verlag, Berlin, 1967.

[66] E. J. Haug, K. K. Kyung, and V. Komkov, *Design sensitivity analysis of structural systems*, vol. 177 of Mathematics in Science and Engineering, Academic Press, Orlando, FL, 1986.

[67] D. Henry, *Geometric Theory of Semilinear Parabolic Equations*, Springer-Verlag, New York, 1981.

[68] I. Herron, *Observations on the role of vorticity in the stability theory of wall bounded flows*, Stud. Appl. Maths, 85 (1991), pp. 269–286.

[69] ——, *The linear stability of circular pipe flow to axisymmetric disturbances*, Stability & Applied Analysis of Continuous Media, 2 (1992), pp. 293–303.

[70] A. T. Hill and E. Süli, *Dynamics of a nonlinear convection-diffusion equation in multidimensional bounded domains*, Proceedings of the Royal Society of Edinburgh, 125A (1995), pp. 439–448.

[71] E. Hopf, *The partial differential equation* $u_t + uu_x = \mu u_{xx}$, Communications on Pure and Applied Mathematics, 3 (1950), pp. 201–230.

[72] D. Iftimie and G. Raugel, *Some results on the Navier-Stokes equations in thin 3D domains*, Journal of Differential Equations, 169 (2001), pp. 281–331.

[73] M. R. Jovanović and B. Bamieh, *Modeling flow statistics using the linearized Navier-Stokes equations*, in Proceedings of the 40th IEEE Conference on Decision and Control, Orlando, FL, 2001, pp. 4944–4949.

[74] ——, *The spatio-temporal impulse response of the linearized Navier-Stokes equations*, in Proceedings of the 2001 American Control Conference, Arlington, VA, 2001, pp. 1948–1953.

[75] ——, *Componentwise energy amplification in channel flows*, to appear in Journal of Fluid Mechanics, (2004).

[76] ——, *Unstable modes versus non-normal modes in supercritical channel flows*, submitted to Journal of Fluid Mechanics, (2004).

[77] T. Kato, *Perturbation Theory for Linear Operators*, Springer-Verlag, New York, 1976.

[78] J. Kim, *Control of turbulent boundary layers*, Physics of Fluids, 15 (2003), pp. 1093–1105.

[79] B. B. King and D. A. Krueger, *Burgers equation: Galerkin least-squares approximations and feedback control*, Mathematical and Computer Modeling, 38 (2003), pp. 1075–1085.

[80] G. Kreiss and H.-O. Kreiss, *Convergence to steady state of solutions of Burgers' equation*, Applied Numerical Mathematics, 2 (1986), pp. 161–179.

[81] H.-O. Kreiss and J. Lorenz, *Resolvent estimates and quantification of nonlinear stability*, Acta Mathematica Sinica, English Series, 16 (2000), pp. 1–20.

[82] E. Kreyszig, *Introductory Functional Analysis with Applications*, John Wiley & Sons, 1978.

[83] K. Kunisch and S. Volkwein, *Control of the Burgers equation by a reduced-order approach using proper orthogonal decomposition*, Journal of Optimization Theory and Applications, 102 (1999), pp. 345–371.

[84] S. Kutluay, A. Esen, and I. Dag, *Numerical solutions of the Burgers equation by the least-squares quadratic B-spline finite element method*, Journal of Computational and Applied Mathematics, 167 (2004), pp. 21–3.

[85] O. A. Ladyzhenskaya, *The Mathematical Theory of Viscous Incompressible Flow*, Gordon and Breach, New York, second english ed., 1969.

[86] O. A. Ladyzhenskaya, V. A. Solonnikov, and N. N. Ural'ceva, *Linear and Quasi-linear Equations of Parabolic Type*, vol. 23 of Translations of Mathematical Monographs, American Mathematical Society, Providence, Rhode Island, 1968.

[87] J. G. Laforgue and R. E. O'Malley, *Supersensitive boundary value problems*, in Asymptotic and Numerical Methods for Partial Differential Equations with Critical Parameters, H. G. Kaper and M. Garbey, eds., Kluwer Academic Publishers, Dordrecht, The Netherlands, 1993, pp. 215–223.

[88] ——, *Shock layer movement for Burgers' equation*, SIAM Journal on Applied Mathematics, 55 (1995), pp. 332–347.

[89] ——, *Viscous shock motion for advection-diffusion equations*, Studies in Applied Mathematics, 95 (1995), pp. 147–170.

[90] ——, *Exponential asymptotics, the viscid Burgers' equation, and standing wave solutions for a reaction-advection-diffusion model*, Studies in Applied Mathematics, 102 (1999), pp. 137–172.

[91] H. Langer and C. Tretter, *Spectral properties of the Orr-Sommerfeld problem*, Proceedings of the Royal Society of Edinburgh, 127A (1997), pp. 1245–1261.

[92] H. Li, H. Wu, and H. Ma, *The Legendre GalerkinChebyshev collocation method for Burgers-like equations*, IMA Journal of Numerical Analysis, 23 (2003), pp. 109–124.

[93] M. Liefvendahl and G. Kreiss, *Bounds for threshold amplitudes in subcritical shear flows*, Journal of Nonlinear Mathematical Physics, 9 (2002), pp. 311–324.

[94] ——, *Analytical and numerical investigation of the resolvent for plane Couette flow*, SIAM Journal on Applied Mathematics, 63 (2003), pp. 801–817.

[95] J. L. Lions, *Controle Optimal des Systèmes Gouvernés par des Équations aux Dérivées Partielles*, Dunod, Paris, 1969. English translation Springer-Verlag, New York, 1971.

[96] W.-J. Liu and M. Krstić, *Backstepping boundary control of Burgers' equation with actuator dynamics*, Systems & Control Letters, 41 (2000), pp. 291–303.

[97] H. V. Ly, K. D. Mease, and E. S. Titi, *Distributed and boundary control of the viscous Burgers' equation*, Numerical Functional Analysis and Optimization, 18 (1997), pp. 143–188.

[98] H. Marrekchi, *Dynamic compensators for a nonlinear conservation law*, PhD thesis, Department of Mathematics, Virginia Polytechnic Institute and State University, 1993.

[99] K. Massa, *Control of Burgers' equation with mixed boundary conditions*, master's thesis, Department of Mathematics, Virginia Polytechnic Institute and State University, 1998.

[100] M. Miklavčič, *Nonlinear stability of asymptotic suction*, Transactions of the American Mathematical Society, 281 (1984), pp. 215–231.

[101] ——, *Applied Functional Analysis and Partial Differential Equations*, World Scientific, Singapore, 1998.

[102] R. K. Miller and A. N. Michel, *Ordinary Differential Equations*, Academic Press, Orlando, Florida, 1982.

[103] T. Murdoch, *An error bound for the product approximation of nonlinear problems in the finite element method*, Numerical Analysis Group Research Report 86/17, Oxford U. Computing Laboratory, 1986.

[104] S. A. Orszag, *Accurate solution of the Orr-Sommerfeld equation*, Journal of Fluid Mechanics, 50 (1971), pp. 689–703.

[105] A. Pazy, *Semigroups of Linear Operators and Applications to Partial Differential Equations*, vol. 44 of Applied Mathematical Sciences, Springer-Verlag, New York, 1983.

[106] P. Poláčik, *Convergence in smooth strongly monotone flows defined by semilinear parabolic equations*, Journal of Differential Equations, 79 (1989), pp. 89–110.

[107] J. Prüss, *On the spectrum of C_0-semigroups*, Transactions of the American Mathematical Society, 284 (1984), pp. 847–857.

[108] S. Pugh, *Finite element approximation of Burgers' equation*, master's thesis, Department of Mathematics, Virginia Polytechnic Institute and State University, 1995.

[109] S. M. Rankin III, *Semilinear evolution equations in Banach spaces with application to parabolic partial differential equations*, Transactions of the American Mathematical Society, 336 (1993), pp. 523–535.

[110] K. R. Raslan, *A collocation solution for Burgers' equation using quadratic B-spline finite elements*, International Journal of Computer Mathematics, 80 (2003), pp. 931–938.

[111] G. Raugel and G. Sell, *Navier-Stokes equations on thin 3D domains. I: Global attractors and global regularity of solutions*, Journal of the American Mathematical Society, 6 (1993), pp. 503–568.

[112] S. C. Reddy and D. S. Henningson, *Energy growth in viscous channel flows*, Journal of Fluid Mechanics, 252 (1993), pp. 209–238.

[113] S. C. Reddy, P. J. Schmid, and D. S. Henningson, *Pseudospectra of the Orr-Sommerfeld operator*, SIAM Journal on Applied Mathematics, 53 (1993), pp. 15–47.

[114] M. Reed and B. Simon, *Functional Analysis I*, Academic Press, San Diego, CA, 1980.

[115] M. Renardy, *On the linear stability of hyperbolic PDEs and viscoelastic flows*, Zeitschrift für Angewandte Mathematik und Physik, 45 (1994), pp. 854–865.

[116] L. G. Reyna and M. J. Ward, *On exponential ill-conditioning and internal layer behavior*, Numerical Functional Analysis and Optimization, 16 (1995), pp. 475–500.

[117] ——, *On the exponentially slow motion of a viscous shock*, Communications on Pure and Applied Mathematics, 48 (1995), pp. 79–120.

[118] S. Roch and B. Silbermann, *C^*-algebra techniques in numerical analysis*, Journal of Operator Theory, 35 (1996), pp. 241–280.

[119] V. A. Romanov, *Stability of plane-parallel Couette flow*, Functional Analysis and its Applications, 2 (1973), pp. 137–146.

[120] H. Salwen, F. W. Cotton, and C. E. Grosch, *Linear-stability of Poiseuille flow in a circular pipe*, Journal of Fluid Mechanics, 98 (1980), pp. 273–284.

[121] P. J. Schmid, *Linear stability theory and bypass transition in shear flows*, Physics of Plasmas, 7 (2000), pp. 1788–1794.

[122] P. J. Schmid and D. S. Henningson, *Optimal energy growth in Hagen-Poiseuille flow*, Journal of Fluid Mechanics, 277 (1994), pp. 197–225.

[123] ——, *Stability and Transition in Shear Flows*, no. 142 in Applied Mathematical Sciences, Springer-Verlag, New York, 2001.

[124] T. Shinbrot, W. Ditto, C. Grebogi, E. Ott, M. Spano, and J. A. Yorke, *Using the sensitive dependence of chaos (the butterfly effect) to direct orbits to targets in an experimental chaotic system*, Physical Review Letters A, 68 (1992), pp. 2863–2866.

[125] T. Shinbrot, C. Grebogi, E. Ott, and J. A. Yorke, *Using chaos to target stationary states of flows*, Physics Letters A, 169 (1992), pp. 349–354.

[126] H. L. Smith and H. R. Thieme, *Convergence for strongly order-preserving semiflows*, SIAM Journal on Mathematical Analysis, 22 (1991), pp. 1081–1101.

[127] L. Smith, *Finite element approximation of Burgers' equation with Robin's boundary conditions*, master's thesis, Department of Mathematics, Virginia Polytechnic Institute and State University, 1997.

[128] S. S. Sritharan, *Invariant Manifold Theory for Hydrodynamic Transition*, vol. 241 of Pitman Research Notes in Mathematics Series, Longman Scientific & Technical, Harlow, Essex, UK, 1990.

[129] L. G. Stanley, *Computational Methods for Sensitivity Analysis with Applications to Elliptic Boundary Value Problems*, PhD thesis, Department of Mathematics, Virginia Polytechnic Institute and State University, 1999.

[130] ——, *Sensitivity equation methods for parameters dependent elliptic equations*, Numerical Functional Analysis and Optimization, 22 (2001), pp. 721–748.

[131] L. G. Stanley and D. L. Stewart, *A comparison of local and global projections in design sensitivity computations*, in Computational Methods in Optimal Design and Control, J. Borggaard, J. Burns, E. Cliff, and S. Schreck, eds., vol. 24 of Progress in Systems and Control Theory, AFOSR Workshop on Optimal Design and Control, Birkhäuser, 1998, pp. 361–373.

[132] ——, *Design Sensitivity Analysis: Computational Issues of Sensitivity Equation Methods.*, vol. 25 of Frontiers in Applied Mathematics, SIAM, Philadelphia, PA, 2002.

[133] D. L. Stewart, *Numerical Methods for Accurate Computation of Design Sensitivities*, PhD thesis, Department of Mathematics, Virginia Polytechnic Institute and State University, 1998.

[134] R. Temam, *Navier-Stokes Equations and Nonlinear Functional Analysis*, SIAM, Philadelphia, PA, second ed., 1995.

[135] ——, *Infinite-Dimensional Dynamical Systems in Mechanics and Physics*, vol. 143 of Applied Mathematical Sciences, Springer, Berlin, 1997.

[136] ——, *Navier-Stokes Equations: Theory and Numerical Analysis*, American Mathematical Society, Providence, Rhode Island, reprint of the 1984 ed., 2001.

[137] Y. Tourigny, *Product approximation for the nonlinear Klein-Gordon equation*, IMA Journal of Numerical Analysis, 9 (1990), pp. 449–462.

[138] A. E. Trefethen, L. N. Trefethen, and P. J. Schmid, *Spectra and pseudospectra for pipe Poiseuille flow*, Computer Methods in Applied Mechanics and Engineering, 1926 (1999), pp. 413–420.

[139] L. N. Trefethen, *Pseudospectra of matrices*, in Numerical Analysis 1991, D. F. Griffiths and G. A. Watson, eds., vol. 260 of Pitman Research Notes in Mathematics Series, Longman Scientific & Technical, Harlow, Essex, UK, 1992, pp. 234–266.

[140] ——, *Pseudospectra of linear operators*, SIAM Review, 39 (1997), pp. 383–406.

[141] L. N. Trefethen, S. J. Chapman, D. S. Henningson, Á. Meseguer, T. Mullin, and F. T. M. Nieuwstadt, *Threshold amplitudes for transition to turbulence in a pipe*, Tech. Report NA-00/17, Oxford Computing Laboratory, Oxford, UK, 2000.

[142] L. N. Trefethen and M. Embree, *Spectra and Pseudospectra: The Behavior of Non-Normal Matrices and Operators*, Princeton University Press, to appear, July 2005.

[143] L. N. Trefethen, A. E. Trefethen, S. C. Reddy, and T. A. Driscoll, *Hydrodynamic stability without eigenvalues*, Science, 261 (1993), pp. 578–584.

[144] S. Volkwein, *Distributed control problems for the Burgers equation*, Computational Optimization and Applications, 18 (2001), pp. 115–140.

[145] J. A. Walker, *Dynamical Systems and Evolution Equations: Theory and Applications*, Plenum Press, New York, N. Y., 1980.

[146] M. J. Ward, *Exponential asymptotics and convection-diffusion-reaction models*, in Analyzing Multiscale Phenomena Using Singular Perturbation Methods, vol. 56 of Proceedings of Symposia in Applied Mathematics, Providence, RI, 2000, American Mathematical Society, pp. 151–184.

[147] M. J. Ward and L. G. Reyna, *Internal layers, small eigenvalues, and the sensitivity of metastable motion*, SIAM Journal on Applied Mathematics, 55 (1995), pp. 425–445.

[148] T. G. Wright, *Eigtool software package*. Web site: http://www.comlab.ox.ac.uk/pseudospectra/eigtool/.